PD-AAW-318
52129
4180

Third Quarterly Report
Oct. 19, 1986 - Feb. 19, 1987

Grant No. DPE-5542-G-Ss-4057-00

RESEARCH AND DEVELOPMENT OF SOLAR-POWERED DESICCANT REFRIGERATION FOR COLD-STORAGE APPLICATIONS

Illinois Institute of Technology
Chicago, Illinois

and

Asian Institute of Technology
Bangkok, Thailand

Rec'd in SCI: JUN 26 1987

The third report includes:

1. An analysis of a closed-cycle solid desiccant cooling system prepared by IIT, Chicago.

2. Testing of a Zeolite-water refrigerator and investigation of other potential desiccant-refrigerant pairs.

CLOSED CYCLE ADSORPTION

by

Illinois Institute of Technology
Chicago, IL

CHAPTER I

THERMODYNAMICS OF SOLID ADSORPTION PHENOMENA AND PROCESSES

1-1 SOLID ADSORPTION PHENOMENA

Solid adsorption is the process by which molecules of a certain fluid substance ("adsorbate") adhere to the surface of a solid material ("adsorbent"). Two types of adsorption at fluid-solid interfaces are usually distinguished: physical adsorption (or physio-sorption) and chemical adsorption (or chemisorption).

Chemisorption is the result of strong binding forces comparable to those which accompany chemical reactions. Thus the energies involved are of the same order of magnitude as heats of reaction (10^4-10^5 calories per mole). As a consequence of the formation of a chemisorbed compound, the process is usually irreversible and terminates after the formation of a single layer at the interface. A typical example of chemisorption is the adsorption of oxygen by charcoal at 100 °C which when heated and exposed to low pressures releases CO.

On the other hand, physical adsorption involves forces of Van der Waals type and the energy effects are comparable to heats of phase change such as condensation. The amount adsorbed at a given temperature T increases with the relative pressure p/p_s, where p_s is the saturation vapor pressure of liquid adsorbate at the temperature T. Several superimposed layers of adsorbed substance may form. The process is essentially reversible except when

capillary condensation occurs in adsorbents containing fine pores. This usually leads to hysterisis in the sorption isotherm.

The following discussion addresses the phenomena of physical gas-solid adsorption which constitutes the fundamental aspect of the present research. First the general principles of adsorption theory are briefly discussed with emphasis on the recent developments. A phenomenological law for adsorption equilibrium is proposed and compared to known potential theories. Then formulas are derived for thermodynamic description of adsorption processes encountered in the applications of closed-cycle adsorption heating and cooling systems. The use of these formulas will be illustrated in the numerical simulations presented in this thesis.

1-2 EXPERIMENTAL AND THEORETICAL DESCRIPTION OF ADSORPTION

Adsorption is most generally described in terms of **isotherms** which give the amount of gas adsorbed per unit mass of adsorbent as function of the relative pressure at constant temperature. Figure 1-1 shows isotherms of the pair chabazite-Methanol [5] as an example.

1-2-1 Experimental determination of Isotherms

The experimental apparatus should allow to measure the amount of gas adsorbed, the pressure of the vapor phase and the temperature of the adsorbent-adsorbate system. Two experimental methods are typically used. Their basic principles are shown in figure 1-2 although the apparatus can be more sophisticated for

more accurate and faster runs [1].

1. Gravimetric method: the amount of gas adsorbed is measured by the gain in weight of an adsorbent sample placed in a glass tube at a preset relative pressure. In order to obtain the desired relative pressure, a large sample of initially frozen adsorbate is contained in the glass tube which is initially evacuated prior to any measurements. The temperature of the liquid adsorbate (which imposes the pressure of the gas phase) and the temperature of the adsorbent are then controlled by two regulated ovens.

2. Volumetric method: All volumes in the experimental setup are calibrated. The amount of gas adsorbed is calculated from the pressure measured by a manometer M and the volume adsorbed read on a buret B. The adsorbent sample is contained in a thermostatic tube.

1-2-2 Types of adsorption Isotherms

Figure 1-3 shows Brunauer's 5 types of adsorption isotherms. Although a qualitative interpretation of thes isotherms can be made [2], a more precise description is made difficult by overlapping phenomena involved in physical adsorption: monolayer adsorption, multilayer adsorption and capillary condensation. The type-II isotherm illustrates this difficulty as the first portion of the S-shaped curve correspondes to monolayer adsorption up to relative pressure (p/p_s) 0.1, a multilayer adsorption region follows until about p/p_s=0.4 and at larger values of the relative pressure, capillary condensation occurs.

1-2-3 Equilibrium thermodynamics of adsorption

In applying thermodynamic principles to adsorption

equilibrium, two different approaches can be adopted. It is possible to regard adsorption as a transformation from the gas phase to the adsorbed phase according to:

Gaseous molecule ⇔ *Adsorbed molecule*

The adsorbent is assumed to have the unique role of creating a force field and otherwise be exterior to the adsorbed phase. Another perspective considers the surface layer (adsorbent and adsorbate) as single phase comparable to a solution. In both approaches, the equilibrium condition is:

$$\mu_g = \mu_s \tag{1-1}$$

or since $\mu = \bar{H} - T\bar{S}$

$$\bar{H}_g - \bar{H}_s = T(\bar{S}_g - \bar{S}_s) \tag{1-2}$$

1-2-3-1 Equilibrium constant

Introducing the relation $\mu = \mu^o + RT\ Ln(a/a^o)$ where a is the activity and "o" designates a standard state, equation (1-1) yields:

$$\mu_s^o - \mu_g^o = -RT\ Ln\ K \tag{1-3}$$

where,

$$K = (a_s a_g^o) / (a_s^o a_g) \tag{1-4}$$

is the equilibrium constant. A simplified expression for K is obtained by choosing the standard activities to equal 1 and assuming an ideal gas phase for which $a_g = p$:

$$K = a_s/p \tag{1-5}$$

To obtain the isotherms a_s need to be determined using statistical

thermodynamics [3]. To illustrate the procedure, for ideal localized sorption:

$$a_s = \theta / (1-\theta) \tag{1-6}$$

where θ is the degree of saturation of the adsorbing surface. Substituting in (1-5) yields:

$$K = \theta / [p(1-\theta)] \tag{4-7}$$

which is the well known **Languimir isotherm** originally derived using kinetic arguments.

1-2-3-2 Gibbs's adsorption Isotherm

Consider a solid-gas interface with area A, n moles of adsorbed species at temperature T and pressure p. The Gibbs free energy is given by:

$$G = G(p,T,A,n) \tag{1-8}$$

Differentiating (1-8) and using thermodynamic principles, we obtain:

$$dG = Vdp - SdT - \pi dA - \mu_s\, dn \tag{1-9}$$

where π is the *spreading pressure* defined by :

$$\pi = -(\partial G/\partial A)_{p,T,n} \tag{1-10}$$

Integrating (1-9) at constant p and T yields:

$$G = \pi A + \mu_s n \tag{1-11}$$

Upon differentiation of (1-11) and after substraction of (1-9), we obtain:

$$d\pi = (n/A)\, d\mu_s \tag{1-12}$$

Introducing the surface concentration $\Gamma = n/A$ and using the condition of equilibrium, equation (1-1) yields:

$$d\pi = \Gamma\, d\mu_g \tag{1-13}$$

If we further assume an ideal gas phase, $d\mu_g = RT\, d(Lnp)$. Thus

$$d\pi = RT\Gamma\, d(Lnp) \tag{1-14}$$

This relation between the spreading pressure and the surface concentration is called ***Gibbs's adsorption isotherm.*** Equation (1-14) can be integrated at constant temperature from 0 to p from which one obtains:

$$p = (RT/A_{sp}) \int_0^p x\, d(Lnp) \tag{1-15}$$

where $A_{sp} = A/m$ is the area per unit mass of adsorbent and x is the number of adsorbed moles per unit mass of adsorbent.

To obtain the isotherm from Gibbs's relation (1-14), an equation of state for the two dimensional adsorbed phase is needed. Such an equation relates the spreading pressure π to the surface concentration Γ . To illustrate the procedure, assume an equation of state in which deviation from ideality is expressed by an excluded area correction:

$$\pi(\sigma - \sigma^0) = RT \tag{1-16}$$

where $\sigma = A_{sp} w/n$. Differentiating (1-16) and substituting in (1-14) yields:

$$d\theta/[\,\theta(1-\theta^2)\,] = d(Lnp) \tag{1-17}$$

where $\theta = \sigma/\sigma^0$. Integrating (1-17) gives:

$$Ln[\theta/(1-\theta)] + \theta/(1-\theta) = Lnp + LnK \tag{1-18}$$

which is **Volmer's isotherm.**

1-2-3-3 <u>Other adsorption isotherms</u>

An alternative method of deriving adsorption isotherms is the use of statistical thermodynamics. The procedure is exposed in some detail in [3-4]. Another important isotherm for multilayer adsorption was drived by Brunauer, Emett and Teller. This theory and final equation are known by the initials of the authors: ***BET***. The BET isotherm is the basis of an experimental method of determining the specific surface area of adsorbents. A thermodynamic analysis based on a virial equation is also available [3] and has the advantage of including nonlocalized sorption.

1-2-3-4 Heats of adsorption

Barrer [3] gives the following definitions for the isosteric heat of adsorption q_{st} the differential heat of adsorption ΔH and the integral heat of adsorption ΔH:

$$q_{st} = RT^2 (\partial Lnf/\partial T)_n \qquad (1\text{-}20)$$

$$\Delta H = H_s - H_g \qquad (1\text{-}21)$$

$$\Delta H = (1/n) \int \Delta H \, dn \qquad (1\text{-}21)$$

H_s is the partial molar enthalpy of adsorbed species and H_g is the same quantity for the gas phase. Replacing μ in equation (1-1) by $\mu^o + RTLn(f/f^o)$, dividing by T and using the Gibbs-Helmholtz relation $[\partial(\mu/T)/\partial T] = -H/T^2$ yield:

$$-\frac{\bar{H}_s}{T^2} = \frac{\tilde{H}_g}{T^2} + R\left(\frac{\partial Lnf}{\partial T}\right)_n \qquad (1\text{-}23)$$

Assuming an ideal gas phase $H_g = H_g$ and equation (1-23) implies:

$$\Delta\bar{H} \equiv \bar{H}_s - \bar{H}_g = R\,T^2\left(\frac{\partial Lnf}{\partial T}\right)_n \equiv q_{st} \qquad (1\text{-}24)$$

This establishes the equality of ΔH and q_{st} . An application of this relation is to test equilibrium data from which q_{st} is determined by means of an independent calorimetric method allowing the measure of ΔH [4]. An other important equation involving q_{st} is derived from the following Clausius-Clapeyron type of relation:

$$\left(\frac{\partial p}{\partial T}\right)_n = \frac{\bar{S}_g - \bar{S}_s}{\bar{V}_g - \bar{V}_s} \qquad (1\text{-}25)$$

Using equation (1-2), we obtain:

$$\left(\frac{\partial p}{\partial T}\right)_n = \frac{\bar{H}_g - \bar{H}_s}{T(\bar{V}_g - \bar{V}_s)} \qquad (1\text{-}26)$$

Assuming ideal gas, $\bar{H}_g - \bar{H}_s = q_{st}$ and $\bar{V}_s << \bar{V}_g = RT/p$

and equation (1-26) becomes:

$$\left(\frac{\partial Lnp}{\partial 1/T}\right)_n = \frac{q_{st}}{R} \qquad (1\text{-}27)$$

This last equation shows that q_{st} can be obtained from the slope of the curve Lnp versus 1/T.

1-2-4 Potential theories of adsorption

1-2-4-1 Dubinin-Polanyi Theory

A different approach to the theoretical determination of isotherms was developed by Polanyi and extended by Dubinin (see for example [6]) . The sorbed species is considered to be liquid like and incompressible, however the properties of this phase will be different from those of bulk fluid. The difference in free energy between the two phases is measured by the ***adsorption potential***, ε, defined by:

$$\varepsilon = - RT \, Ln(p/p_s) \tag{1-27}$$

The pressures p and p_s are the saturation pressure at temperature T for the adsorbed phase and the bulk liquid respectively. Dubinin-Polanyi theory is based on the assumption that the relationship between ε and the volume sorbed, which is estimated as liquid is temperature independent. Thus using a "characteristic curve" obtained at a suitable temperature, an isotherm can be obtained at any other sorbent temperature.

For micropore adsorbents such as activated carbon or zeolites, an empirical isotherm equation of the form :

$$w = w_0 \exp(-D\varepsilon^2) \tag{1-29}$$

with two adjustable parameters is sometimes sufficiently adequate to fit the experimental data. A posssible generalization of equation (1-29) is to replace the exponent 2 by a third adjustable parameter n. Although equation (1-29) is known to deviate from experimental data for very small and very large uptakes, it is a very useful tool in correlating adsorption data for design purposes.

1-2-4-2 <u>"Linearized Potential" Theory</u>

In a recent paper, Pons and Grenier [7] extended the Polanyi

assumption by proposing that ε is a linear function of temperature:

$$\varepsilon = A(w) + B(w)\,T \tag{1-30}$$

A(w) and B(w) are then choosen as second-order polynomials of the variable X defined by:

$$X=[Ln(w_0/w)]^{0.25} \tag{1-31}$$

The seven parameters of the model are determined by a best fit of the experimental data. This model was applied to the pair Activated Carbon-Methanol for which they obtained:

$$A(w) = 68.619 + 199.9X - 15.489X^2 \tag{1-32}$$

$$B(w) = -0.28811 - 0.52414X + 0.69153X^2 \tag{1-33}$$

$$X = [Ln(0.34/w)]^{0.25} \tag{1-34}$$

Their experimental conditions were:

$-10<T<130^oC$; $0.1<p<70$ kPa; $0.007<w<0.321$

1-2-5 A proposed phenomenological law for Adsorption Equilibrium

A convenient graphical representation of adsorption data is to plot the *isosters* (curves of constant uptake) in a (T_s,T) diagram; T is the temperture of the system and T_s the saturation temperature of the liquid adsorbate at the pressure of the system. Such graphs which are obtained from the isotherms (figure 1-4 gives the isosters for the pair Chabazite-Methanol obtained form data of [5]) and prove to be very convenient in the analysis of adsorption cycles encountered in heating and cooling applications .

Available data on adsorption by microporous adsorbents such as zeolites and activated carbon show that the isosters in a (T_s,T) diagram are straight lines over a sufficiently wide range of

temperature and adsorbate uptake. This naturally leads to the idea that a linear law of the form:

$$T_s = \mathbf{A}(w)T + \mathbf{B}(w) \tag{1-32}$$

will be suitable for representing adsorption data over a range of T and w conditions which hopefully will include the important range for engineering applications.

A linear relation such as (1-32) is obviously very convenient to numerical calculations since it is explicit in T_s and T and requires an iterative method only if w is desired. This is the advantage sought in the present thesis since we are mainly concerned with the numerical simulation of practical adsorption machines. Nevertheless an attempt is made to provide some theoretical basis for this law and to give a physical interpretation of **A**(w) and **B**(w) .

1-2-5-1 Relation to Potential Theories

A certain theoretical justification of the proposed law can be found by investigating its relation to potential theories. Recalling Clausius-Clapeyron's equation for the bulk liquid adsorbate:

$$\frac{d\mathrm{Ln}p}{dT} = \frac{L(T)}{RT^2} \tag{1-33}$$

and writing L(T) in the functional form

$$L(T) = L_0 + f(T) \tag{1-34}$$

[f(T) need not be specified at this stage but one can think of it as the first term in a Taylor expansion of L(T)] we obtain after substitution of (1-34) in (1-33) and integration:

$$\mathrm{Ln}p = -\frac{L_o}{RT} + \frac{1}{R}\int^{T} \frac{f(T)}{T^2}\,dT \qquad (1\text{-}35)$$

The expression of the adsorption potential becomes:

$$\varepsilon = -RT\left[-\frac{L_o}{R}\left(\frac{1}{T_s} - \frac{1}{T}\right) + \frac{1}{R}\int_{T}^{T_s} \frac{f(T)}{T^2}\,dT\right] \qquad (1\text{-}36)$$

Using equation (1-32) yields:

$$\varepsilon = L_o\left(\frac{1}{A(w)} - 1\right) + g(w,T) \qquad (1\text{-}37)$$

where,

$$g(w,T) = L_o\frac{B(w)}{T_s} - \frac{1}{R}\int_{T}^{T_s} \frac{f(T)}{T^2}\,dT \qquad (1\text{-}38)$$

Equation (1-37) indicates that when g(T,w) is constant, we have a temperature independent potential (Polanyi assumption) and if the first order term in T is considered, we obtain the linear potential of [7]. A more precise information about the form of the functions **A**(w) and **B**(w) can be obtained from the comparison of the present law to Dubinin-Polanyi theory. In effect, substituting (1-36) in (1-29) and taking the logarithm of each side yields:

$$\mathrm{Ln}\frac{w}{w_o} = -DR^2T^2\left[-\frac{L_o}{R}\left(\frac{1}{T_s} - \frac{1}{T}\right) + \frac{1}{R}\int_{T}^{T_s} \frac{f(T)}{T^2}\,dT\right]^2 \qquad (1\text{-}39)$$

which can be rewritten as:

$$\frac{1}{\sqrt{D}}\left[\mathrm{Ln}\frac{w}{w_o}\right]^{0.5} = -L_o\left(\frac{1}{T_s} - \frac{1}{T}\right) + \frac{1}{R}\int_{T}^{T_s} \frac{f(T)}{T^2}\,dT \qquad (1\text{-}40)$$

This relation illustrates the role of the quantity $[\ Ln(w_o/w)^{0.5}\ ]$. To see it more clearly, let's examine the case of constant latent heat L_o for which f(T)=0. In this case equation (1-40) reduces to:

$$\frac{1}{\sqrt{D L_o}} \left[Ln \frac{w}{w_o}\right]^{0.5} = \frac{T}{T_s} - 1 \qquad (1\text{-}41)$$

or for $T>T_s$:

$$T = \left\{\frac{1}{\sqrt{D L_o}} \left[Ln \frac{w}{w_o}\right]^{0.5} + 1\right\} T_s \qquad (1\text{-}42)$$

This suggests that Dubinin's equation (1-29) may reduce to the form proposed by (1-32). Furthermore the coefficients **A**(w) and **B**(w) should be simple functions of $[Ln(w_o/w)]^{0.5}$.

1-2-5-2 Expressions of q_{st} using equation (1-32)

A relation between the isosteric heat of adsorption q_{st} at conditions (T,p) and the latent heat of vaporization of the bulk liquid adsorbate at conditions (T_s,p) is obtained by a simple combination of relation (1-20) defining q_{st} and Clausius-Clapeyron equation (1-33). We obtain:

$$q_{st} = L(T_s)\ [T/T_s]^2\ (\partial T_s/\partial T)_w \qquad (1\text{-}43)$$

If equation (1-32) is used $(\partial T_s/\partial T)_w = \mathbf{A}(w)$, thus:

$$q_{st} = L(T_s)\ [T/T_s]^2\ \mathbf{A}(w) \qquad (1\text{-}44)$$

This relation shows that q_{st} depends not only on w but also on T.

1-2-6 Application of the proposed law

Figure 1-5 is a plot of the adsorption equilibrium data for the

pair synthetic Zeolite 13X-Water [9] in the $[(T-T_s)/T_s]^{0.5}$ versus Ln(w) diagram. The best curvefitting of this data is given by:

$$w = 0.2578 \exp\{-6.4516[(T-T_s)/T_s]^2\}$$

According to Dubinin's formula (1-29), all the data points should fall on a straight line. This is obviously not the case even in the region apart from the limits w small and w large where such deviation is expected. This poor representation of the equilibrium data justifies the use of a more accurate equation such as Pons and Grenier's equation (1-30) or the proposed law (1-32).

Figures (1-6,7,8) show the functions **A**(w) and **B**(w) for three sets of adsorption equilibrium data. The fact that the curves exhibit similar trends for the three cases supports the existence of a physical significance to the functions **A**(w) and **B**(w). Figure (1-8) presents these functions versus the scaling term $[Ln(0.25/w)]^{0.5}$ Although the curve **A**(w) is almost a straight line in this diagram, the curve **B**(w) does not indicate a simple expression for this function. For this reason, third order polynomials in w are used to correlate the equilibrium data for use in the simulation of adsorption systems. The data of reference [9] for example are very well represented only by the second order expressions:

$$\mathbf{A}(w) = 0.711 - 0.3177w + 6.003w^2$$

$$-\mathbf{B}(w) = 220.6 - 1256.6632w + 1532.6928w^2 \quad (°F)$$

Figure (1-9) shows **A**(w) and **B**(w) for the pair Chabazite-Methanol. In this case the data points are well correlated by the following linear expressions:

$$A(w) = 10.0w - 0.5 \qquad B(w) = -2125.0w + 252.75 \ (K)$$

Figures (1-10) gives the variations of the isosteric heat of

adsorption q_{st} and the ratio q_{st}/L with w at constant temperature according to equation (1-44). Figure (1-11) presents the variations of q_{st} with T and w. The data used are for the pair Synthetic 13X-Water [9]. The general features of these results are similar to the ones presented in other references such as [3] which indicate the weak dependence of q_{st} on T and the decrease of q_{st} with increasing w to approach the latent heat of condensation L near saturation.

1-3 THERMODYNAMIC DESCRIPTION OF ADSORPTION PROCESSES

1-3-1 General considerations

The important property of changing uptake with temperature and the energy effects that accompany the transformation:

Gaseous molecule $\Leftrightarrow$ adsorbed molecule

can be used in thermal processes to produce heating and/or cooling. In such processes, the system is constrained to undergo a cycle during which the desired effect is produced. The most important phases in adsorption cycles occur at one of the following conditions:

- constant pressure (isobaric process)
- constant volume
- constant uptake (isosteric process)

A natural question that arises when modeling adsorption machines is how the parameters T, w and T_s (or p) are related during one of the above phases. It is the purpose of this section to obtain formulas describing adsorption cycles. The following assumptions

are made to symplify the analysis:

(i) Ideal gas phase

(ii) Uniform pressure

(iii) Thermodynamic equilibrium

Assumption (i) is valid for all heating/cooling applications given their very low pressure conditions. Assumption (ii) is acceptable for adsorbents with large intercrystalline voids such as pellets of zeolite 13X which are usually used. Assumption (iii) is equivalent to saying that mass diffusion in the adsorbent is infinitely fast. This assumption can be expected to give good results for systems with sufficiently slow temperature variations such as solar energy powered adsorption machines. However deviations from equilibrium may occur with systems operating in fast conditions. In such cases an additional mass balance equation is needed which will relate the uptake w to its equilibrium value w_{eq} under the system conditions T and T_s. A simple model of the driving force to mass transfer can be assumed to be the difference $(w_{eq}-w)$. Hence the mass flux can be written as:

$$(\partial w/\partial t) = h_m(w_{eq} - w) \qquad (1\text{-}45)$$

where h_m is a constant proportional to the resistance to mass transfer. The formulas derived below using assumption (iii) will still hold if w is replaced by w_{eq} when necessary. For each phase, general formulas are derived with space dependent temperature field and simplified expressions are obtained for the case of uniform conditions. The equilibrium relation is written in the form .

$$T_s = F(T,w) \tag{1-46}$$

A function G(T,w) which measures the change in uptake per degree of temperature change is introduced by:

$$G(T,w) \equiv dw/dT \tag{1-47}$$

and called " adsorptivity function . G characterizes the response of the adsorbent to imposed temperature variations in terms of the consequent uptake change. From the computational point of view the use of G reduces the number of unkowns by eliminating for example w. This reduction is advantageous when a convenient expression of G can be found. This is in particular the case in the simulation of a solar adsorption refrigerator presented in Chapter 3.

1-3-2 Constant-pressure Process

We assume that the pressure of the system is imposed by an external source and remains constant. Differentiating (1-46) at constant p (or T_s) yields:

$$0 = (\partial F/\partial T)_w \, dT + (\partial F/\partial w)_T \, dw \tag{1-48}$$

This equation gives the expression of G as follows:

$$G_p(T,w) = - \frac{(\partial F/\partial T)_w}{(\partial F/\partial w)_T} \tag{1-49}$$

when equation (1-32) is used we obtain:

$$G_p(T,w) = - A(w) / [A'(w)T + B'(w)] \tag{1-50}$$

Since p is known, the equilibrium relation (1-46) gives T explicitly when w is known and allows the solution of w by an iterative method when T is known.

1-3-3 Constant-volume Process

In this case, the system is confined to a constant closed volume. Let ν_a be the total volume of the adsorbent and ν_g the total volume of the gas phase. ν_g is the sum of two terms: $\varepsilon\nu_a$ the void fraction of ν_a , and the portion of the total volume not occupied by the solid adsorbent.

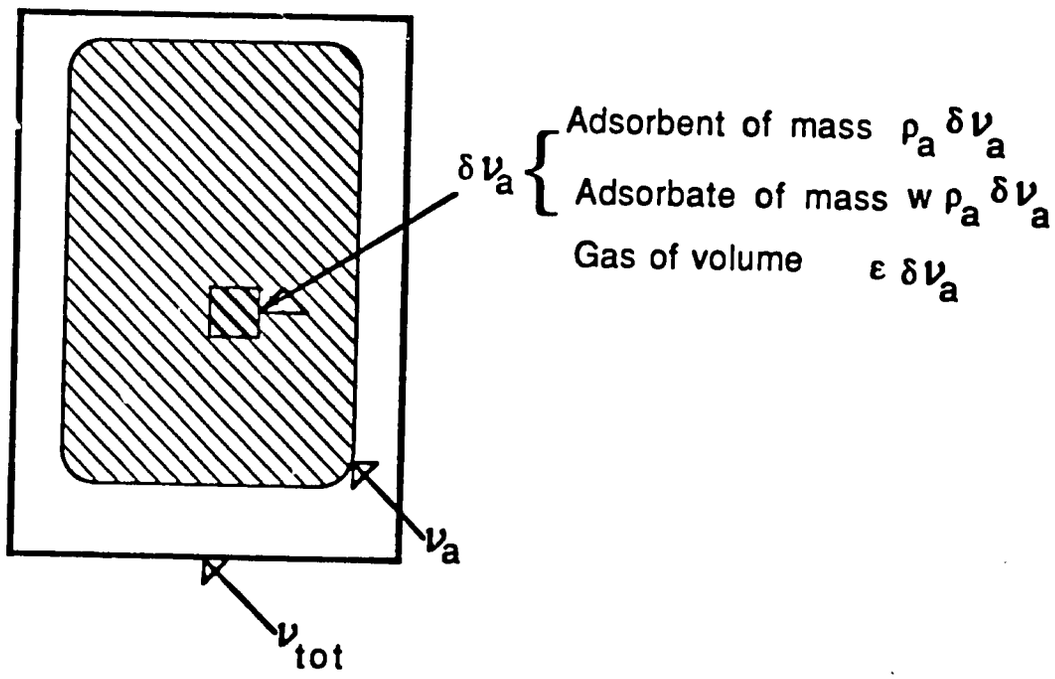

$$\nu_g = \varepsilon\nu_a + (\nu_{total} - \nu_a) \tag{1-51}$$

The term $(\nu_{tot}-\nu_a)$ is usually small and is neglected in the following analysis. A small adsorbent element of volume $\delta\nu_a$ is considered. It contains "dry" adsorbent of mass $\rho_a\delta\nu_a$, adsorbed species of mass $w\rho_a(\delta\nu_a)$ and gas phase of volume $\varepsilon(\delta\nu_a)$ and mass δm_v . The ideal gas equation for the gas phase is :

$$p\,(\varepsilon\delta\nu_a) = (\delta m_v)\, r\, T \tag{1-52}$$

21

Assuming constant porosity, for an infinitesimal transformation we have by differentiating (1-52):

$$\frac{dp}{p} = \frac{d(\delta m_v)}{\delta m_v} + \frac{dT}{T} \qquad (1\text{-}53)$$

An additional equation is obtained by considering that the change in the mass of the gas phase is of opposite sign and equal to the change in the mass of the adsorbed phase:

$$\int_{\nu_a} d(\delta m_v) = \int_{\nu_a} -\rho_a(dw)\ \delta\nu_a \qquad (1\text{-}54)$$

Solving for the term $d(\delta m_v)$ in (1-53) and integrating over ν_a yields:

$$\frac{dp}{p} \int_{\nu_a} \delta m_v = \int_{\nu_a} d(\delta m_v) + \int_{\nu_a} \frac{dT}{T}\ \delta m_v \qquad (1\text{-}55)$$

Taking into account (1-53) and (1-54) we obtain:

$$dp \int_{\nu_a} \frac{\delta \nu_a}{T} = \frac{-\rho_a r}{\varepsilon} \int_{\nu_a} dw\ (\delta \nu_a) + p \int_{\nu_a} \frac{dT}{T^2}\ \delta \nu_a \qquad (1\text{-}56)$$

This equation is a linear equation in p which can be solved for known distributions of of dT and dw. If we call t the varying parameter and define a(t) and b(t) by:

$$a(t) = \frac{\int_{\nu_a} \frac{1}{T^2}\frac{dT}{dt}\,\delta\nu_a}{\int_{\nu_a} \frac{\delta\nu_a}{T}} \quad ; \quad b(t) = \frac{\frac{\rho_a r}{\varepsilon}\int_{\nu_a} \frac{dw}{dt}(\delta\nu_a)}{\int_{\nu_a} \frac{\delta\nu_a}{T}} \qquad (1\text{-}57)$$

we can write:

$$p(t) = [\, p(0) + \int_0^t a(\eta)\, e^{-\int_0^\eta b(x)dx} \,]\, e^{\int_0^t b(\eta)\, d\eta} \qquad (1\text{-}58)$$

An expression of the function G_v can be derived as follows. Differentiating (1-46) yields:

$$dT_s = \left(\frac{\partial F}{\partial T}\right)_w dT + \left(\frac{\partial F}{\partial w}\right)_T dw \qquad (1\text{-}59)$$

Making use of Clausius-Clapeyron's equation, equation (1-56) transforms to :

$$\frac{L(T_s)}{R\,T_s^2}\, dT_s = \frac{-\frac{\rho_a r}{\varepsilon p}\int_{\nu_a} dw\,(\delta\nu_a) + \int_{\nu_a} \frac{1}{T^2}\, dT\, \delta\nu_a}{\int_{\nu_a} \frac{\delta\nu_a}{T}} \qquad (1\text{-}60)$$

Eliminating dT_s between (1-59) and (1-60) yields:

$$G_v = \frac{\left\{ \frac{R\,T_s^2}{L(T_s)} \frac{-\frac{\rho_a r}{\varepsilon p}\int_{\nu_a} dw\,(\delta\nu_a) + \int_{\nu_a} \frac{1}{T^2}\, dT\, \delta\nu_a}{(dT)\int_{\nu_a} \frac{\delta\nu_a}{T}} - \left(\frac{\partial F}{\partial T}\right)_w \right\}}{\left(\frac{\partial F}{\partial w}\right)_T} \qquad (1\text{-}61)$$

1-3-3-1 Approximation for small temperature change

In most heating/cooling adsorption cycles, the change in pressure during the constant-volume phase is caused by the change in the uptake. The contribution of the temperature change (2nd term in RHS of (1-53)) can in general be neglected. Thus

$$\delta m_v \, (dp/p) \approx d(\delta m_v) \tag{1-62}$$

Integrating over the volume ν_a gives:

$$(dp/p) \approx (dm_v/m_v) \tag{1-63}$$

where m_v is the total mass of the vapor phase. Integrating equation (1-63) with respect to the parameter t yields:

$$p(t) = p(0) \, [\, m_v(t)/m_v(0) \,] \tag{1-64}$$

From the mass balance given by (1-54) we obtain:

$$m_v(t) = m_v(0) - \int_{\nu_a} \rho_a \, [\, w(t) - w(0) \,] \, \delta\nu_a \tag{1-65}$$

Thus:

$$p(t) = p(0) \, \{ \, 1 - \frac{\rho_a}{m_v(0)} \int_{\nu_a} [w(t) - w(0)] \, \delta\nu_a \, \} \tag{1-66}$$

Using the ideal gas law to express $m_v(0)$, we obtain:

$$p(t) = p(0) \, \{ \, 1 - \frac{\rho_a \, r}{\varepsilon} \, \frac{\int_{\nu_a} [w(t) - w(0)] \, \delta\nu_a}{\int_{\nu_a} \frac{1}{T(0)} \, \delta\nu_a} \} \tag{1-67}$$

1-3-3-2 The case of uniform conditions

When the parameters T and w are constant over the volume ν_a,

24

the previous equations (1-54) and (4-56) can be greatly simplified. The mass balance equation (1-54) when integrated with respect to t yields:

$$m_v(t) = m_v(0) - \rho_a \nu_a \, [\, w(t) - w(0) \,] \tag{1-68}$$

Equation (1-55) becomes:

$$\frac{dp}{p} = \frac{dT}{T} - \frac{dw}{\dfrac{m_v(0)}{\rho_a \nu_a} - [\, w(t) - w(0) \,]} \tag{1-69}$$

or in integrated form:

$$\frac{p(t)}{p(0)} = \left\{ 1 - \frac{\rho_a \nu_a}{m_v(0)} [\, w(t) - w(0) \,] \right\} \frac{T(t)}{T(0)} \tag{1-70}$$

Equation (1-60) reduces to:

$$\frac{L(T_s)}{R T^2} dT_s = \frac{dT}{T} - \frac{dw}{\dfrac{m_v(0)}{\rho_a \nu_a} - [\, w(t) - w(0) \,]} \tag{1-71}$$

Assuming a linear variation of $L(T_s)$ with T_s of the form:

$$L(T_s) = L_o - a_L T_s \tag{1-72}$$

We can the integrate (1-71) with respect to t to obtain:

$$\frac{L_o}{R\, T_s(t)} + \mathrm{Ln}\left\{ \frac{T(t)\left\{ \dfrac{m_v(0)}{\rho_a \nu_a} - [\, w(t) - w(0) \,] \right\}}{[T_s(t)]^{a_L / R}} \right\} = \mathrm{Const} \tag{1-73}$$

Equation (1-71) expresses a differential relationship between

T, T_s and w for a constant-volume process whereas (1-73) gives an implicit relation between the three parameters. If starting from a known initial state characterized by two of the parameters ($T(0), T_s(0), w(0)$), we would like to determine the conditions of an adsorption system at the final state of a constant-volume process for which one parameter (for example T_s) is specified. Equations (1-46) and (1-73) form a set that can be solved for w(t) and T(t).

The expression of the function G_v given by (1-61) reduces to:

$$G_v = \frac{\left(\frac{\partial F}{\partial T}\right)_w + \frac{R}{L(T_s)} \frac{F^2(T,w)}{T}}{\left(\frac{\partial F}{\partial w}\right)_T + \frac{R}{L(T_s)} \frac{F^2(T,w)}{\frac{m_v(0)}{\rho_a \nu_a} - [w(t) - w(0)]}} \qquad (1\text{-}74)$$

1-3-4 " Globally-Isosteric " Process

Usually a constant-volume process corresponds to a very small change in the global uptake. But in general, a globally isosteric process is achieved when no adsorbate species is allowed to leave the adsorbed phase. Such a process satisfies:

$$d \int_{\nu_a} \rho_a w \, \delta \nu_a = 0 \qquad (1\text{-}75)$$

Since ν_a is stationary, we can write

$$\int_{\nu_a} \rho_a (dw) \, \delta \nu_a = 0 \qquad (1\text{-}76)$$

Using equation (1-59), we obtain:

$$\int_{\nu_a} \rho_a \frac{dT_s - \left(\frac{\partial F}{\partial T}\right)_w dT}{\left(\frac{\partial F}{\partial w}\right)_T} \delta \nu_a = 0 \qquad (1\text{-}77)$$

Solving for dT_s (which is uniform) and assuming ρ_a constant yields:

$$dT_s = \frac{\int_{\nu_a} \left[\left(\frac{\partial F}{\partial T}\right)_w / \left(\frac{\partial F}{\partial w}\right) \right](dT)\, \delta \nu_a}{\int_{\nu_a} \frac{1}{(\partial F/\partial w)_T} \delta \nu_a} \qquad (1\text{-}78)$$

It is obvious that for uniform conditions, equation (1-78) reduces to

$$dT_s = (\partial F/\partial T)_w \, dT \qquad (1\text{-}79)$$

Which can be directly derived from (1-59) since in this case the process is described by dw=0.

1-3-4 Verification of the derived formulas

No experimental data now exists which can be used in a direct verification of the formulas derived in this section. Therefore the only method of their validation is by comparison of the results obtained from these formulas when used in the numerical simulation of adsorption systems with available test results. This indirect procedure is not rigorous as other approximations involved in such analysis are possible sources of errors.

In the simulation of a solar energy powered adsorption refrigerator, the formulas relative to uniform conditions are used along with data from reference [8]. The predicted transient regime and machine performance show sufficient agreement with the experimental results.

Using equilibrium data provided by Tchernev [9], the functions

27

G_p and G_v are computed for a chosen set of experimental data. The results are given in figures 1-12 and 1-13 . Although Tchernev didn't specify the type of process for he determined experimentally the variations with T of a quantity analogous to **G** , his results of figure A15 show similar trend as figures 1-12,13.

The agreement mentioned above between the derived formulas and the available experimental results substantiate somewhat their validity. However, in the absence of more direct verification, the following remarks should be made:

1. No detailed comparison with experimental data is attempted here due to lacking data in references [8,9].
2. Most of the derived formulas involve differentiations of the experimentally determined equilibrium function F(T,w), which process is known to may induce large errors. Thus these formulas will certainly be more accurate if the quantities $(\partial F/\partial T)_w$ and $(\partial F/\partial w)_T$ are determined experimentally.

1-4 CONCLUSIONS

A phenomenological law for solid adsorption is proposed and proved to lead to precise and convenient representation of equilibrium data especially for numerical calculations. Formulas describing the processes involved in heating and cooling applications of solid adsorption are also derived. These formulas are substantiated by an indirect verification through the results obtained in their application to numerical simulation of actual adsorption heating and cooling systems.

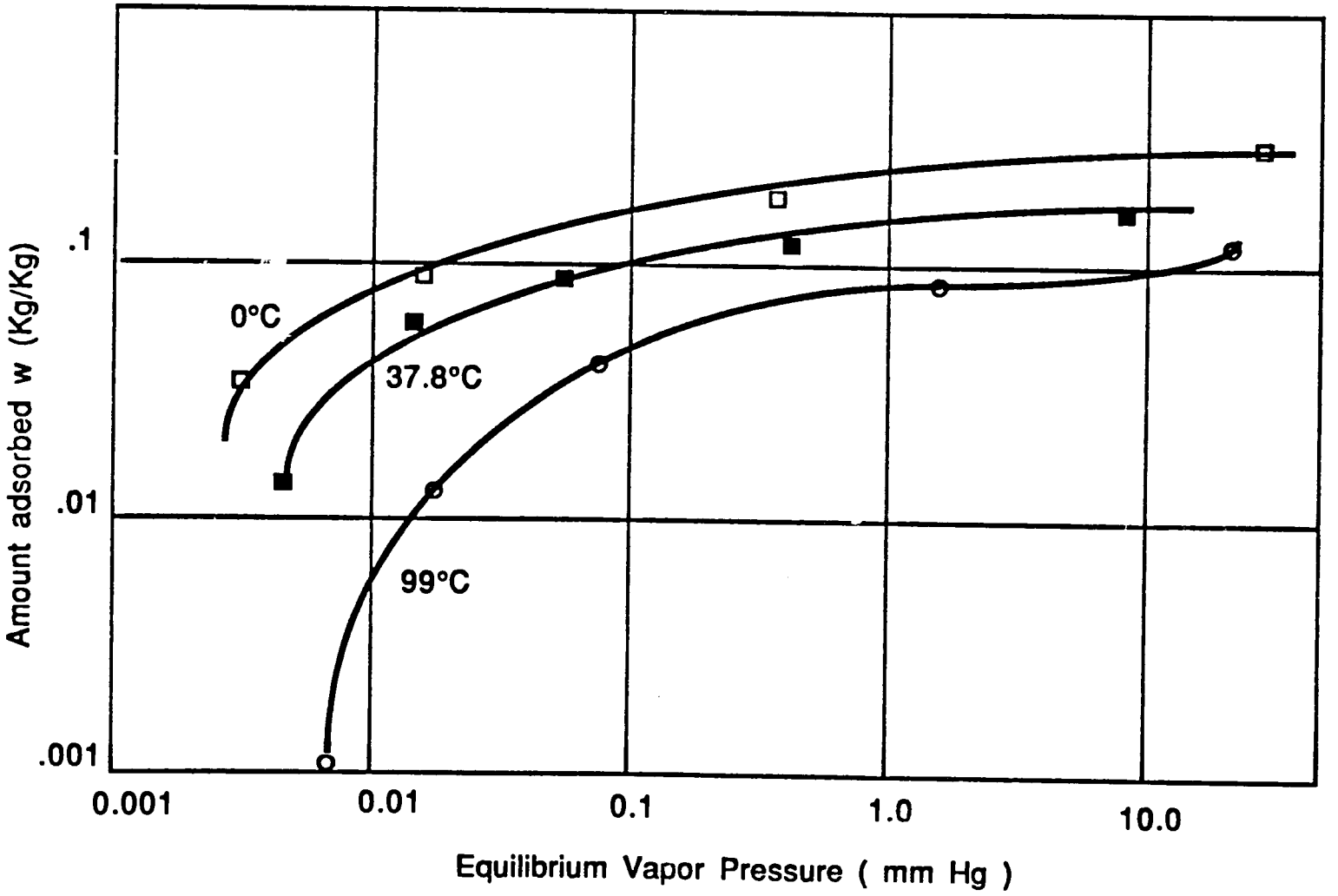

Figure 1-1 : Isotherms for the pair Chabazite-Methanol [5]

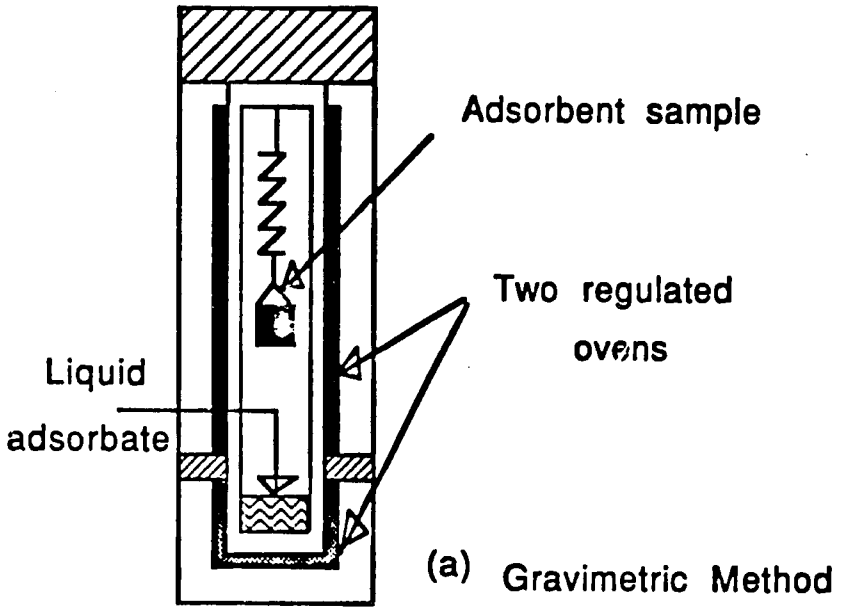

(a) Gravimetric Method

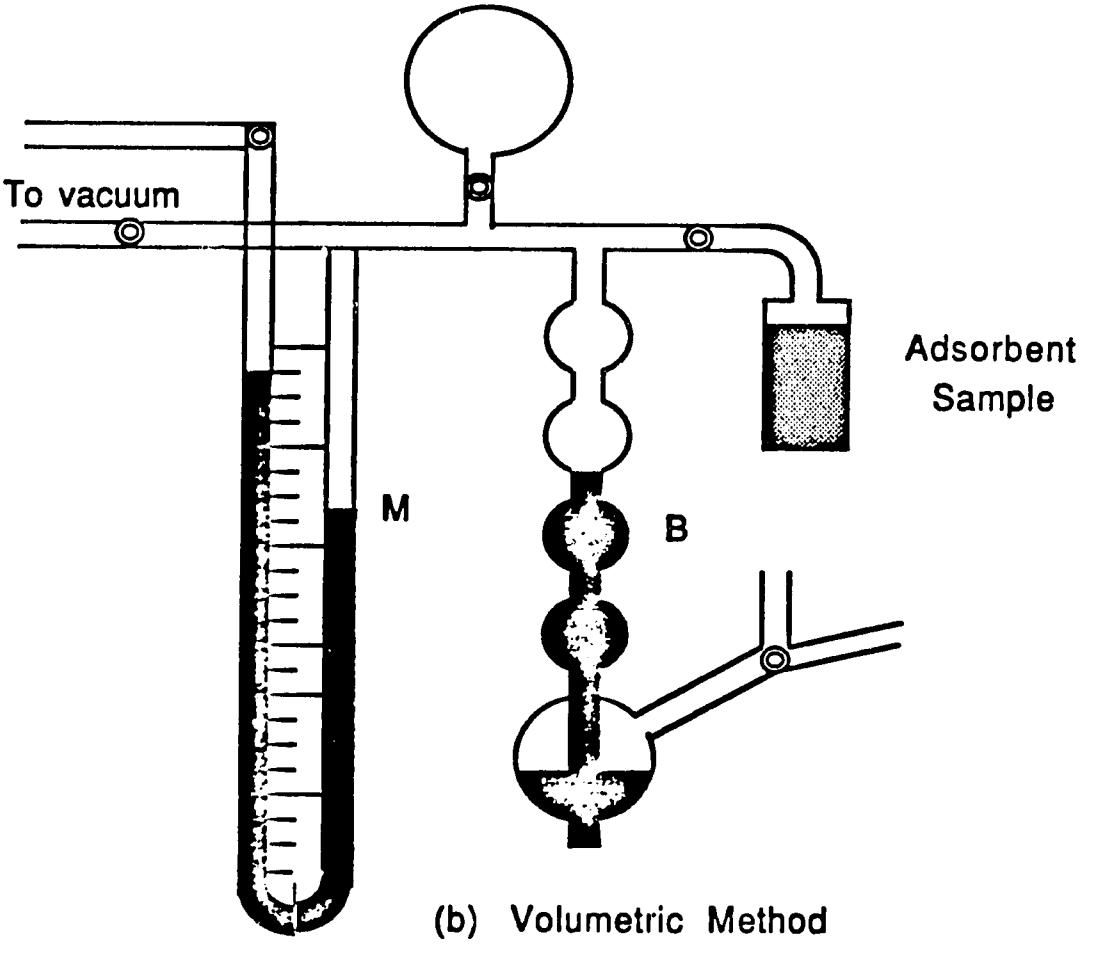

(b) Volumetric Method

Figure 1-2: Experimental determination of Isotherms

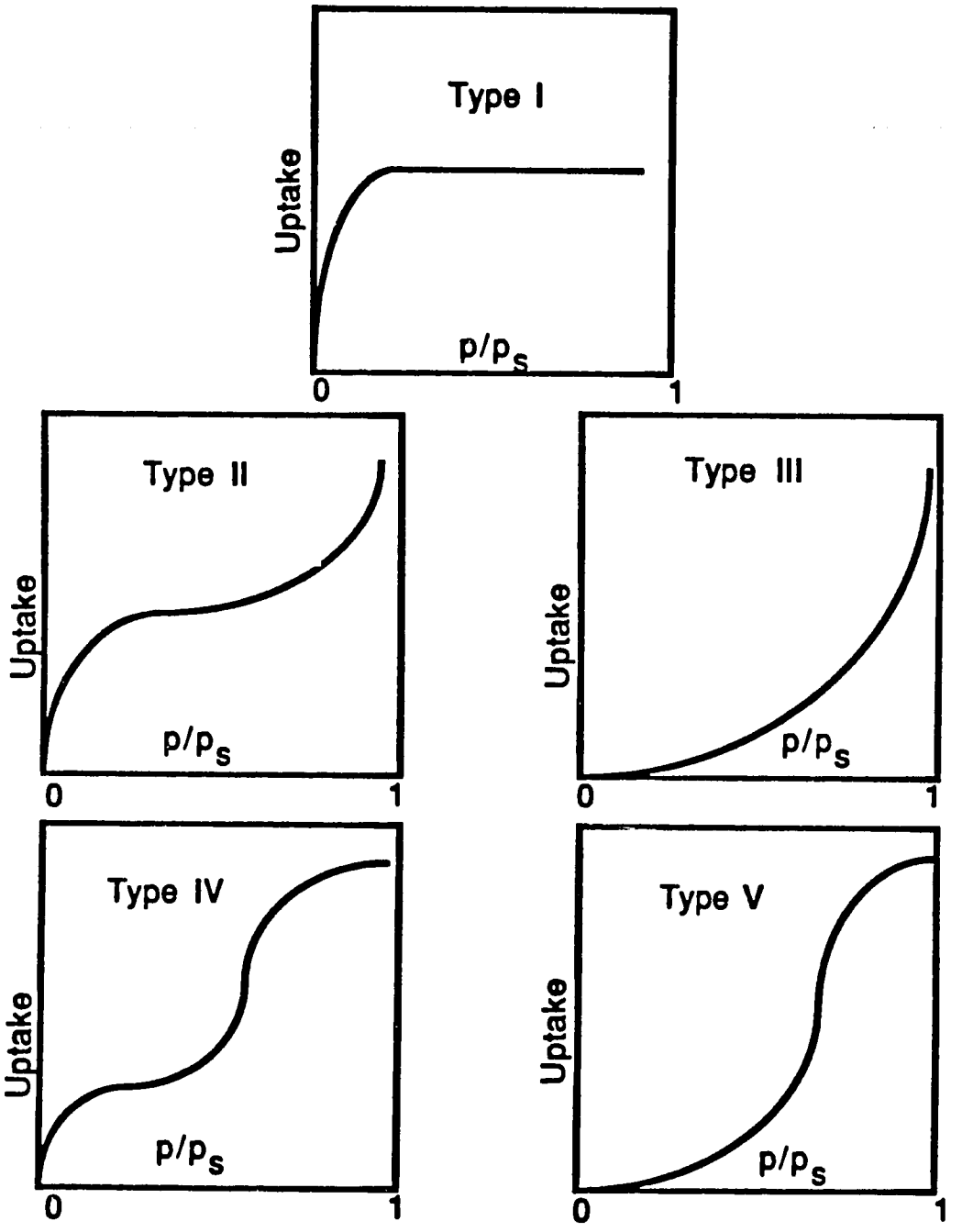

Figure 1-3 : Brunauer's five types of Adsorption Isotherms.

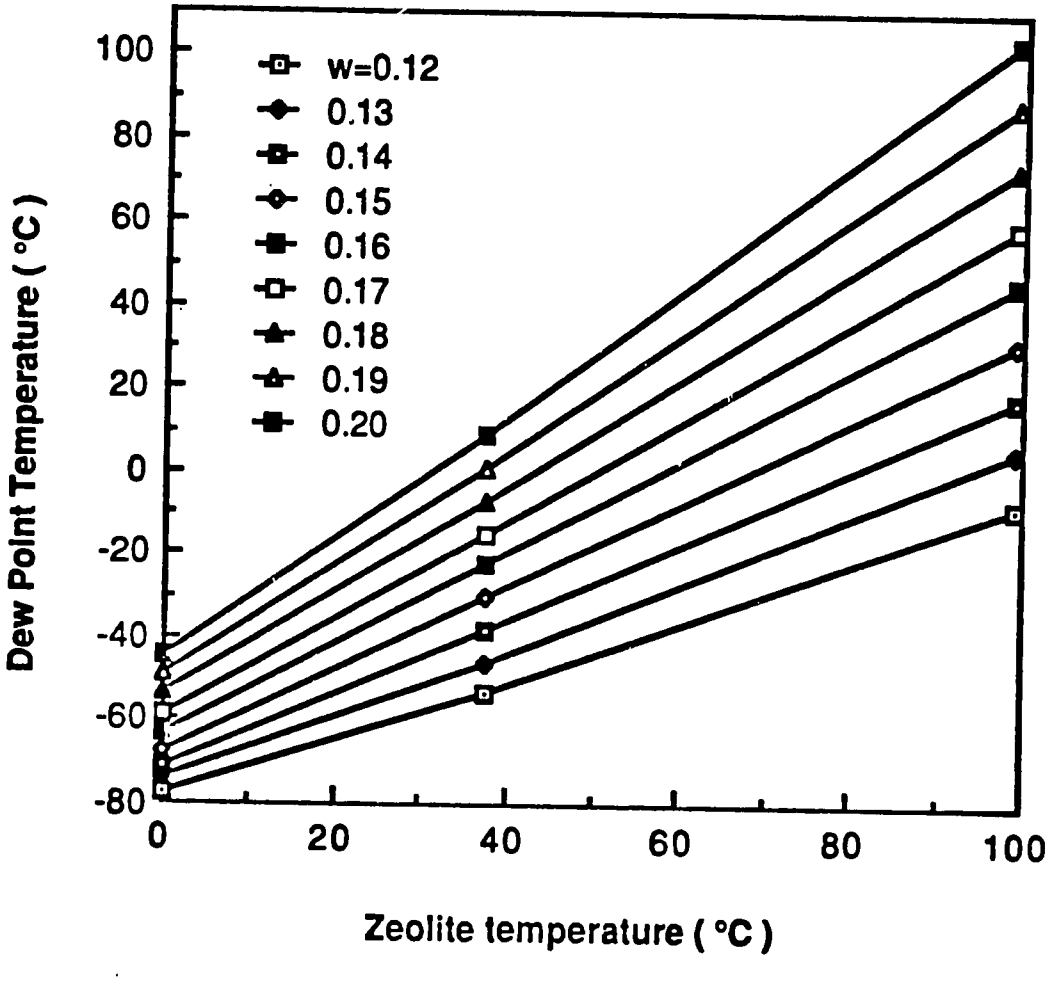

Figure 1-4: Isosters for the pair Chabazite-Methanol.

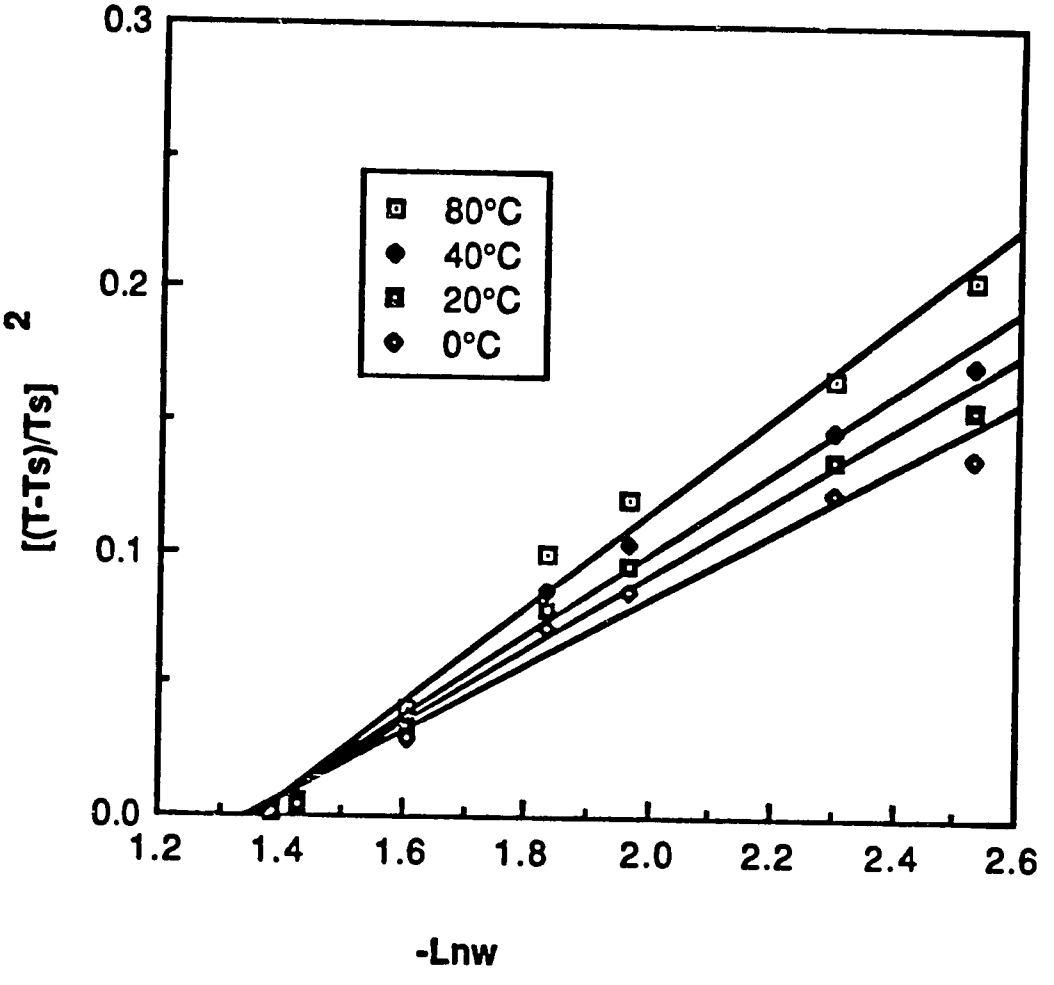

Figure 1-5: Plot of $[(T-Ts)/Ts]^2$ vs -Lnw for the data of [10].

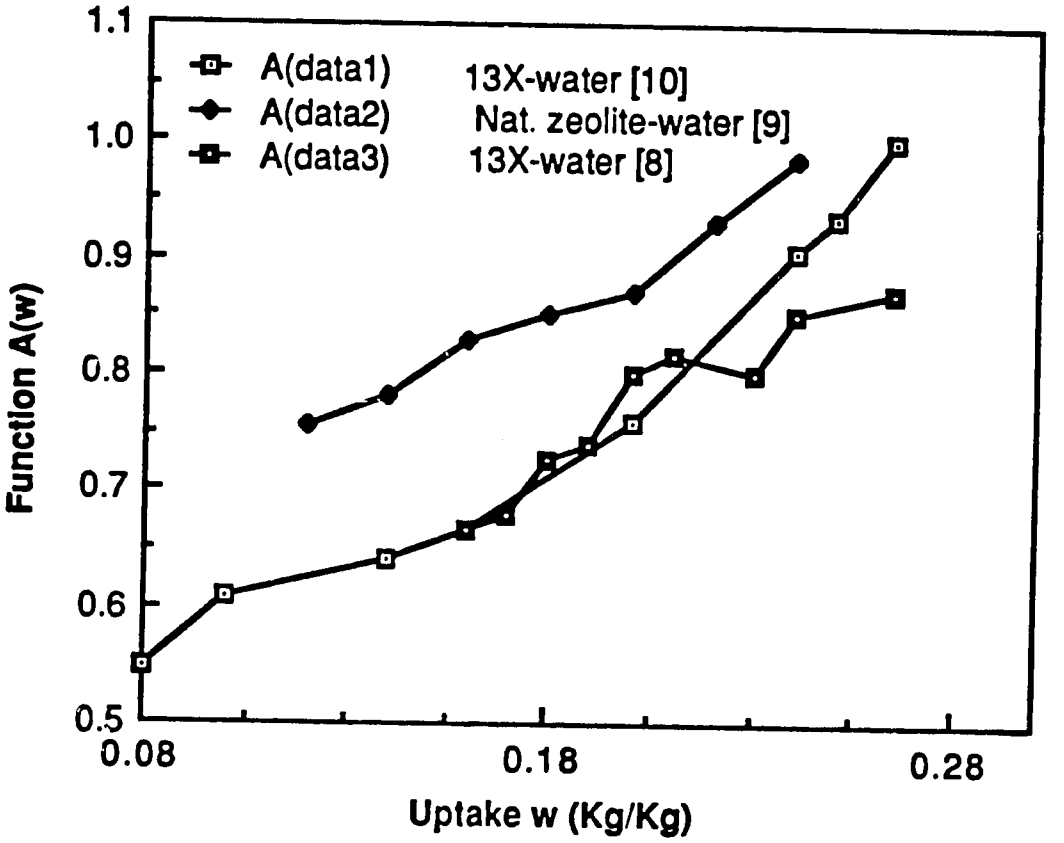

Figure 1-6 : Function A(w) For 3 Adsorption pairs.

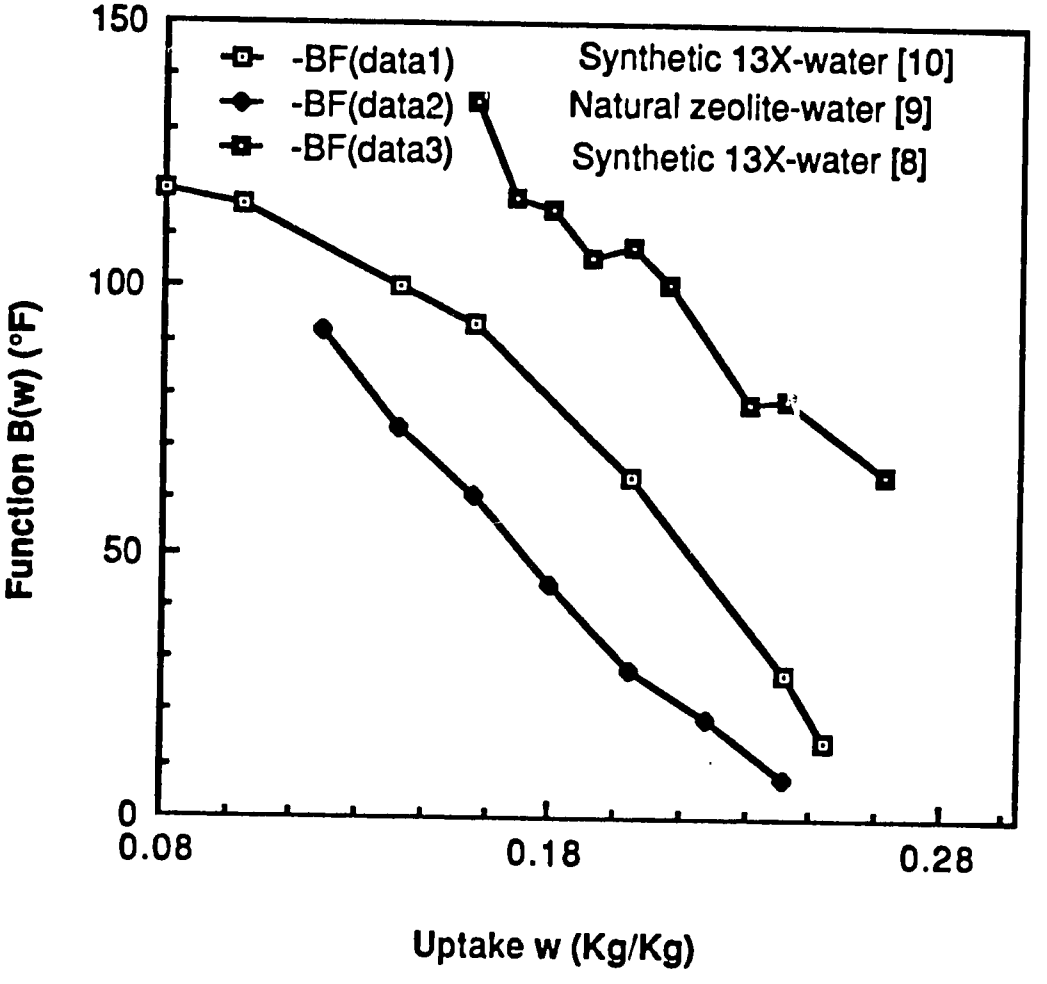

Figure 1-7 : Function B(w) (°F) for 3 Adsorption pairs.

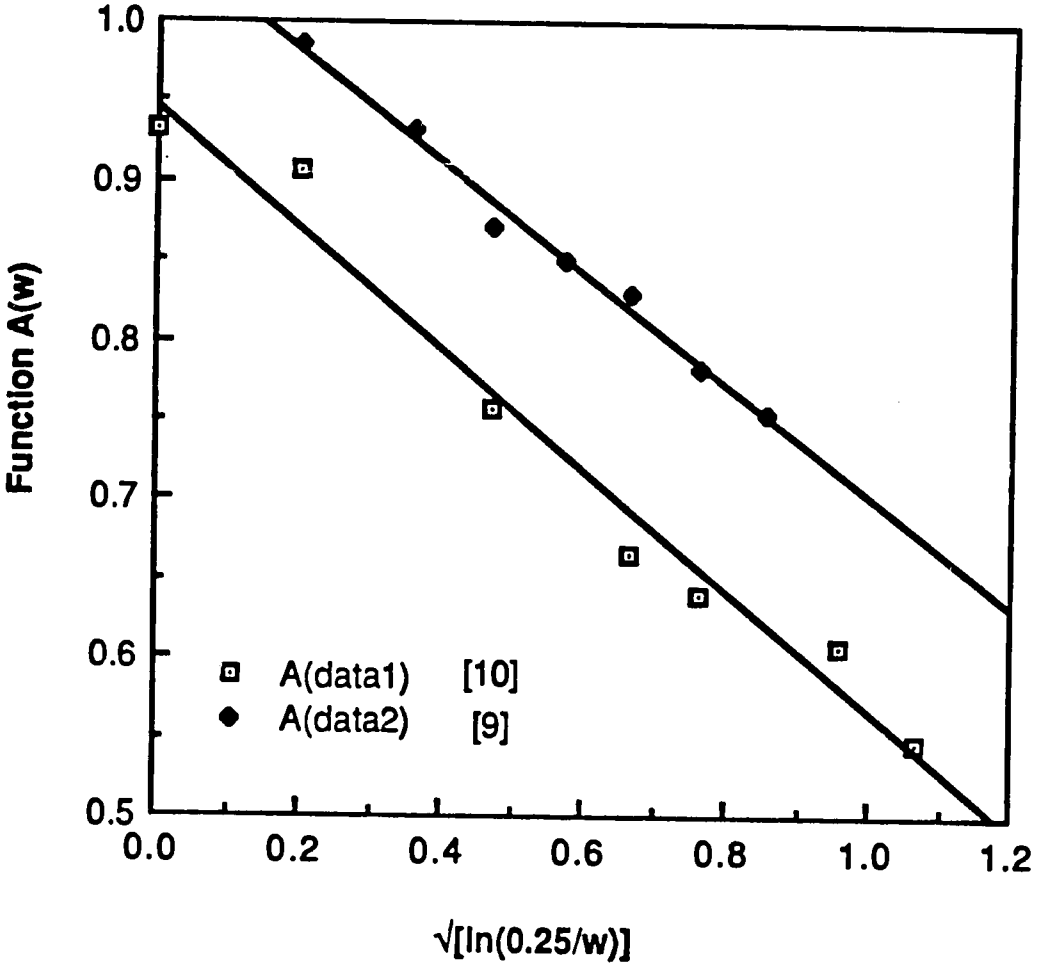

Figure 1-8a: Function A(w) vs √[Ln(.25/w)].

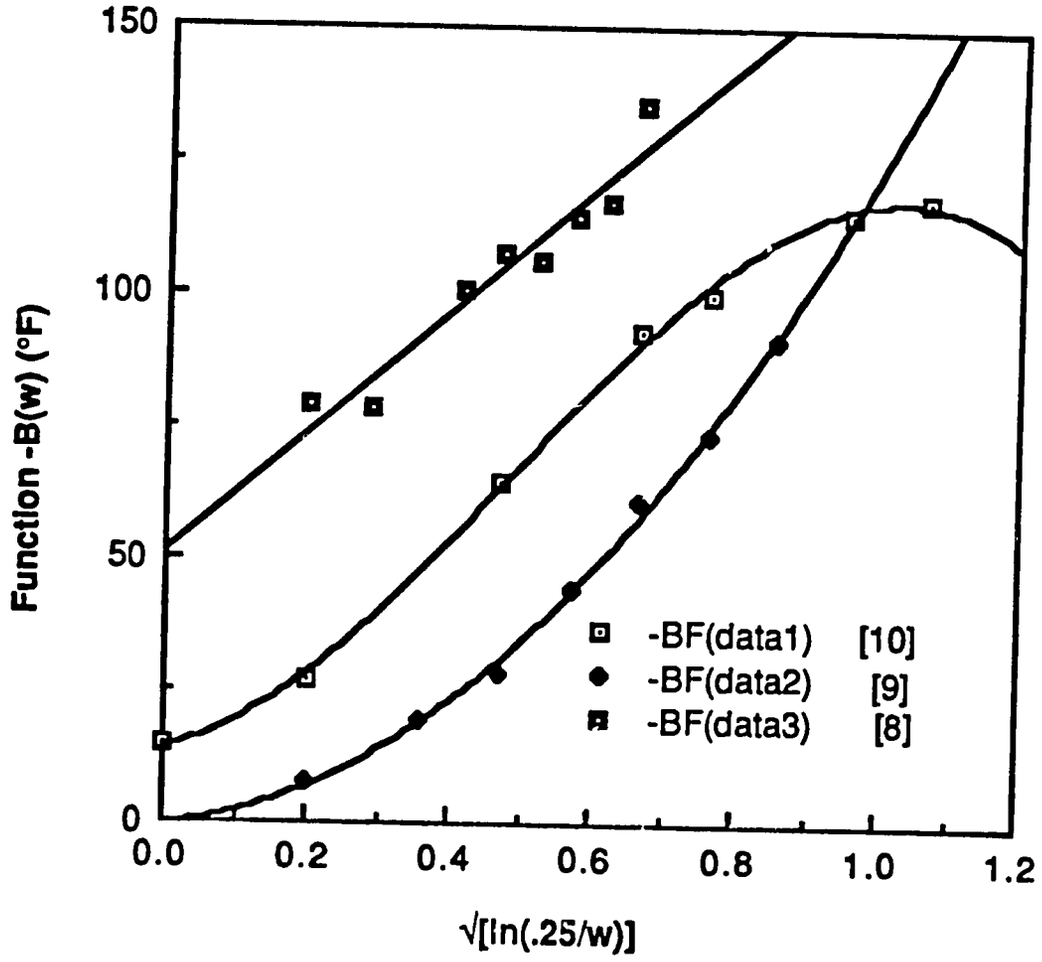

Figure 1-8b: Function -B(w) (°F) vs √[ln(.25/w)].

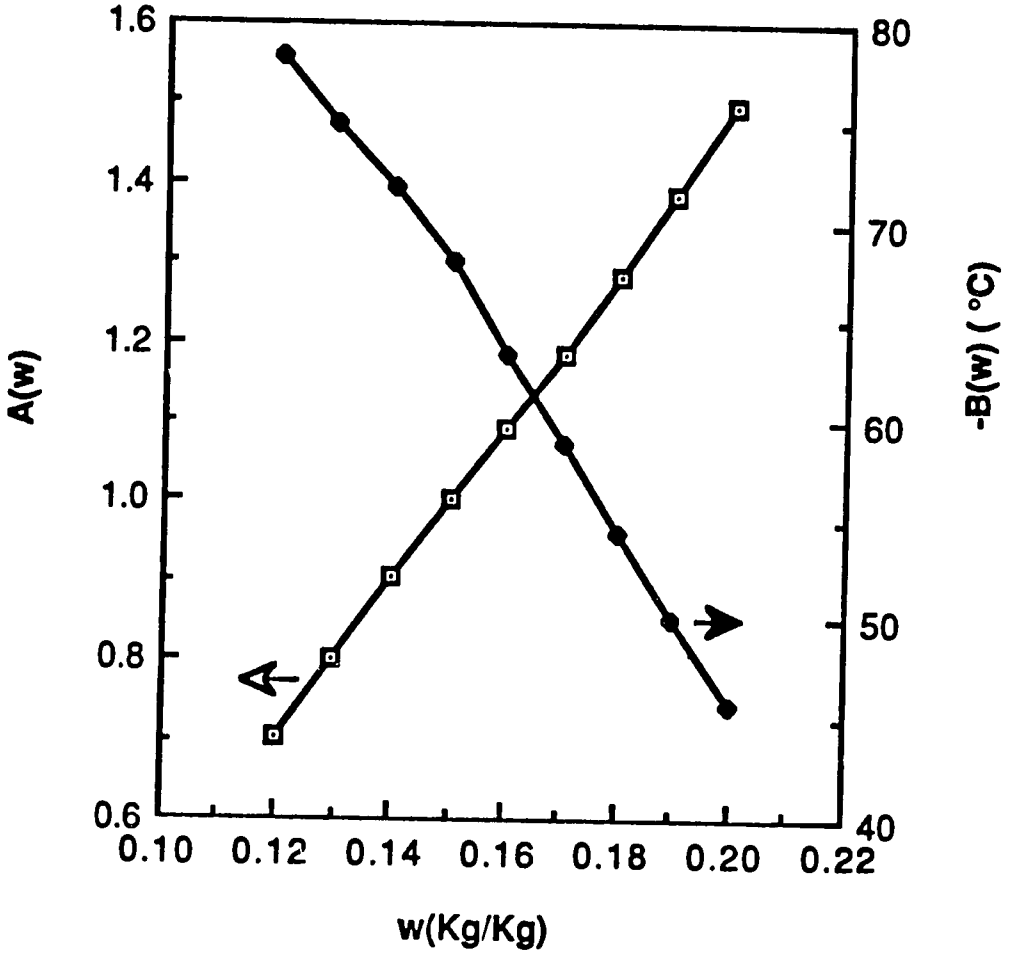

Figure 1-9 : Functions A(w) and B(w) for the pair Chabazite-Methanol.

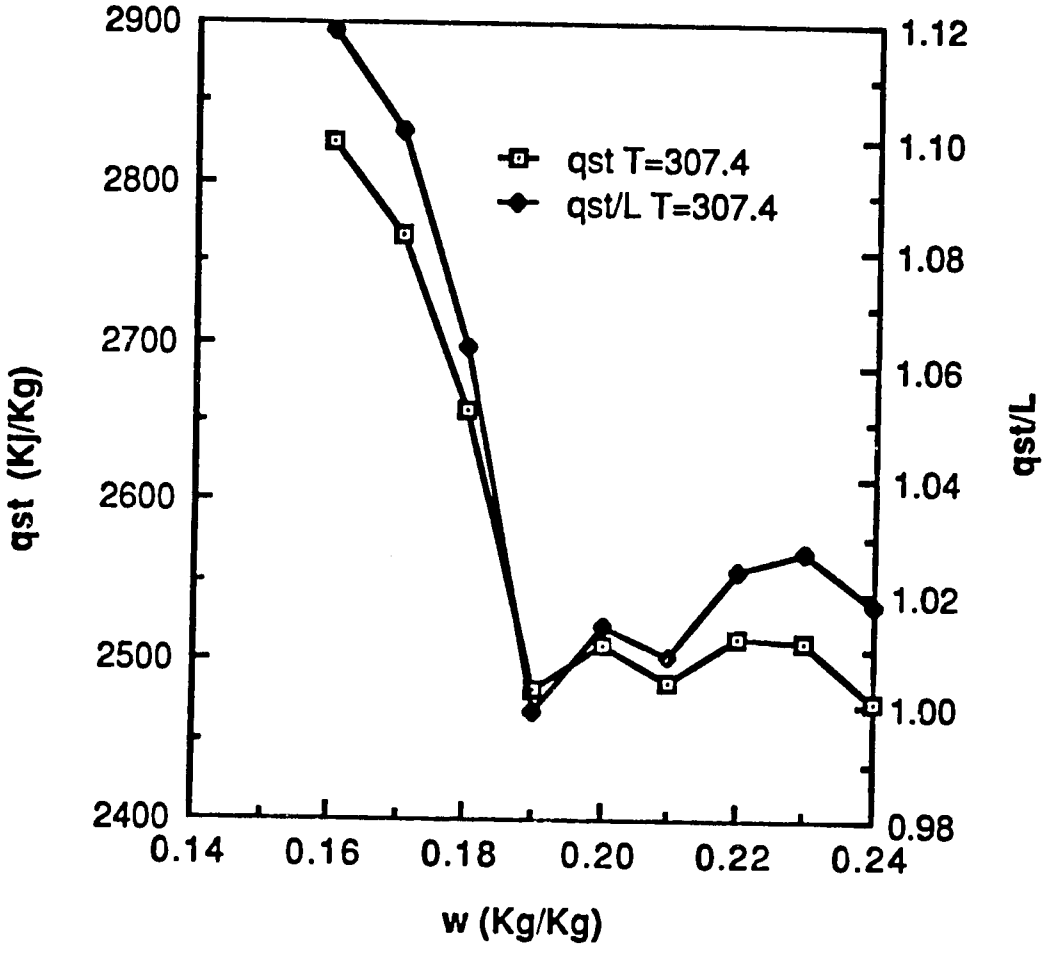

Figure 1-10: variations of qst and qst/L with w at constant T as computed using (1-44) and the data of [9].

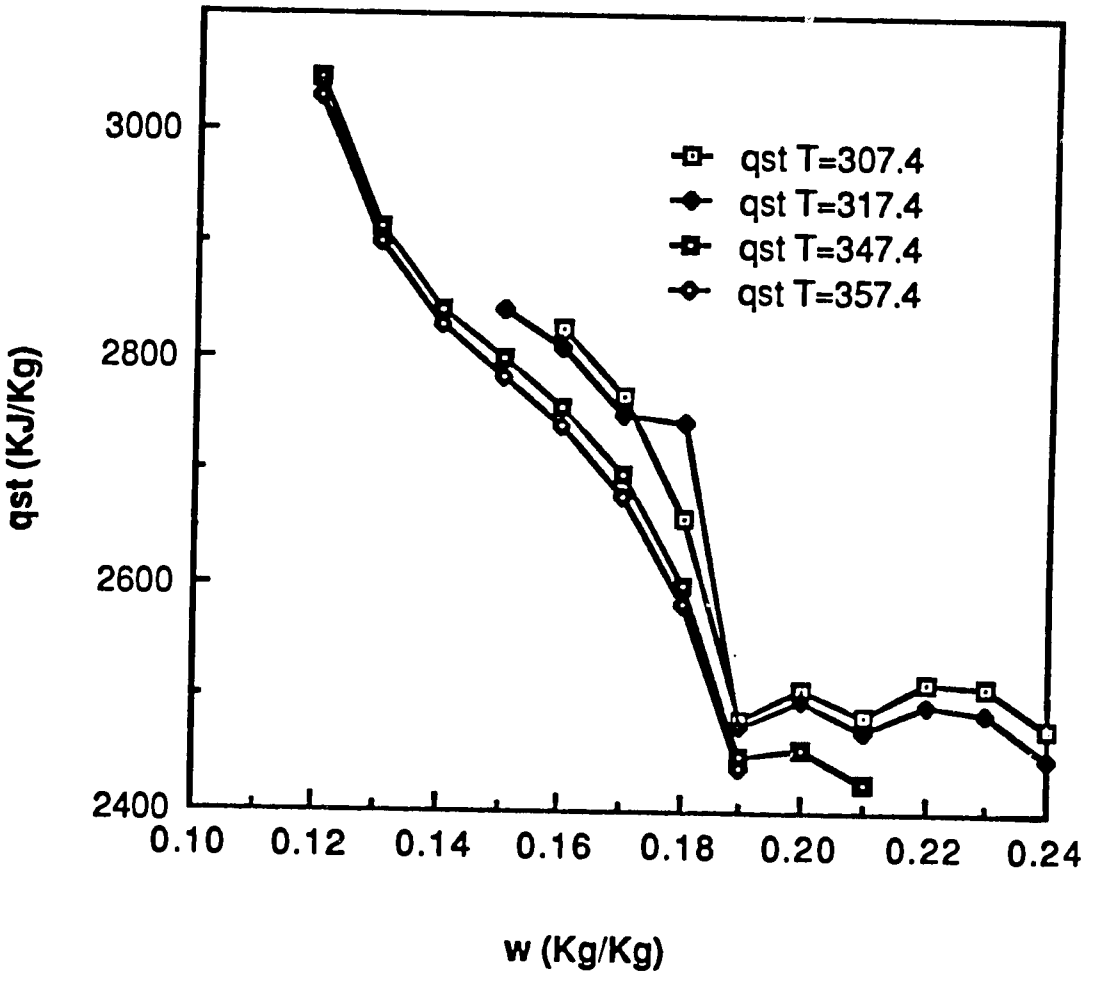

Figure 1-11: Variations of qst with w and T as computed by equation (1-44) and the data of [9].

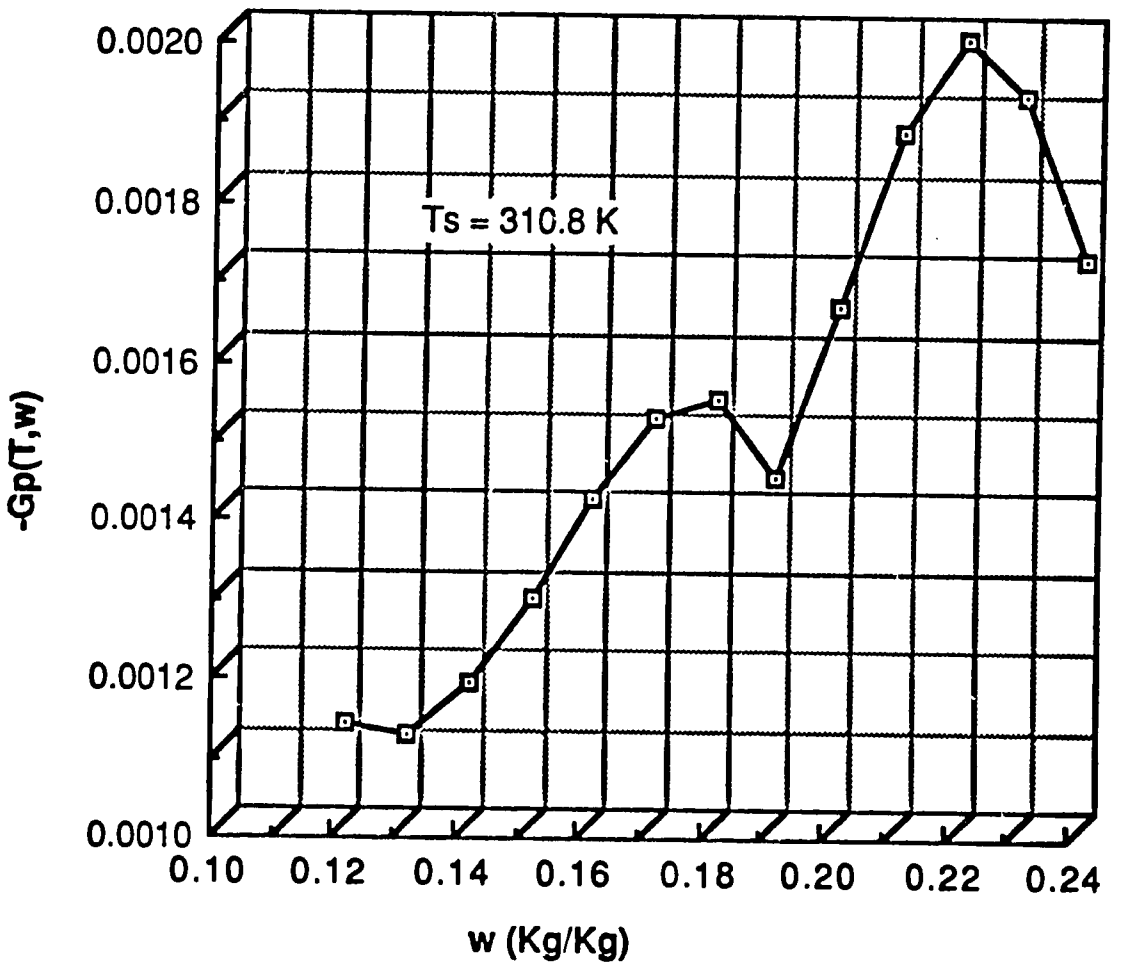

Figure 1-12: Function G(T,w) as computed from equation (1-50) and the data of [9].

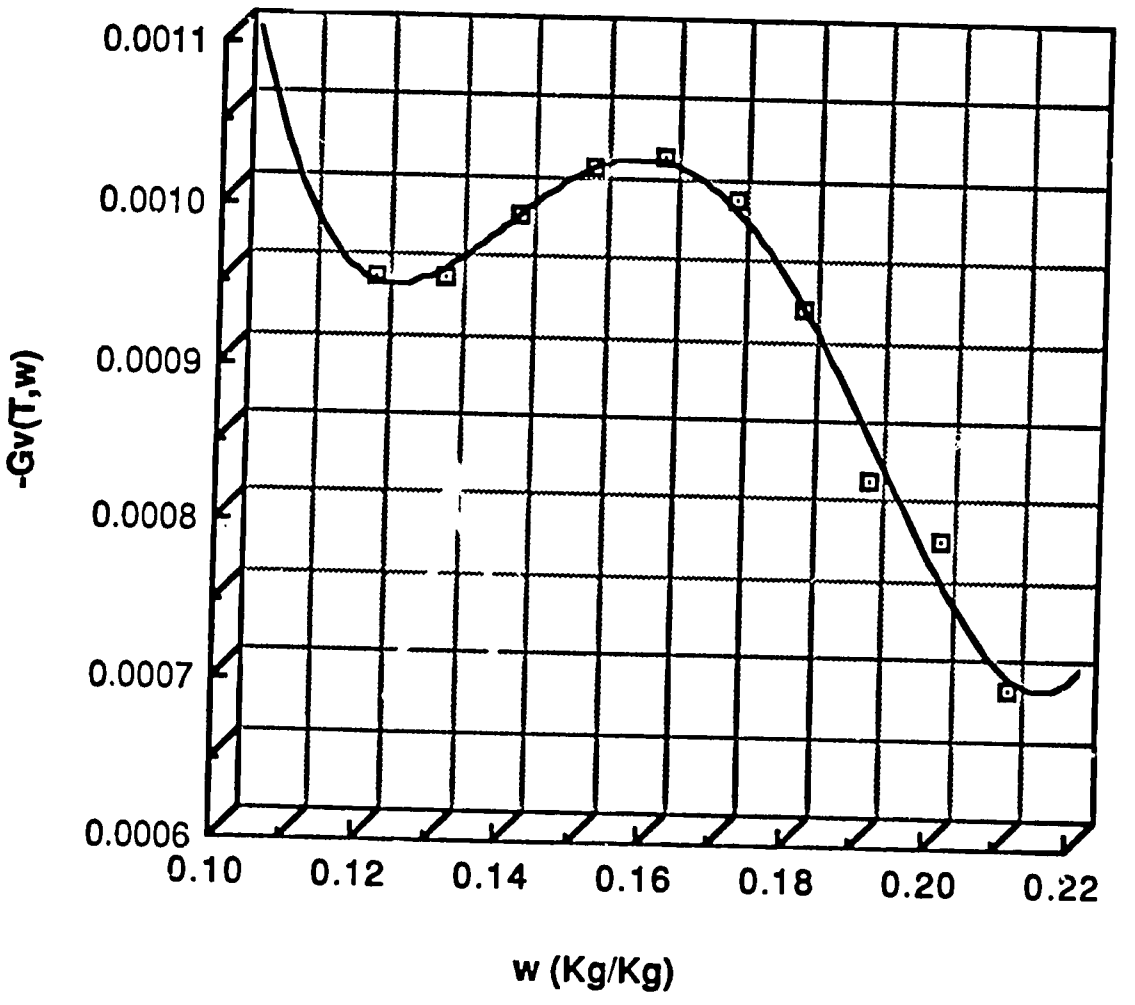

Figure 1-13: Function Gv(T,w) as computed from equation (1-74) and the data of [9].

NOMENCLATURE

Abbreviation	Term
a	Activity
A	Area
a(t)	Function introduced in equation (1-57)
A(w)	Function introduced in equation (1-32)
b(t)	Function introducedin equation (1-57)
B(w)	Function introducedin equation (1-32)
D	Constant introduced in equation (1-29)
f(T)	Function introduced in equation (1-33)
F(T,w)	Function introduced in equation (1-32)
g(T,w)	Function introduced in equation (1-38)
G	Gibbs's free energy
G	Absorptivity function defined in equation (1-47)
H	Enthalpy.
K	Equilibrium constant
L(T)	Latent heat of vaporization at temperature T
m	Mass
n	Number of adsorbed moles
p	Pressure
q_{st}	Isosteric heat of adsorption
r	Ideal gas constant for the adsorbate (R/Molar mass)
R	Universal ideal gas constant=8.314 (J/mol.K)
S	Entropy
t	varying parameters (for example time)
T	Temperature
	Volume

w	uptake (mass of adsorbed species per unit mass of adsorbent
X	Variable defined by equation (1-31)

Greek symbols:

Γ	Surface concentration
ε	Adsorption potential in section 1-2
	Porosity (or void fraction) in section 1-3
μ	Chemical potential
π	Spreading pressure defined in equation (1-10)
ρ	Mass density
θ	Degree of saturation of adsorbing surface

Subscripts:

a	Adsorbent
g	Gas phase
o	At reference state
p	at constant pressure
s	sorbed state or saturation
sp	specific
V	At constant volume

Superscript:

-	partial molar quantity
~	Integral quantity

REFERENCES

[1] Dini, S., "Analysis of Cross-Cooled Desiccant Cooling Systems", PhD Thesis, IIT Chicago, 1981.

[2] Osipow, L.I., "Surface Chemistry: Theory and industrial Applications", Reinhold Corp., N.Y., 1962.

[3] Barrer, R.M., "Zeolites and Clay Minerals as Sorbents and Molecular Sieves", Academic Press, 1978.

[4] Hiemenz, P.C., "Principles of Colloid and Surface Chemistry", Dekker Inc. , N.Y., 1977.

[5] Collier Engineering Services, "determination of Properties of Zeolite-Refrigerant Combinations for Solar Refrigeration Systems", Report to the US Department of Energy, 1986.

[7] Pons M. and Ph. Grenier, "A Phenomenological Adsorption Equilibrium Law extracted from Experimental and Theoretical Considerations Applied to Activated Carbon-Methanol Pair", to be published in Carbon, 1987.

[8] Guilleminot, J.J. and F. Meunier, "Etude Experimentale d'une glaciere solaire Utilisant le cycle zeolithe 13X-eau", Rev. Gen. Therm., No. 239, 825, 1981.

[9] Tchernev D.I., Private Communication.

[10] Tchernev D.I., "Closed-Cycle Regenerative Heat-Pump", Paper presented at at Desiccant Review Conference, Chattanova, Tennessee, June 1986.

[11] Gallant, R.W., "Physical Properties of Hydrocarbons", Gulf Publishing Co., 1974.

45

CHAPTER TWO

LITERATURE SURVEY ON THE USE OF ZEOLITES IN SOLAR ADSORPTION REFRIGERATION

2.1 INTRODUCTION

Sorption refrigeration is based on the property that some gases like H_2O , CO_2 and NH_3 are "pumped" by liquids or solids at low temperature and "released" at high temperature. This phenomena discovered since 1824 [7] was the subject of intensive research in the last 30 years . The energy crises and the development of solar technology served to renew the interest in these technologies. Several pairs sorbent-sorbate such as LiBr-H_2O, LiCl-H_2O ... etc were studied theoretically and prototypes were built to test the results of these models.

Adsorption (sorption by a solid) cooling was studied in recent years and presents the advantages of working without mobile parts and avoiding the difficult problem of crystallization which handicaps the liquid desiccant systems. The closed-cycle solid desiccant cooling systems are suited only for air- conditioning applications when water is used as refrigerant. But other fluids such as alcohols can be used to provide refrigeration at temperatures below freezing. These systems can be solar energy powered in which the adsober is incorporated to the solar collector.

The operating principle of adsorption cooling was described in the late 70's by Tchernev [3] and Meunier & al. [4]. These authors proved both on a thermodynamic basis and by building test prototypes the reliability of such systems. The adsorbents used are different types of microporous alumino-silicates also called

zeolites which are capable of adsorbing considerable amount of several refrigerant gases. A detailed description of the nature and use of zeolites, as well as the physics of solid sorption on these materials can be found in references [1-4]. In this Chapter we will recall the operating principle of adsorption cooling and review the thermodynamic analyses of such systems as well as the results of experimental studies obtained in this domain.

2.2 OPERATING PRINCIPLE OF ADSORPTION COOLING SYSTEMS

The principle of intermittent single effect cooling cycles using solid adsorption is described in detail in [3-6]. It is usually found convenient to represent such cycles in the (T, T_s) diagram where the isosters (lines of constant mass fraction of adsorbate w) approximately straight lines. Figure 2-1 shows the (T,T_s) diagram for the pair Zeolite 13X-H_2O [6] on which a cooling cycle is represented by the points a-b-c-d-a. This cycle is followed daily by a solar refrigerator in a periodic regime and consists of two operating modes (figure 2-2) :

- **Regeneration mode.** At the end of adsorption (point a), the collector is at temperature T_{ad} and the gas sorbate at pressure p_{ev} of the evaporator. As solar radiation heats up the system, the pressure of the gas phase increases and the one-way valve C_2 closes. When the pressure reaches p_{co} (point b) -the temperature of the collector is then T_{ss}-, the one-way valve C_1 opens and allows the condensation to begin and continue until the adsorbent is at its maximum temperature T_{re} (point c).

Adsorption mode. When the collector is cooled down at night, the pressure of gas adsorbate decreases and the valve C_1 closes. At the value p_{ev} of the pressure, the valve C_2 opens and the evaporation starts (point d). This phase of cooling production continues until the adsorbent is at its minimum temperature T_{ad} (point a).

3.2 THERMODYNAMIC ANALYSIS OF ADSORPTION COOLING SYSTEMS

3.2.1 First Law Analysis and Coefficient of Performance

To perform a thermodynamic analysis of an adsorption cooling machine, the following data are needed:

- Equilibrium isotherms for the pair adsorbent-adsorbate used
- Adsorption enthalpies and entropies as functions of T and w
- Physical properties (ρ, C_p, etc) of both the sorbent and the adsorbate as pure substances and in the adsorbed state.
- Data on the inert parts of the machine (heat capacity, efficiency, etc).
- The temperatures of the cycle which are:

  T_{ad} : temperature at the end of adsorption

  T_{ev} : temperature of the evaporator

  T_{co} : temperature of the condenser

  T_{re} : temperature at the end of regeneration

It is then possible to obtain the minimum value T_{ss} of T_{re} below which the cycle does not work. Assuming constant values of

the latent heat L and the isosteric heat of adsorption q_{st} and using Clapeyron-Clausius equations (1. 27) and (1.33), it is easy to obtain:

$$(1/T_{ss}) = (1/T_{ad}) - (L/q_{st})[(1/T_{ev}) - (1/T_{co})] \qquad (2.1)$$

The following heat quantites can also be calculated. If we designate by m_L the amount of cycled adsorbate , we have

$$m_L = M_a (w_{ab} - w_{cd}) \qquad (2.2)$$

The cooling effect: $$Q_L = L(T_{ev}) m_L \qquad (2.3)$$

The heat of regeneration : $$Q_{ad} = \int_{T_{ss}}^{T_{re}} q_{st} (T,w) \, dm_L \qquad (2.4)$$

Sensible heat to bring the condensate from T_{co} to T_{ev} :

$$Q_1 = m_L \int_{T_{ev}}^{T_{co}} C_L (T) \, dT \qquad (2.5)$$

Sensible heat needed to bring the collector from point a to b:

$$Q_{sen} = \int_{T_{ss}}^{T_{re}} (M_c C_c + M_a C_a + w_{ab} M_a C_s) \, dT \qquad (2.6)$$

Sensible heat needed to bring the collector from point b to c :

$$Q_r = \int_{T_{ss}}^{T_{re}} (M_c C_c + M_a C_a + w M_a C_s) \, dT \qquad (2.7)$$

The coefficient of performance of the machine is defined as follows:

$$COP = (Q_L - Q_1)/(Q_{ad} + Q_s + Q_r) \qquad (2.8)$$

Figure 2-3 [6] shows the typical curve COP vs T_{re} . In this figure C_0 is the COP of an ideal trithermal machine operating between T_{re} ,T_{ad}

and T_{ev} ,i.e. $[T_{ev}(T_{re}-T_{ad})]/[T_{re}(T_{ad}-T_{ev})]$. C_o' is the COP of an ideal quadrithermal cycle operating between T_{re} , T_{ss} , T_{co} and T_{ev} , i.e. $[(1/T_{re})-(1/T_{ss})]/[(1/T_{co})-(1/T_{ev})]$. C_1 is the COP obtained by neglecting the collector thermal capacity and a solar efficiency of unity. C_2 is the COP ontained by taking into account the thermal capacity of the collector but still an efficiency of 1. Finally the curves S and V are obtained by taking the efficiency of the collector into account. The letters P, S and V refer to a simple plane collector, a collector with selective surface and an evacuated collector respectively.

It is evident that when the efficiency of the solar collector is taken into account, the COP reaches a maximum value of about 0.25-0.38 at a certain optimum value of T_{re} before declining. Equation (2.8) shows that the COP depends on the operating temperatures, the properties of the pair adsorbent-adsorbate used and the efficiency of the solar collector. A comparison of several pairs by Guilleminot & al. [6] proved that no pair is appropriate for all applications. In particular they found that the pair Activated Al-H_2O is more efficient for air-conditioning with a water cooled condenser whereas Zeolite 13X-H_2O is better with an air-cooled condenser. The use of other refrigerants such as methanol instead of water permits evaporator temperatures below freezing and decreases the value of T_s (which is favorable to COP) but the overall COP with the Zeolite 13X-Water pair is larger than with Zeolite 13X-Methanol. The effect of the solar collector was also found to be very important: at low values of the difference

$(T_{co}-T_{ev})$, the use of a plane collector is sufficient whereas at large values of this parameter, it is necessary to use a more efficient collector at high temperatures.

Chang and Roux [8] confirmed the above observations about the factors influencing the COP. They also showed that the slope of the isosters in $\log(p_s)$ vs $1/T$ diagram (which as seen in Chapter 1 determines the heat of adsorption) has competing effects on the COP. A large value of the slope decreases T_s and therefore T_{re} allowing high efficiency of the collector . But at the same time the efficiency of the cooling cycle is decreased thus lowering the overall COP of the machine.

As a mean of reducing the heat losses, Guilleminot & al. [6] proposed the possibility of recovering the sensible heat used during the regeneration phase. A fluid is heated up by circulation throught the hot collector and can be used for domestic purposes.

3.3.2 <u>Second Law Analysis of Adsorption Cycles</u>. An other representation of adsorption cycles was adopted by Dahome & Meunier [14]: They plotted the entropy of the working fluid (water in their case) versus its temperature as it follows the cycle (figure 2-4). The entropy in the adsorbed phase was calculated from the heat of adsorption q_{st} as follows:

$$S = S(T_1 , p_1) + q_{st} (T_1 ,p_1)/T \qquad (2.9)$$

The COP was defined by:

$$COP=(Q_{4-5} + Q_{5-6})/(Q_{8-1} + Q_{1-2}) \qquad (2\text{-}10)$$

The heat quantities Q's are defined by:

$$Q_{4-5} = \int_{T_2}^{T_4} C\ (T)\, dT \qquad (2\text{-}11)$$

$$Q_{5-6} = L(T_4) \qquad (2\text{-}12)$$

$$Q_{8-1} = \int_{T_3}^{T_1} C_s\,(T)\, dT \qquad (2\text{-}13)$$

$$Q_{1-2} = H_2 - H_1 = q_{st}\,(T_1\,,\, p_1) \qquad (2\text{-}14)$$

The authors compared the actual adsorption cycle to an ideal quadri -thermal cycle operating between T_1, T_2, T_3 and T_4 and found that they are close but not identical. This result gives credit to the analysis of section 2.3.1 and comfirms that adsorption cycles are suitable to energy storage, cooling and heat transforming processes.The influence of internal irreversibilities was also examined in terms of "discontinuities" of the pressure and the temperature at the interfaces of phase change. The results how that irreversibilities have little effect on the COP but cause a significant drop of the ratio COP/COP_{ideal} and an important loss of available energy ("noncompensated energy").

2.4 EXPERIMENTAL RESULTS

Tchernev [3] presented experimental efficiencies of solar energy powered adsorption refrigerators using natural zeolites Zeosorb 3.5A and 5.0A as adsorbents. His results given in figure 2-5 show a maximum value of the efficiency of about 0.40-0.45 reached around 75° C temperature. The shape of the efficiency curve is similar to the theoretical curve of figure 2-3a except

at low temperatures of desorption. The Dubinin approach discussed in Chapter 1 and known to be inadequate at the limits $\theta \approx 0$ and $\theta \approx 1$ which is used by the theoretical investigators is probably the cause of this discrepancy. It is also evident from figure 2-5 that the pair Zeosorb 5.0-H_2O exhibits a large maximum efficiency (at about T=80°C) whereas the pair Zeosorb 3.5A-H_2O has a better efficiency at lower adsorption T_{ad} between 50 and 70°C.

Guilleminot and Meunier [9] tested a refrigerator using the pair Zeolite 13X-H_2O. Their results given in figure 2-6 show a clear difference between the calculated and the measured temperatures of the upper and lower plates of the collector-adsorber. This lead the authors to define an apparent adsorption temperature T_z which agrees with the theoretical analysis. However the experimental COP of about 0.44 is well predicted by the relatively simple theory presented in section 2.2. This demonstrates the little effect of the irreversibilities due to heat and mass transfer which are neglected in the theory of this type of experiments which are characterized by a slow periodidity and a favorable integration of the adsorber into the collector.

Adell [3] gave experimental results obtained with the pair Zeolite 13X-H_2O. He found a solar COP of about 0.08-0.09 (all losses included). His exergy analysis which neglects some causes of irreversibilities such as mass diffusion and temperature gradients in the zeolite gave a COP of 0.95.

2.5 OTHER STUDIES

The discrepancies between the theoretical value of the COP obtained from the exergy analysis and the experimental COP lead normally Adell [11] to consider the non-uniformity of the temperature in the adsorber. An analytic model was developed assuming the dependency T=T(z,t) where z is the coordinate normal to the adsorbent layer and other simplifying approximations. The model was used to predict the heat diffusivity of the "mixture" zeolite 13X -adsorbed water and the " apparent diffusivity" during during desorption. Fair agreement with the experimental profiles of temperature was obtained but the model predicts a value for a parameter defined in a linearized representation of equilibrium data which is much larger than its experimental value.

Monnier and Dupont [10] used a finite difference scheme to solve the equation of transient heat and mass transfer. Their calculation assumed as in [13] variations of temperature in the z-direction only. Their results seemed to correlate well the measured temperature profiles only in the first hours of the desorption phase. An interesting finding of their study was the existence of an optimum zeolite thickness (4cm in their case) for which the COP is maximum.

Adell [12] presented a theoretical investigation of a possible application of adsorption cooling in agriculture in tropical regions. He showed in particular how the daily periodic change in temperature can be controlled to allow better conditions for the plants using a very simple technology. This study predicted a COP of about 0.15.

2.6 THE CONCEPT OF REGENERATIVE HEAT EXCHANGE APPLIED TO ADSORPTION SYSTEMS

The systems described above are all based on single effect intermit-cycles. These systems are characterized by COP's less than 1 (as small as 0.1 for the solar COP). Tchernev [16] used the idea of a regenerative heat to recover the heat generated during adsorption phase and the sensible heat stored in the zeolite container as a mean to increase the COP . His system consists of two zeolite containers working alternativeiy in adsorption and desorption mode. An appropriate choice of the period of each mode allows recycling of most the energy used in desorption phase. In addition, the two-container machine provides continuous cooling (or heating in the case of a heat pump). A most detailed description of Tchernev's system along with a mathematical model for its analysis will be presented in Chapter 4. A schematic representation of this system is given in figure 4-1. The author claims a potential increase of the COP to about 2.0. Note that Tchernev's system does not use solar energy as heat source therfore the increase of COP has to be compared with the value of about 0.6 obtained with single container machines when the efficieny of the solar collector is equal to unity.

A prototype was tested and an experimental cooling COP of 1.2 obtained (figure 2-7a). Another important result of Tchernev's tests was confirming the weak dependency of the system performance on the condenser temperature· which demonstrates the possibility of using air cooled condensers even in hot weather conditions (figure 2-7b). The pair used in the tests was Zeolite 13X-H_2O.

Tchernev [16] indicated the major lack of information on zeolite physical properties as well as on heat and mass transfer in regenerators with non-linear temperature dependency of the thermal properties and equilibrium relationships. A first attempt was made by the author and partial results of his unpublished analysis are shown in figure 2-8.

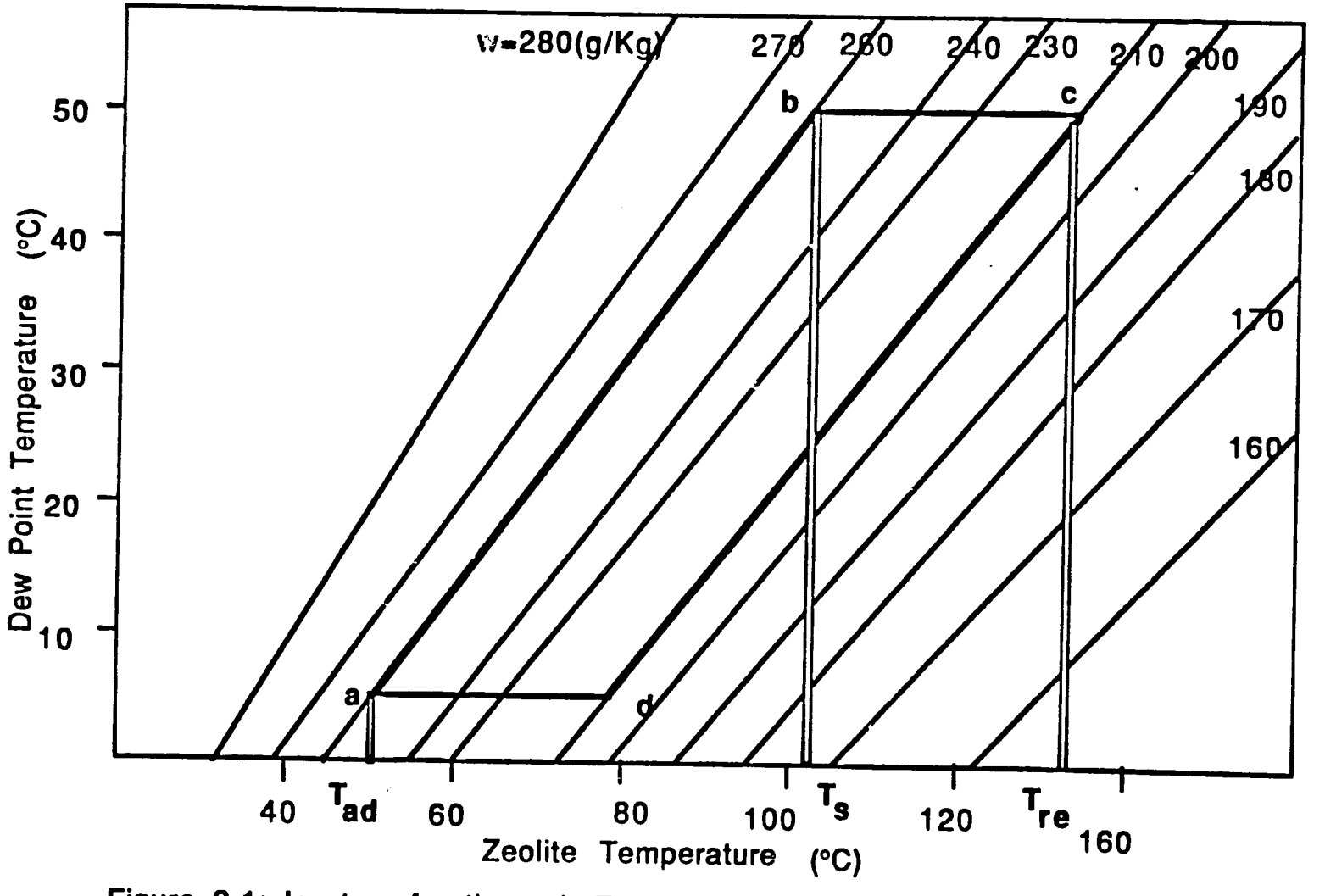

Figure 2-1: Isosters for the pair Zeolite 13X-water . Representation of an adsorption cycle.

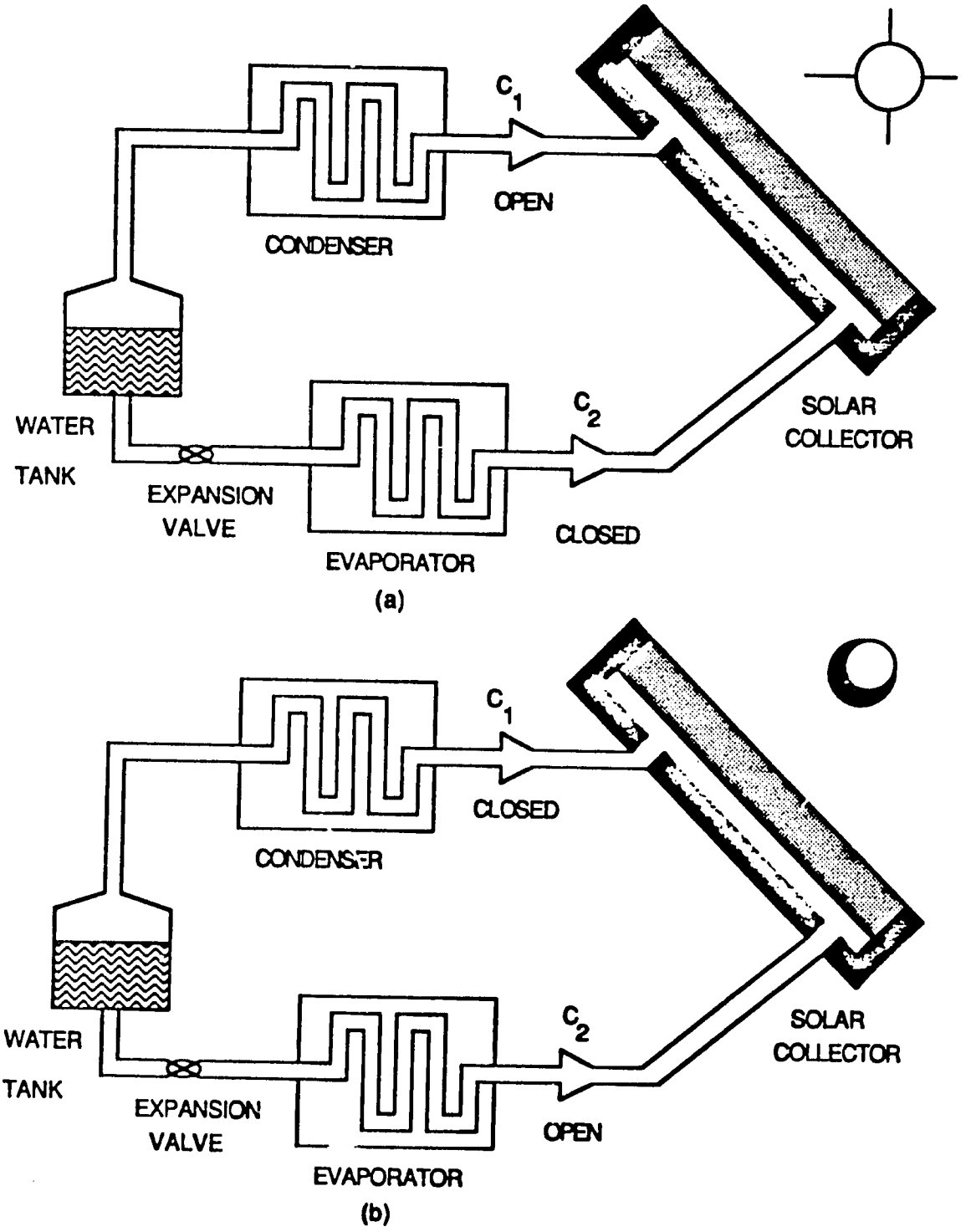

Figure 2-2: The two operating modes of a solar adsorption refrigerator. (a) Adsorption, (b) Desorption.

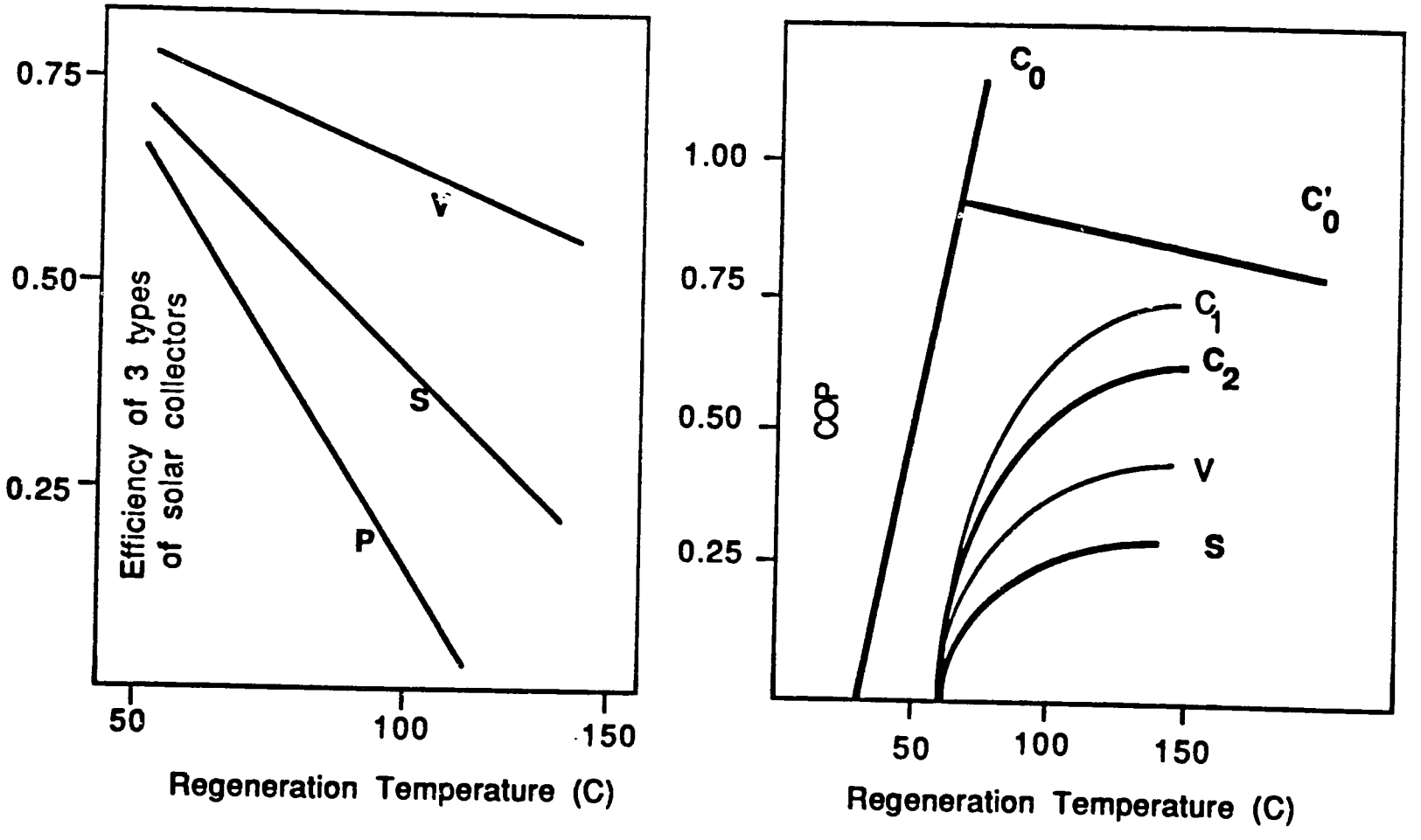

Figure 2-3: Typical curves COP vs T_{re} [6] .

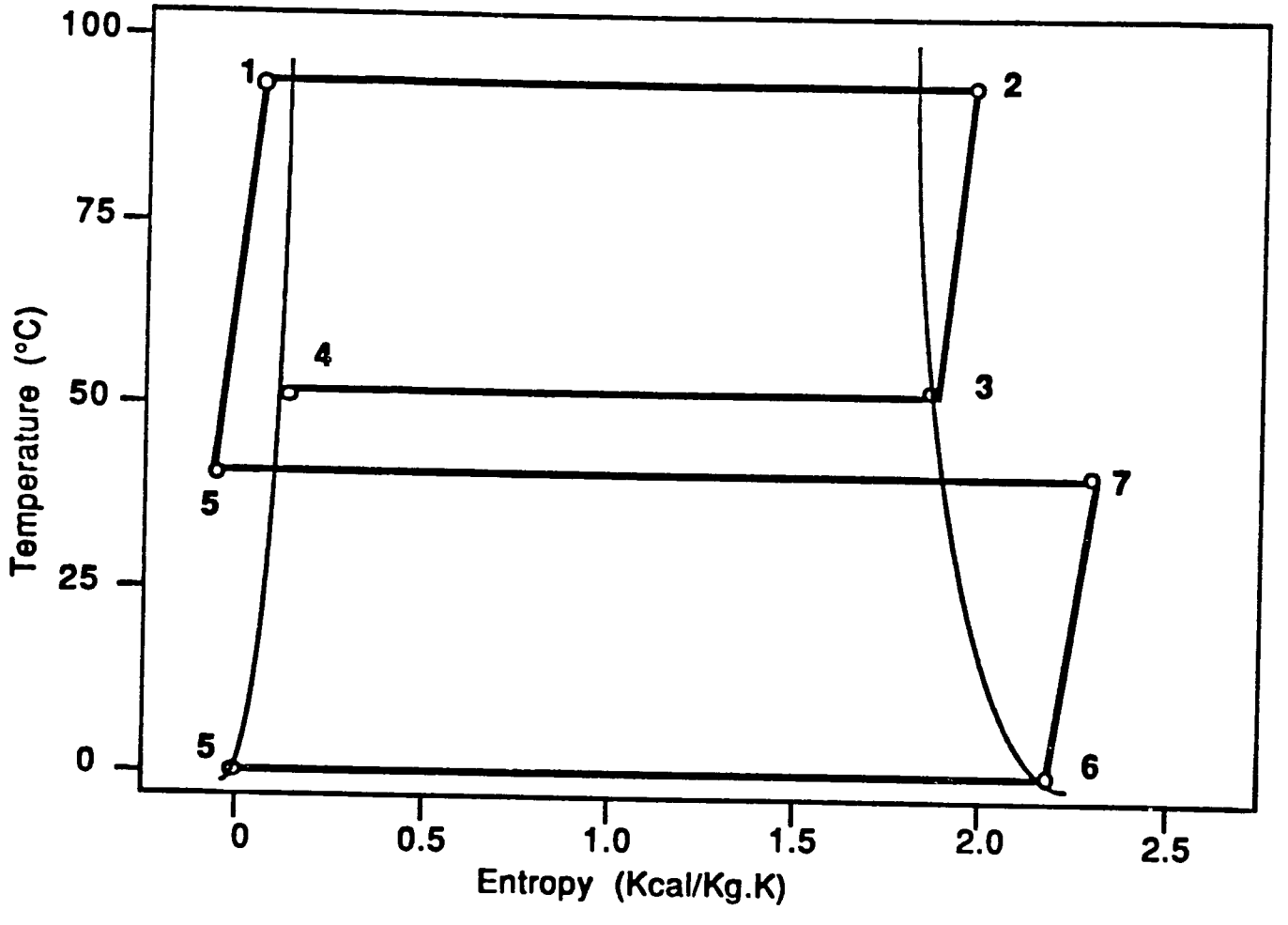

Figure 2-4: Representation of an adsorption cycle on the entropy diagram (ref.[14]).

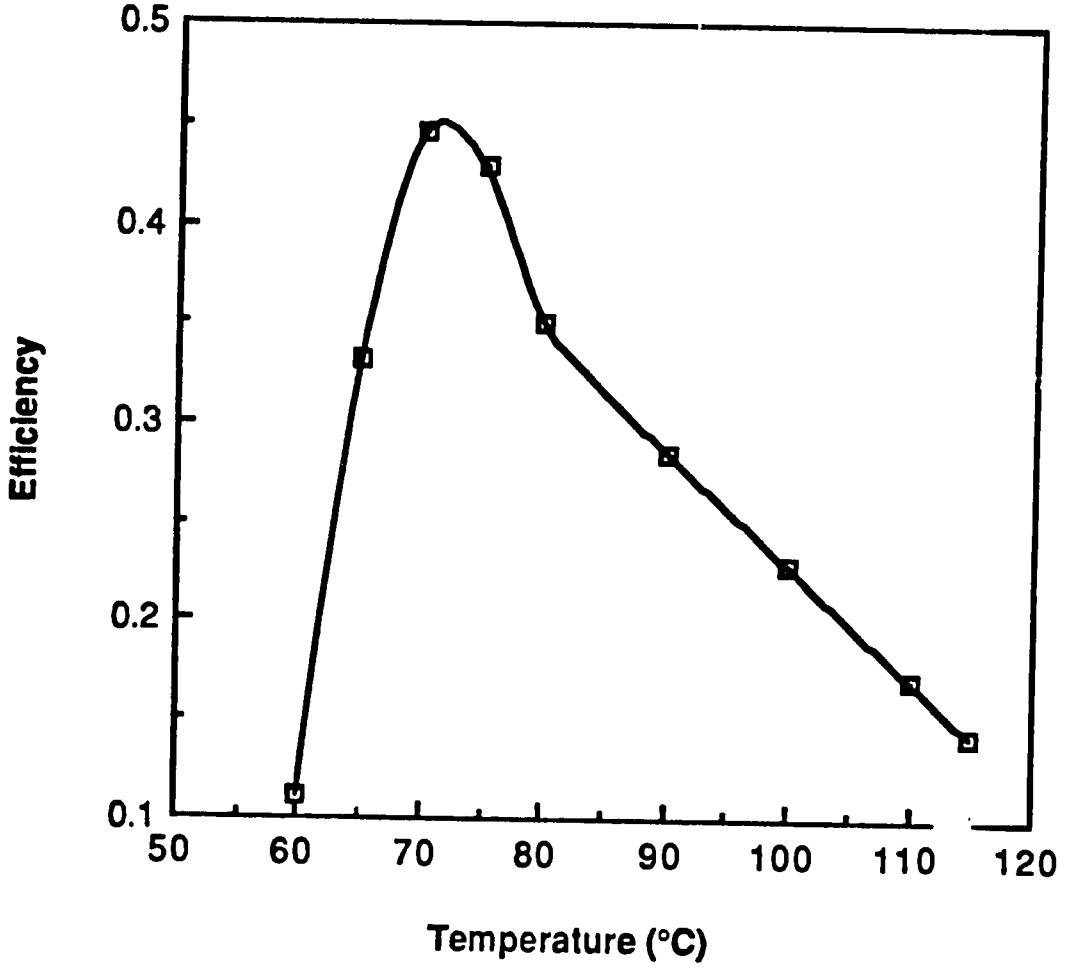

Figure 2-5a: Cooling Efficiency for Zeosorb 5.0A with input power density of 1 Kw/m2 [3].

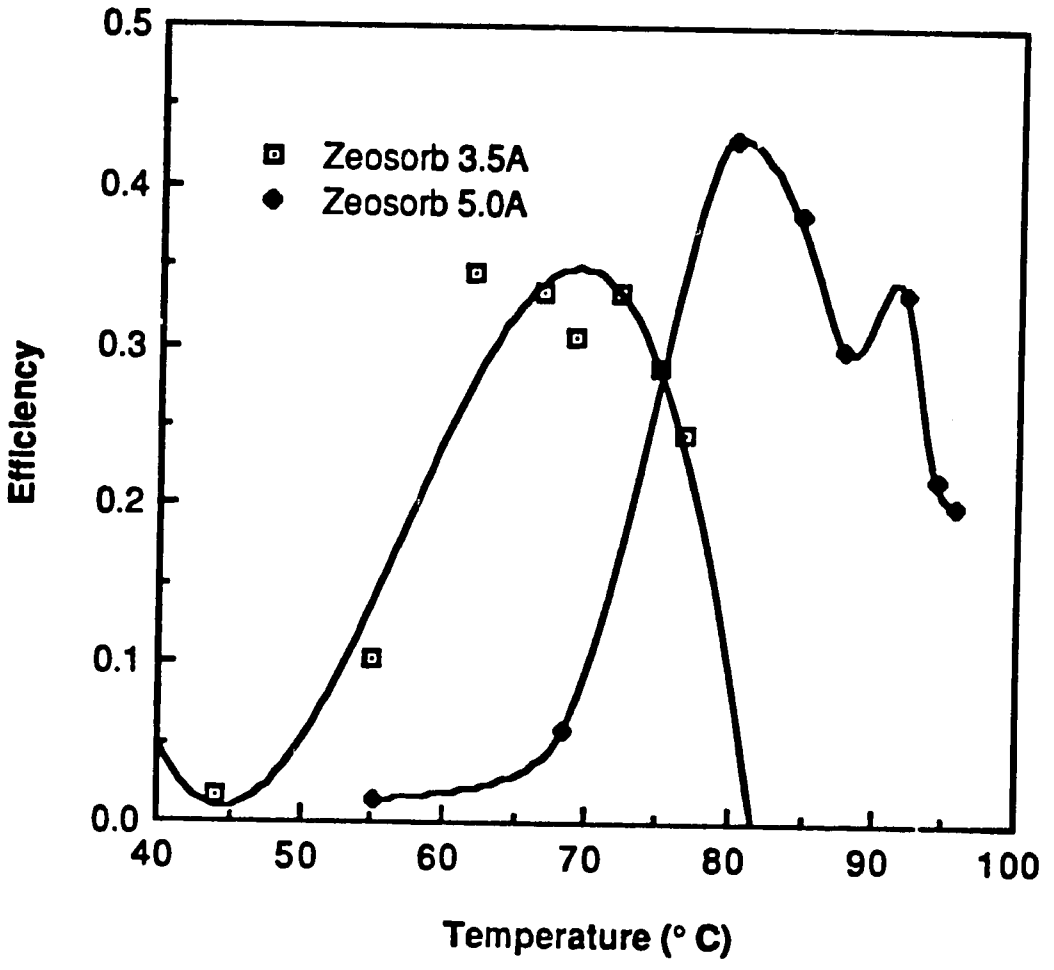

Figure 2-5b : Experimental efficiencies for the pairs Zeosorb 5.0A-water and Zeosorb 3.5A-water with solar heat .

Solar Time	Upper Plate Temperature	Lower Plate Temperature	T^*_z	COP1	COP2
11.30-12	89	70	65	0.43	0.096
12 - 13	97	78	75	0.48	0.23
13 - 14	104	85	82	0.52	0.32
14 - 15	110	92	87	0.52	0.36
15 - 16	108	98	91	0.48	0.39
16 - 17	107	104	94	0.52	0.40
17 - 18	100	101	95	0.52	0.41

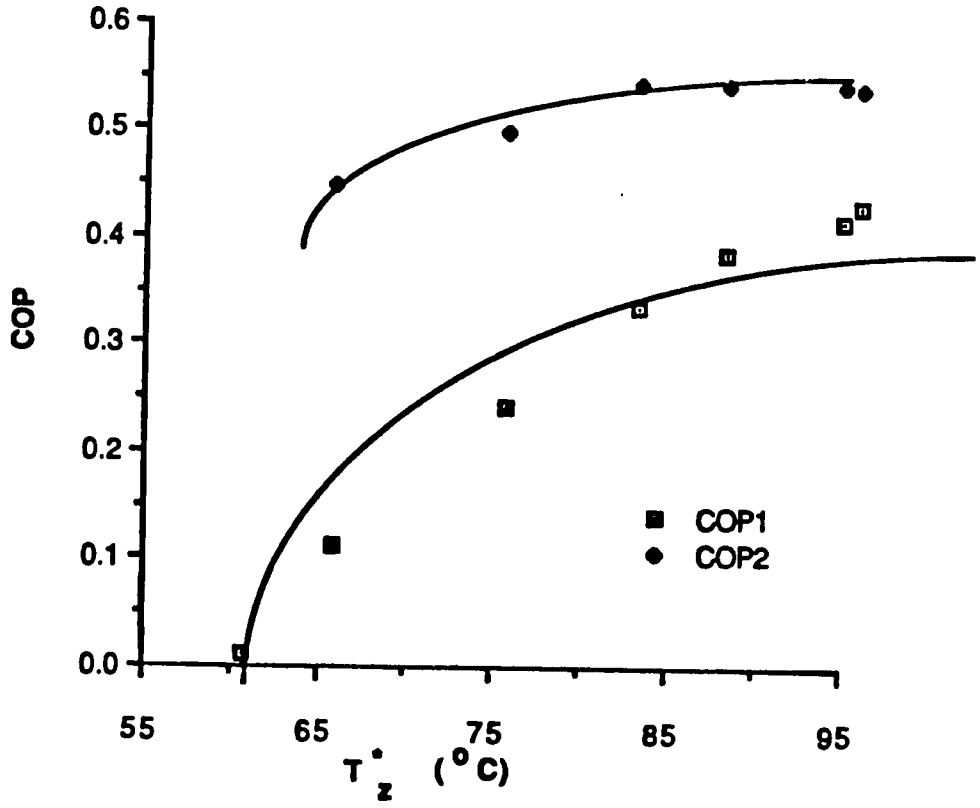

Figure 2-6 · Experimental upper and lower plate temperature T^*_z (apparent zeolite temperature) and the COP. COP1 & COP 2 are the instantaneous and the cumulative COP.

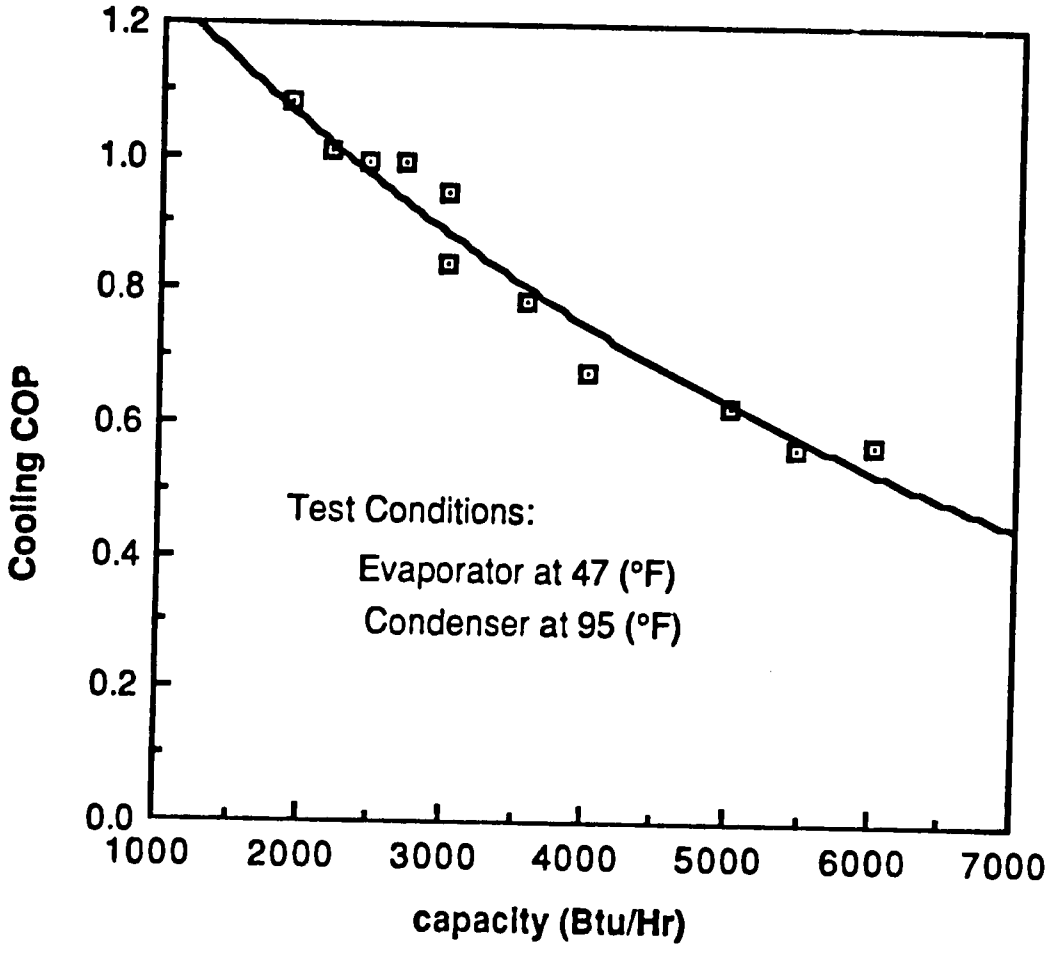

Figure 2-7a: Experimental cooling COP vs Capacity [16].

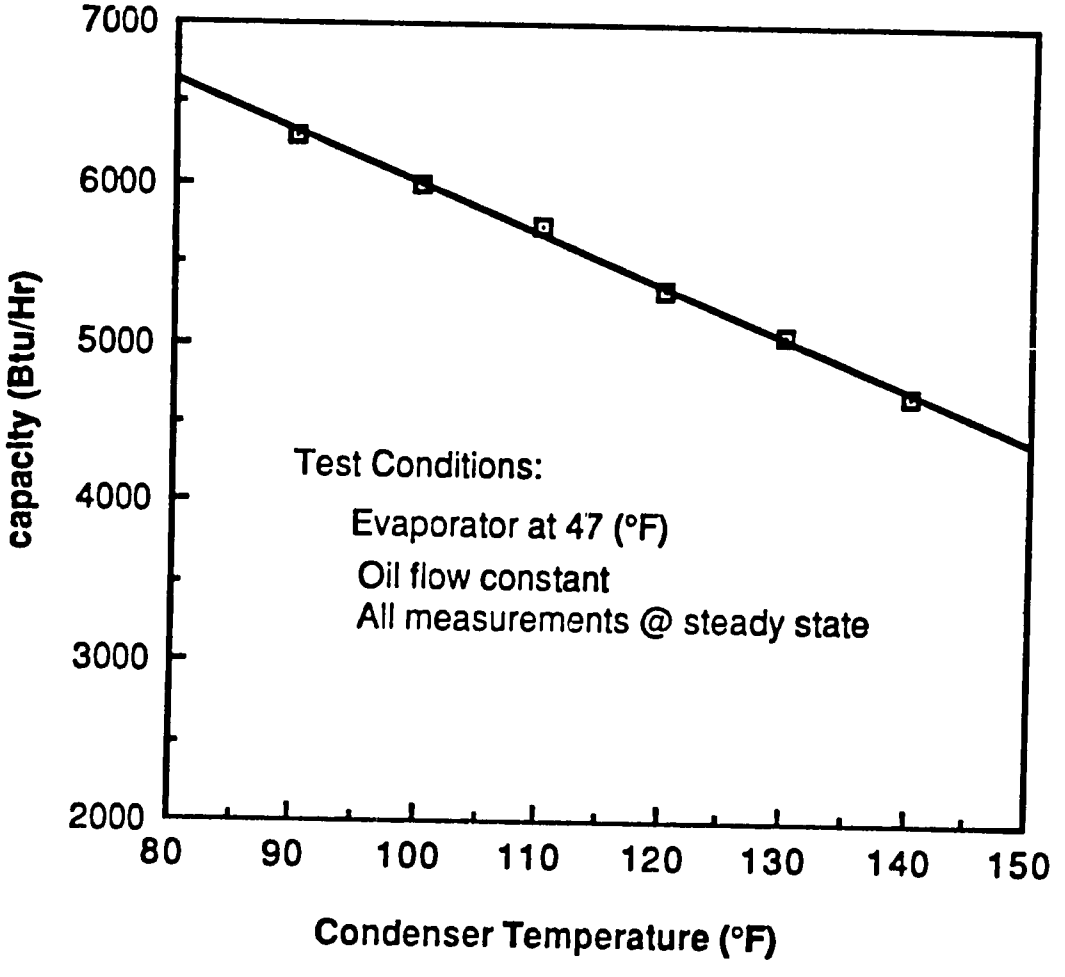

Figure 2-7b: Capacity as function of condenser temperature [16].

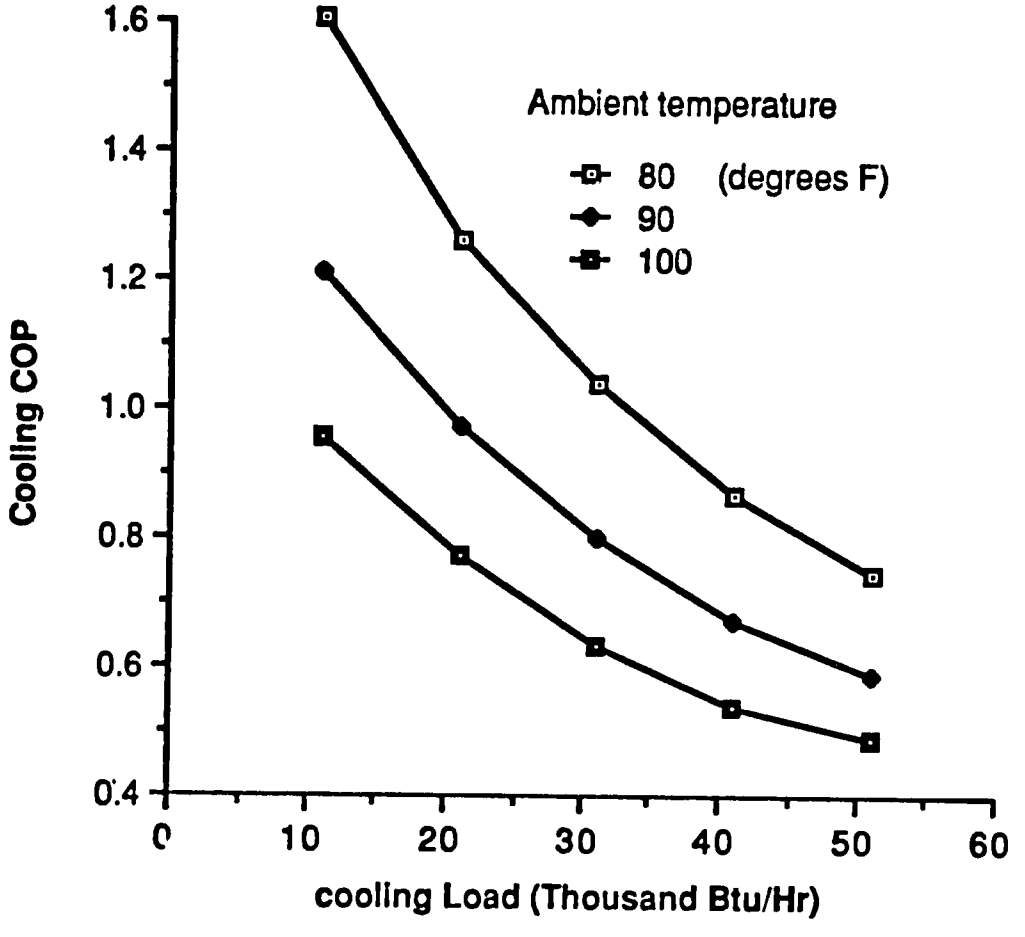

Figure 2-6 Simulation results giving COP vs the cooling load [16].

CHAPTER III
DYNAMIC ANALYSIS OF THE SOLAR COLLECOR IN A CLOSED-CYCLE ADSORPTION REFRIGERATOR

3-1 INTRODUCTION

The critical component of a closed-cycle adsorption refrigerator is the collector. The latter accomplishes the combined functions of receiving solar energy and regenerating the adsorbent material. Previous analyses of closed-cycle machines considered only an idealized cycle on the (T_s,T) diagram [1,2,3]. Although this type of analysis reasonably predicts the system performance in terms of its COP, it does not allow the study of the effect of design parameters and weather conditions. Thus, a dynamic analysis of a real system is useful from the view point of design optimization and also gives more insight in the sorption mechanisms in such systems.

The analysis of solar collectors in general presents unique problems of changing ambient temperature, wind conditions and solar radiation [4]. Besides these problems, an adsorbing collector adds the difficulty associated with adsorption phenomena. Given this complexity, several simplifying assumptions are made in this study:

1. The adsorbent is always assumed to be at thermodynamic equilibrium, i.e., the moisture content w, the temperature T and the pressure of the vapor phase p are related by:

$$T_s(p) = F(T,w) \tag{3-1}$$

This assumption seems reasonable since the system operates on a daily cycle (long time periodicity).

2. The temperature is uniform across the collector. Although it is known that temperature gradients exist [5,6], this assumption is not expected to significantly affect the results of this analysis.

3. The values of specific heats are constant and the specific heat of adsorbed species is taken equal that of the bulk liquid adsorbate.

3-2 THE GOVERNING EQUATIONS

We assume the adsorbent material and the inert parts of the collector to be at a uniform temperature T and the glass cover at T_g. The geometry and design data of the collector are shown in figure 3-1.Two differential equations are derived by writing the energy balances for a unit area of the collector. For the adsorbent, the fraction $(\tau\alpha)_e$ of the incident solar flux $\mathcal{I}$ is transformed into:

- sensible heat
- heat of desorption
- heat lost by convection and radiation to the glass cover.

The energy balance is expressed as follows:

$$(\tau\alpha)_e \mathcal{I} = (M_c C_c + M_a C_a + w M_a C_s)(dT/dt) - q_{st}(T,w)(dw/dt) + (h_{r,a-g} + h_{c,a-g})(T - T_g) \qquad (3\text{-}2)$$

For the glass cover, the inlet energy increase is the sum of the absorbed solar flux and the net heat gain by convection and radiation from the adsorbent and ambient air. Therefore we obtain:

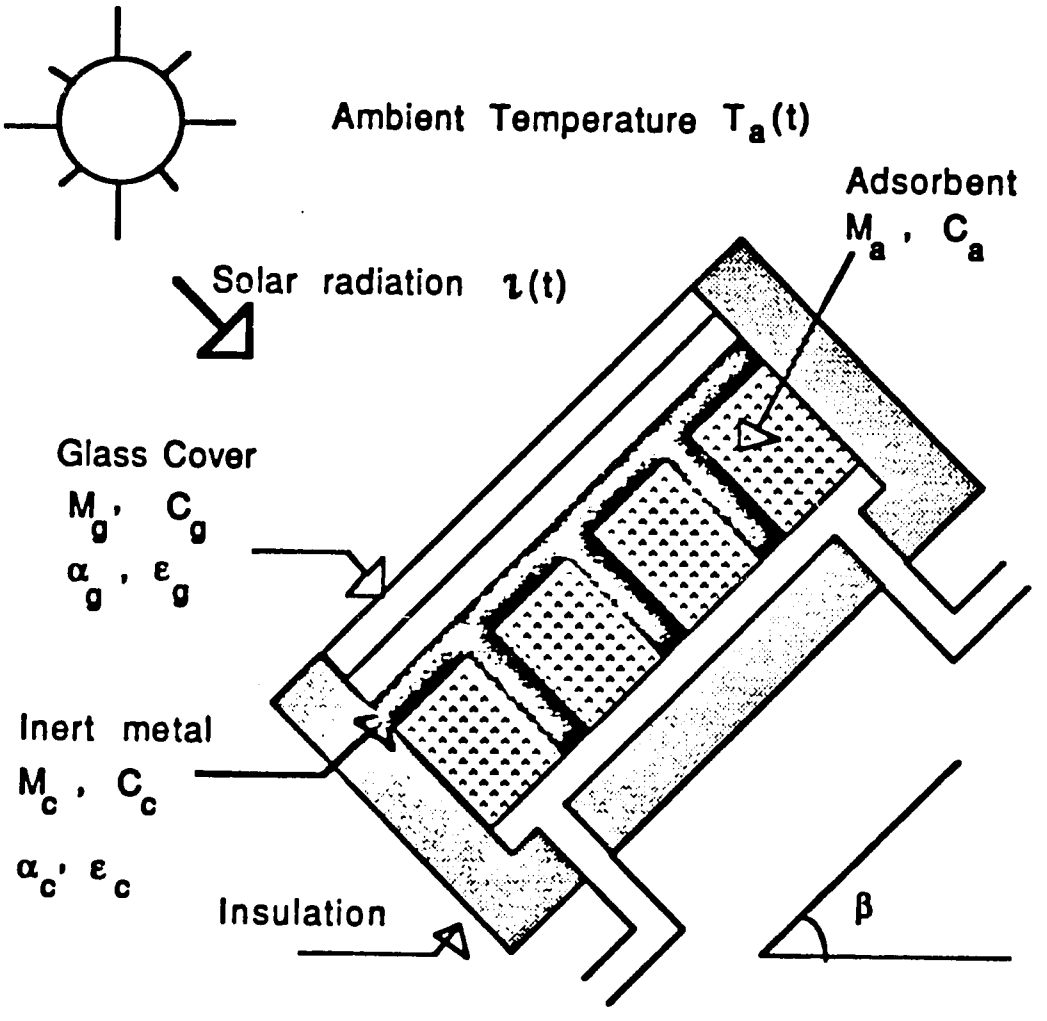

Figure 3-1 : Geometry and design data of the solar collector in an adsorption cooling system.

$$\alpha_g \mathcal{I} + (h_{r,a-g} + h_{c,a-g})(T - T_g) = M_g C_g (dT_g/dt) + (h_{r,g-\infty} + h_{c,g-\infty})(T_g - T_\infty) \quad (3\text{-}3)$$

Equation (3-1) can be modified to eliminate the term (dw/dt) by introducing the function **G** introduced in Chapter I which satisfies:

$$dw = \mathbf{G}(T,w)\, dT \quad (3\text{-}4)$$

Equations (3-2) and (3-3) can be rewritten in a more convenient form for numerical solution as follows:

$$\frac{dT}{dt} = \frac{(\alpha\tau)_e \mathcal{I} - (h_{r,a-g} + h_{c,a-g})(T - T_g)}{M_a (C_a + wC_s) + M_c C_c - q_{st} M_a \mathbf{G}(T,w)} \quad (3\text{-}2')$$

$$\frac{dT_g}{dt} = \frac{\alpha_g \mathcal{I} + (h_{r,a-g} + h_{c,a-g})(T - T_g) - (h_{r,g-\infty} + h_{c,g-\infty})(T_g - T_\infty)}{M_g C_g} \quad (3\text{-}3')$$

Expressions of the function **G** and the relations describing the phases of an adsorption cycle are derived in Chapter 1. We recall here the formulas obtained for uniform conditions:

During a constant-volume process:

$$\frac{L_o}{R\, T_s(t)} + \mathrm{Ln}\left\{ \frac{T(t)\left\{ \frac{m_v(0)}{\rho_a \nu_a} - [\, w(t) - w(0)\,] \right\}}{[T_s(t)]^{a_L / R}} \right\} = \mathrm{Const} \quad (3\text{-}4)$$

$$G_v = \frac{-\left(\frac{\partial F}{\partial T}\right)_w + \frac{R}{L(T_s)} \frac{F^2(T,w)}{T}}{\left(\frac{\partial F}{\partial w}\right)_T + \frac{R}{L(T_s)} \frac{F^2(T,w)}{\frac{m_v(0)}{\rho_a \nu_a} - [w(t) - w(0)]}} \tag{3-5}$$

During a constant-pressure phase we have:

$$T_s = \text{Constant} \tag{3-6}$$

$$G_p = -A(w) / [A'(w)\ T + B'(w)] \tag{3-7}$$

3-2 NONDIMENSIONLIZATION OF THE GOVERNING EQUATIONS

The important parameters influencing the performance of a solar adsorption refrigerator are better seen in the dimensionless form of the governing equations. This form is obtained after introducing the following parameters and functions:

$\eta = t / t_o$

$E_o = M_c C_c / M_a C_a$, $E_1 = C_s / C_a$, $E_2 = M_g C_g / M_a C_a$

$E_3 = L_o / C_a (T_{re} - T_{ad})$, $E_4 = h_o A t_o / M_a C_a$, $E_5 = r T_{ad} \rho_a / \varepsilon p_{ev}$

$E_6 = T_{re} / T_{ad}$, $E_7 = p_{co} / p_{ev}$, $E_8 = T_{co} / T_{ev}$, $E_9 = T_{co} / T_{ad}$

$E_{10} = L_o / r T_{ev}$, $E_{11} = C_L / C_a$, $E_{12} = \mathcal{I}_o A t_o / [M_a C_a (T_{re} - T_{ad})]$

$\theta = (T - T_{ad}) / (T_{re} - T_{ad})$, $\theta_g = (T_g - T_{ad}) / (T_{re} - T_{ad})$

$\theta_\infty = (T_\infty - T_{ad}) / (T_{re} - T_{ad})$, $I(\eta) = \mathcal{I}(t) / \mathcal{I}_o$

$\theta_s = (T_s - T_{ev}) / (T_{co} - T_{ev})$ $\Phi(\theta, w) = (F(T,w) - T_{ev}) / (T_{co} - T_{ev})$

$\varphi(\theta,w)=q_{st}(T,w)/L_o$, $\lambda(\theta_v)=L(T_v)/L_o$, $\gamma(\theta,w)= G(T,w)/(T_{re}-T_{ad})$

where t_o, h_o, L_o and G_o are characteristic values of t, h, L and G respectively. The governing equations therefore become:

$$\frac{d\theta}{d\eta} = \frac{E_{12}(\alpha\tau)_e I(\eta) - E_4 h^*_{a-g} (\theta - \theta_g)}{1+E_o + E_1 w - E_3 \varphi(\theta,w)\Gamma(\theta,w)} \qquad (3\text{-}2^{**})$$

$$\frac{d\theta_g}{d\eta} = \frac{E_{12}(\tau)_g I(\eta) + E_4[h^*_{a-g} (\theta - \theta_g) - h^*_{g-\infty} (\theta_g - \theta_\infty)]}{E_2} \qquad (3\text{-}3^{**})$$

$$w = w_o + \mu_o \left\{ 1 - \frac{[(E_8-1)\theta_s + 1]^\beta}{[(E_6-1)\theta+1]} \frac{1}{C} \exp\left[-\frac{E_{10}}{[E_8-1)\theta_s+1]}\right] \right\} \qquad (3\text{-}4^{**})$$

where C and μ_o are defined by:

$$C = \frac{[(E_8-1)\theta_{so}+1]^\beta}{[(E_6-1)\theta_o+1]} \exp\left[-\frac{E_{10}}{[E_8-1)\theta_{so}+1]}\right]$$

$$\mu_o = \frac{T_{ad}}{T} \frac{p_o}{p_{ev}} \frac{1}{E_5}$$

3-3 METHOD OF NUMERICAL SOLUTION

The first order nonlinear differential equations (3-2,3) can be solved using the following explicit scheme:

$\theta_{,o}=0$ $\qquad$ $\theta_{g,o}=0$ $\qquad$ $\theta_{s,o}=0$

$$\theta_{,n+1} = \theta_{,n} + \frac{E_{12}(\alpha\tau)_e I_n - E_4 h^*_{z-g} (\theta_{,n} - \theta_{g,n})}{1+E_o + E_1 w - E_3 \varphi(\theta_n, w_n)\Gamma(\theta_n, w_n)} \Delta\eta$$

$$\theta_{g,n+1} = \theta_{g,n} + \frac{E_{12}(\tau)_g I_n + E_4[h^*_{a-g} (\theta - \theta_g) - h^*_{g-\infty} (\theta_{g,n} - \theta_{\infty,n})]}{E_2} \Delta\eta$$

W_{n+1} and $\theta_{s,n+1}$ are obtained differently depending on whether $\theta_s<1$ ($T_s<T_{co}$,constant volume phase) or $\theta_s=0,1$ ($T_s=T_{co}$, T_{ev} constant pressure phase):

If $\theta_s<1$, $\theta_{s,n+1}$ and w_{n+1} are solved using the following iterative procedure: - First a value of w_{n+1} is guessed (say w_n).

- Equation (3-1) gives $\theta_{s,n+1}=\Phi(\theta_{,n+1},w_{n+1})$
- Equation (3-4'') gives a corrected value of w_{n+1}:

$$w_{n+1} = w_o + \mu_o \left\{1 - \frac{[(E_8-1)\theta_{s,n+1}+1]^{\beta}}{[(E_6-1)\theta_{,n+1}+1]} \frac{1}{C} \exp\left[-\frac{E_{10}}{[E_8-1)\theta_{s,n+1}+1]}\right]\right\}$$

- This new value of w_{n+1} is compared to the previous one and iterations are continued until w converges. Once θ_s reaches the value 1, it remains constant for the remaining portion of the process. The quilibrium equation (3-1) is then used to determine w_{n+1} for a known $\theta_{,n+1}$.

3-4 CORRELATIONS FOR HEAT TRANSFER COEFFICIENTS

3-4-1 Natural Convection Between the Collector Plate and the Glass Cover:

It is known from hydrodynamic stability that free convection occurs at a certain critical value of Rayleigh Number of about 1708. Below this value, the heat transfer is by conduction. Thus:

$$Nu_L = 1 \qquad (Ra_L < 1708)$$

For larger values of Ra_L, the following relation due to Hollands et al. [8] is widely used:

$$Nu_L = 1 + 1.44\left(1 - \frac{1708}{Ra_L \cos\beta}\right)^* \left[1 - \frac{1708(\sin\beta)^{1.6}}{Ra_L \cos\beta}\right] + \left(\frac{Ra_L \cos\beta}{5830} - 1\right)^* \qquad (3\text{-}8)$$

The symbol (*) means that if the term between brackets is negative, it should be taken equal to zero. This formula is valid for large aspect ratios ((H/L)>12) and for $0<\beta<70°$. These ranges adequately cover the actual operating conditions for solar collectors. Other formulas are reported by Incropera [9] for the other ranges of inclination angle and aspect ratio.

3-4-2 Natural Convection Between a Heated Plate and Ambient Air:

3-4-2-1 Natural Convection Heat Transfer: In absence of wind, only natural convection should be considered for heat transfer between the plate and ambient air. Although the horizontal and vertical plate configurations were extensively studied, there are

few results for intermediate inclinations. For a horizontal plate, Lloyd and Moran [7] suggest:

$$Nu_L^* = 0.76\ Ra^{0.25} \qquad \text{for} \quad 2.6\times10^4 < Ra_L^* < 10^7 \qquad (3\text{-}9a)$$

$$Nu_L^* = 0.15\ Ra^{1/3} \qquad \text{for} \quad 10^7 < Ra_L^* < 10^{11} \qquad (3\text{-}9b)$$

where $L^* = 4(\text{area})/\text{perimeter}$.

For a vertical plate, the following relationship suggested by Churchil and Lou [10] has the advantage of representing the data in the entire range of Ra:

$$Nu_L = \left\{ 0.825 + \frac{0.387\ Ra_L^{1/6}}{\left[\ 1+(0.492/Pr)^{9/16}\ \right]^{8/27}} \right\}^2 \qquad (3\text{-}10)$$

For the intermediate inclinations, Churchil and Lou suggested that the above formula be used for $30 < \beta < 90°$ and $Ra_L > 10^9$. For Ra_L less than 10^9 they gave the following expression:

$$Nu_L = 0.68 + \frac{0.67\ (Ra_L\ \sin\beta)^{1/4}}{\left[\ 1+(0.492/Pr)^{9/16}\ \right]^{8/27}} \qquad (3\text{-}11)$$

For small angles of inclination, no correlation could be found. However in the case of turbulent natural convection, the inclination has little effect, therefore the horizontal plate formula can be used. For the case of smaller Ra we expect a fair result from the same formula after Ra is replaced by Ra cosβ. The above discussion can be summarized in the following table in which All properties are evaluated at the film temperature $T_f=(T_g+T_\infty)/2$.

$0 < \beta < 30°$	$2.4 \times 10^4 < Ra_L^* < 10^7$ $\quad Nu_L^* = 0.76\,(Ra_L^* \cos\beta)^{1/4}$ $10^7 < Ra_L^* < 10^{11}$ $\quad Nu_L^* = 0.15\,(Ra_L^*)^{1/3}$ where $L^* = A/P$
$30 < \beta < 90°$	$Ra_L < 10^9$ $\quad Nu_L = 0.68 + \dfrac{0.67\,(Ra_L \sin\beta)^{1/4}}{[\,1+(0.492/Pr)^{9/16}\,]^{8/27}}$ $Ra_L > 10^9$ $\quad Nu_L = \left\{ 0.825 + \dfrac{0.387\,Ra_L^{1/6}}{[\,1+(0.492/Pr)^{9/16}\,]^{8/27}} \right\}^2$

3-4-2-2 Forced Convection: In windy conditions, the heat transfer by forced convection cannot be neglected. To calculated Nusselt Number in laminar conditions Sparrow et al. [13] gave the expression:

$$Nu_L^* = 0.86\,(Re_L^*)^{1/2}\,(Pr)^{1/3} \qquad Re < 5\times10^5 \qquad (3\text{-}12)$$

At larger values of Re_L^* Assouad [11] proposed the formula:

$$Nu_L^* = 0.0479\,(Re_L^*)^{0.8}\,(Pr)^{1/3} \qquad Re_L^* > 5\times10^5 \qquad (3\text{-}13)$$

Noting the lack of detailed information about the combined natural and wind convection, McAdams [12] recommended that both pure free convection and pure wind convection heat transfer coefficients be calculated and the larger value adopted.

3-4-3 Radiation Heat Transfer Between Two Parallel Plates:

The quantity of energy transfered by radiation from a surface of area A_2 to a surface of area A_1 is given by:

$$Q_{2\rightarrow 1} = \frac{A_1 \sigma(T_2^4 - T_1^4)}{\frac{1-\varepsilon_1}{\varepsilon_1} + \frac{1-\varepsilon_2}{\varepsilon_2}\frac{A_1}{A_2} + \frac{1}{F_{12}}} \qquad (3\text{-}14)$$

where ε is the emissivity, F_{12} the shape factor and $\sigma = 5.67\times10^{-8}$ S.I. This formula gives in the case of two parallel surfaces the following expression for the heat transfer coefficient:

$$h_{2-1} = \frac{\sigma(T_1^2 + T_2^2)(T_1 + T_2)}{\frac{1}{\varepsilon_1} + \frac{1}{\varepsilon_2} - 1} \qquad (3\text{-}15)$$

3-4-4 Radiation heat Transfer between a surface and the surroundings:

It is convenient to consider the surroundings as a black body at some temperature T_{sky} . Equation (3-14) is then applicable with $\varepsilon_2=1$ and $F_{12}=1$. Omitting the subscript 1, we obtain:

$$Q_{s\text{-}sky} = A\varepsilon\sigma(T^4 - T_{sky}^4) \qquad (3\text{-}16)$$

3-5 ANALYSIS OF SYSTEM PERFORMANCE

In order to analyze the system performance, the following energy quantities need be defined:

- the rate of sensible heat gained by the collector,

$$Q_{sen}(t)=(M_aC_a+M_cC_c+M_awC_s)(dT/dt)$$

$$=(M_aC_a(T_{re}-T_{ad})/t_o)(1+E_o+E_1w)d\theta/d\eta \qquad (3\text{-}17)$$

– the rate of energy used in desorption,

$$Q_{ads}(t)=-q_{st}M_a(dw/dt)=-q_{st}M_aG(dT/dt)$$

$$=-[L_oM_a/t_o(T_{re}-T_{ad})]\varphi\,(w,\theta)\,\Gamma(w,\theta)(d\theta/d\eta) \qquad (3\text{-}18)$$

- the rate of desorbed mass,

$$m_{des}(t)= -M_a(dw/dt)=-M_aG(dT/dt))$$

$$=-[M_a/t_o\,(T_{re}-T_{ad})](\,\Gamma(w,\theta)(d\theta/d\eta) \qquad (3\text{-}19)$$

- the rate os solar energy input to the collector:

$$Q_{sol}(t) = A\mathfrak{I}\,(t) = A\mathfrak{I}_oI\,(\eta) \qquad (3\text{-}20)$$

- the rate of cooling effect produced at the evaporator .

$$Q_{ev}(t)=[L(T_{ev})\,-C_L(T_{co}-T_{ev})]\,m_{des}$$

$$=-[L_oM_a/t_o\,(T_{re}-T_{ad})]\,[\lambda(\theta_{ev})-E_{11}(E_8-1)/E_{10}]\,\Gamma(w,\theta)(d\theta/d\eta) \qquad (3\text{-}21)$$

The following COP's are defined:

- the instantaneous cycle COP:

$$COP_{cycle1}=Q_{ev}(t)\,/\,[Q_{sen}(t)+Q_{ads}(t)] \qquad (3\text{-}22)$$

- the cumulative cycle COP:

$$COP_{cycle2}=\int Q_{ev}(t)dt\,/\,(\int Q_{sen}(t)dt + \int Q_{ads}(t)dt) \qquad (3\text{-}22)$$

- the instantaneous solar (or system) COP:

$$COP_{solar1}=Q_{ev}(t)\,/\,Q_{sol}(t) \qquad (3\text{-}23)$$

- the cumulative solar COP:

$$COP_{solar2}=\int Q_{ev}(t)dt\,/\,[\,\int Q_{sol}(t)dt] \qquad (3\text{-}24)$$

The range of integraion is from t=0 (starting of the desorption

phase) to time t at which the quantity is wanted. The difference between the cycle COP and the solar COP is that the latter takes into account the efficiency of the solar collector whereas the former is specified by the cycle operating temperatures: T_{ad}, T_{re}, T_{co} and T_{ev}. If we denote the collector efficiency by η_{solar}, we obtain :

$$COP_{solar} = COP_{cycle}\,\eta_{solar} \qquad (3\text{-}25)$$

3-6 RESULTS OF THE NUMERICAL SIMULATION

A computer program COLLECTG was written to solve for the profiles of the adsorbent temperature, the uptake and the system performance as functions of time. The purpose was to examine the influence of the operating conditions on the dynamic behaviour of a solar adsorption machine as well as the effect of the parameters E_o, E_1, E_2...etc found by the nondimensionalization of the governing equations. To achieve this objective, profiles of ambient temperature and solar radiation shown in figure 3-2 are assumed and a number of runs were made to analyze the effects of different parameters. The type of solar collector and the following data are also common to all the different runs :

M_a=23.3 (kg) C_a=836.0 (J/kg.K) C_c=607.1 (J/kg.K)

M_g=4.58 (kg) C_g=750.0 (J/kg)

$(\tau\alpha)_6$=0.81 ε_c =0.80 ε_g=0.93 α_g=0.085

For the cases in which the adsorbate is H_2O, we used the following:

C_s=C_L=4180.0 (J/kg.K) r=462(J/kg.K)

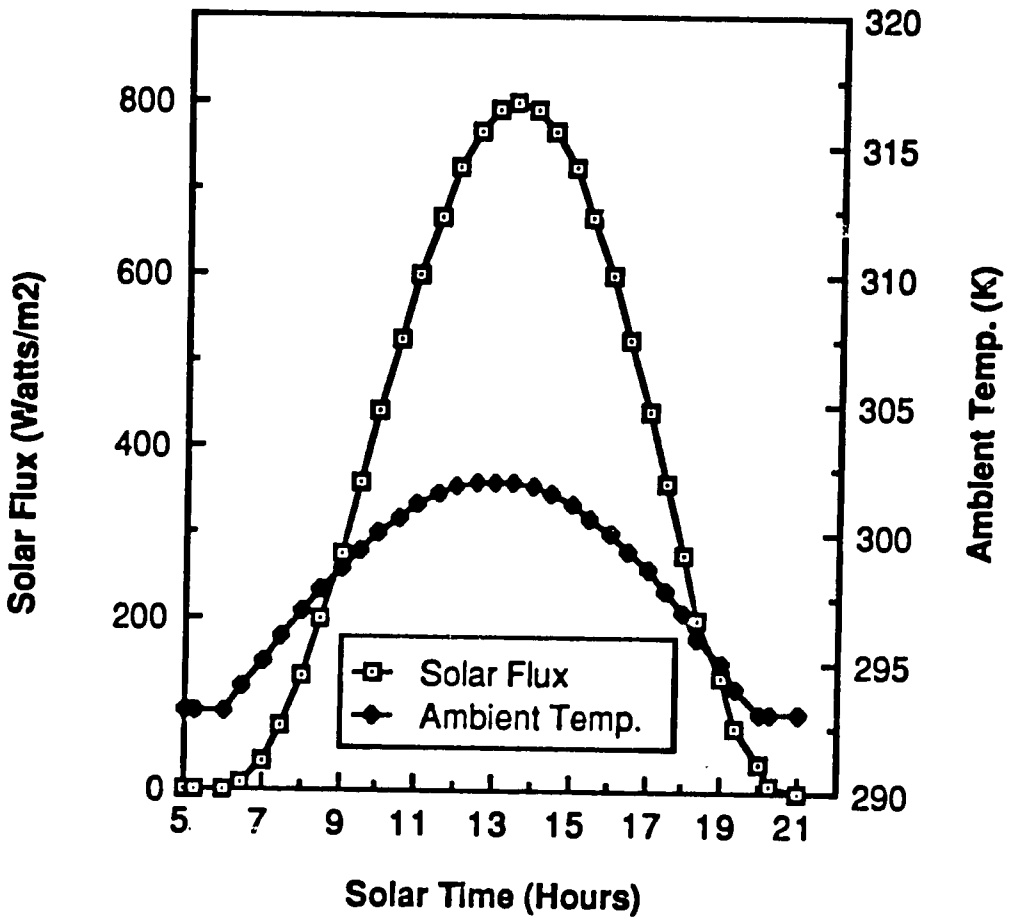

Figure 3-2: Profiles of solar flux and ambient temperature used in the simulation.

L_o=3171.2x10^3 (J/Kg) a_L=-2.4425x10^3 (J/Kg.K)

For the cases in which the adsorbate is methanol, we used:

C_s=C_L=2500.0 (J/Kg.K) r=259.5 (J/Kg.K)

L_o=1718.4x10^3 (J/Kg) a_L=-1.8288x10^3 (J/Kg.K)

3-6-1 General considerations:

To discuss the general aspects of the dynamic behaviour of a solar adsorption refrigerator, the following case is chosen:

Pair adsorbent-adsorbate: Zeolite13X-H_2O (data of [15]).

Evaporator temperature: 0°C

Condenser temperature: 50°C

3-6-1-1 Convergence and stability of the numerical scheme:

It was found that the method is stable for a time step Δt<20mn, and that the temperature profile obtained with Δt=15mn is improved by less than 1% only by taking Δt=7.5mn. Thus the former time step was adopted. It was found that the system attains a "periodic" regime after about three "transient" cycles.

3-6-1-2 System performance:

Figures 3-3a,b show the variations of the COP's with the solar time. In the first hours of the day, the solar energy input is used to increase the temperature of the collector and its content thus practically no mass is desorbed and the COP's are all equal to 0. As the desorption begins, after T_s has reached T_{co}, the instantaneous COP's rapidly increase to finite values: about 0.46 for COP_{cycle1} and 0.22 for COP_{solar1}. This occurs between 11:30 and 12:00. Desorption continues until the collector has reached its maximum temperature

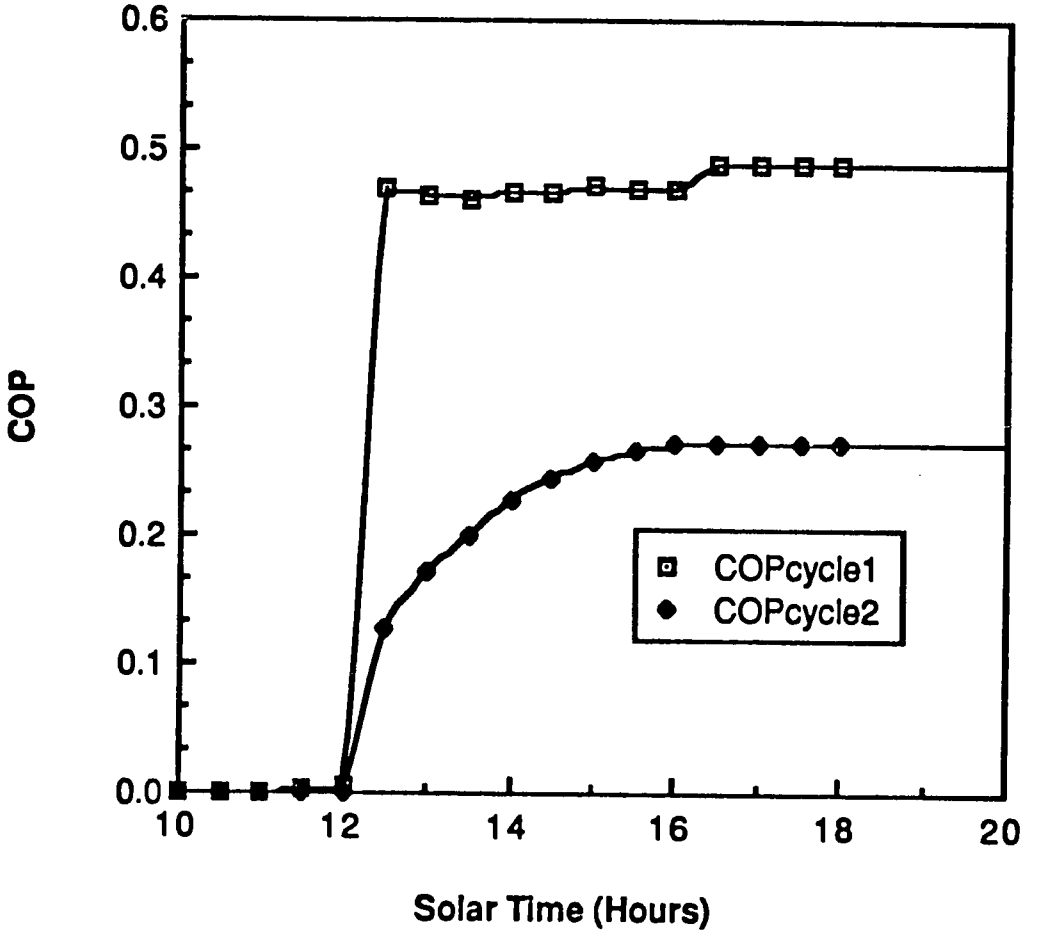

Figure 3-3a: Profiles of the cycle instantaneous and cumulative COP's.

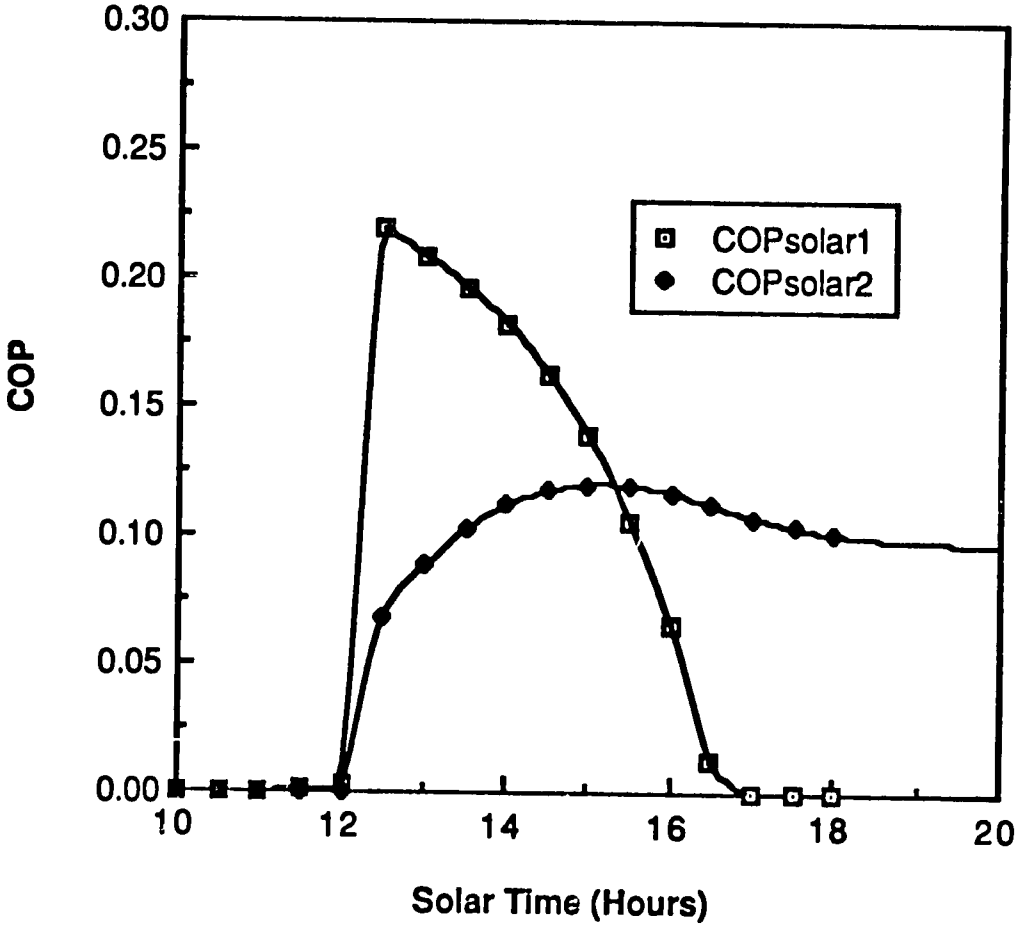

Figure 3-3b: Profiles of the solar instantaneous and cumulative COP's.

of about 139 °C. As the collector temperature rises, it's efficiency decreases causing a decline of COP_{solar1}. As a consequence, COP_{solar2} increases up to a maximum of about 0.11 before coming down to a final value of about 0.095 which constitues the real performance of the machine. Note that an improvement of the collector efficiency to a value of unity will not make the machine performance COP_{solar2} exceed the value 0.50 of the COP_{cycle2}.

3-6-1-3 Profiles of T, w and T_s and **G**

Figure 3-4 shows the adsorption cycle in the form of T_s vs T. During the constant-volume phases, the variations of the uptake w are of the order of 10^{-5} which is smaller than the accuracy on the experimental determination of adsorption isotherms and constitues a rigourous proof of the usual assumption that the constant-volume phase is isosteric.

Figure 3-5a shows the adsorption cycle in the w-T diagram. We notice here again that the constant-volume phase is approximately a horizontal line except at the end of the phase where a sensible deviation can be seen. This figure shows also an interesting linear variation of the uptake with the adsorbent temperature which suggests that the ratio $[T_s-\mathbf{B}(w)]/\mathbf{A}(w)$ is a linear function of w (at constant T_s). The parameters **A**(w) and **B**(w) are the functions introduced in equation (1-32). This remark implies also that the adsorptivity function **G**(w,T) should be essentially constant.

Figure 3-5b shows the variations of the adsorbent

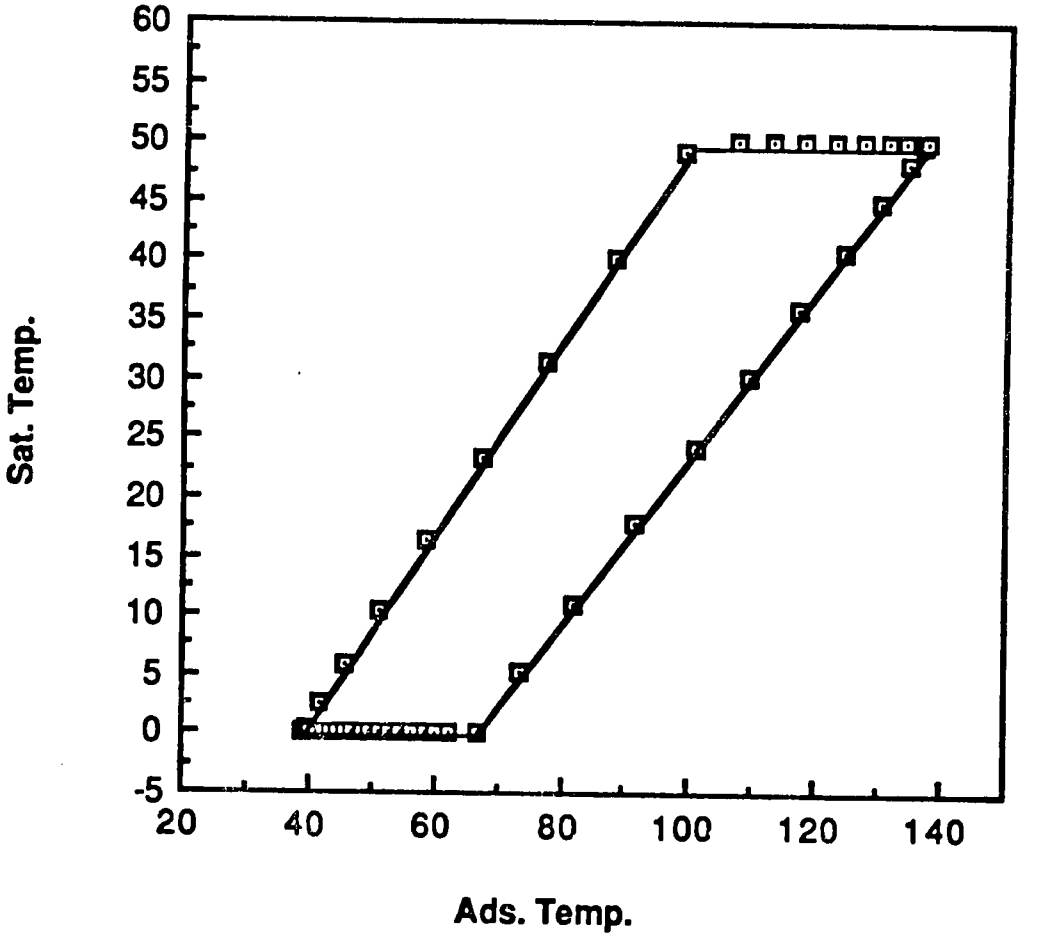

Figure 3-4: Adsorption cycle for the set of data chosen.

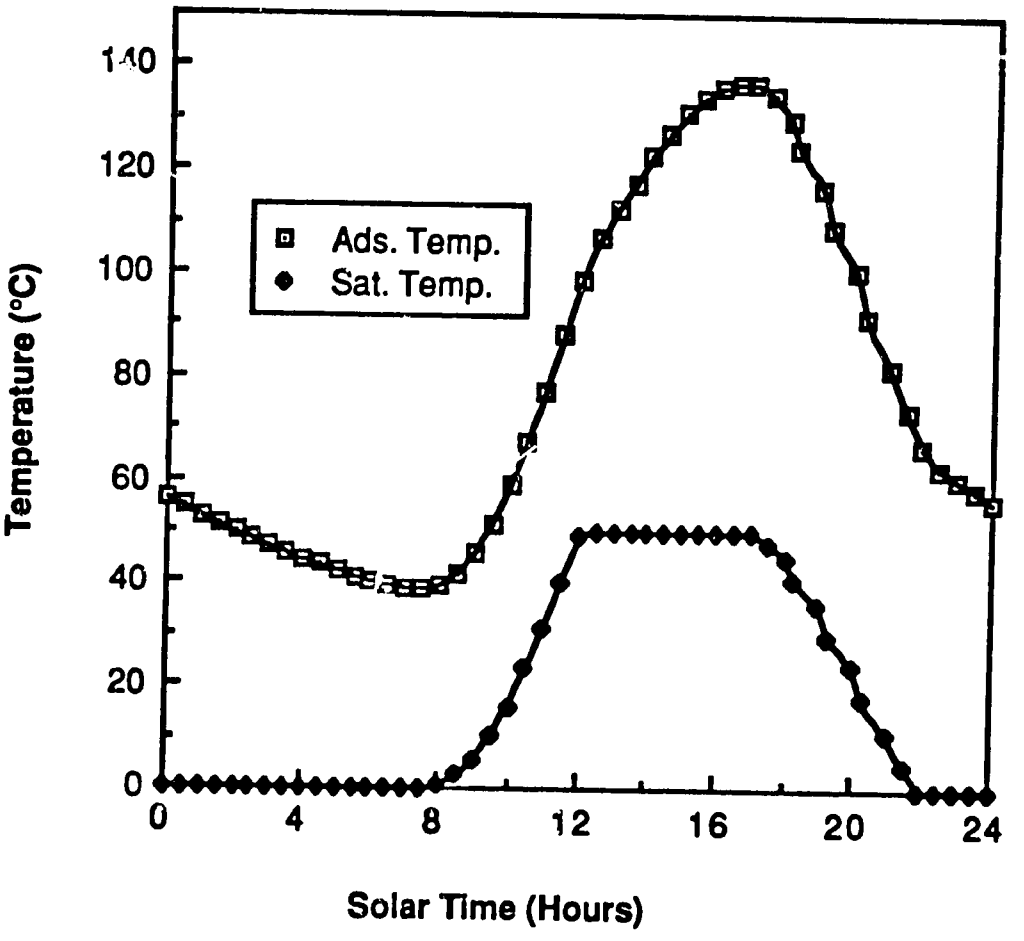

Figure 3-5b: variations of the adsorbent temperature and the saturation temperature with time.

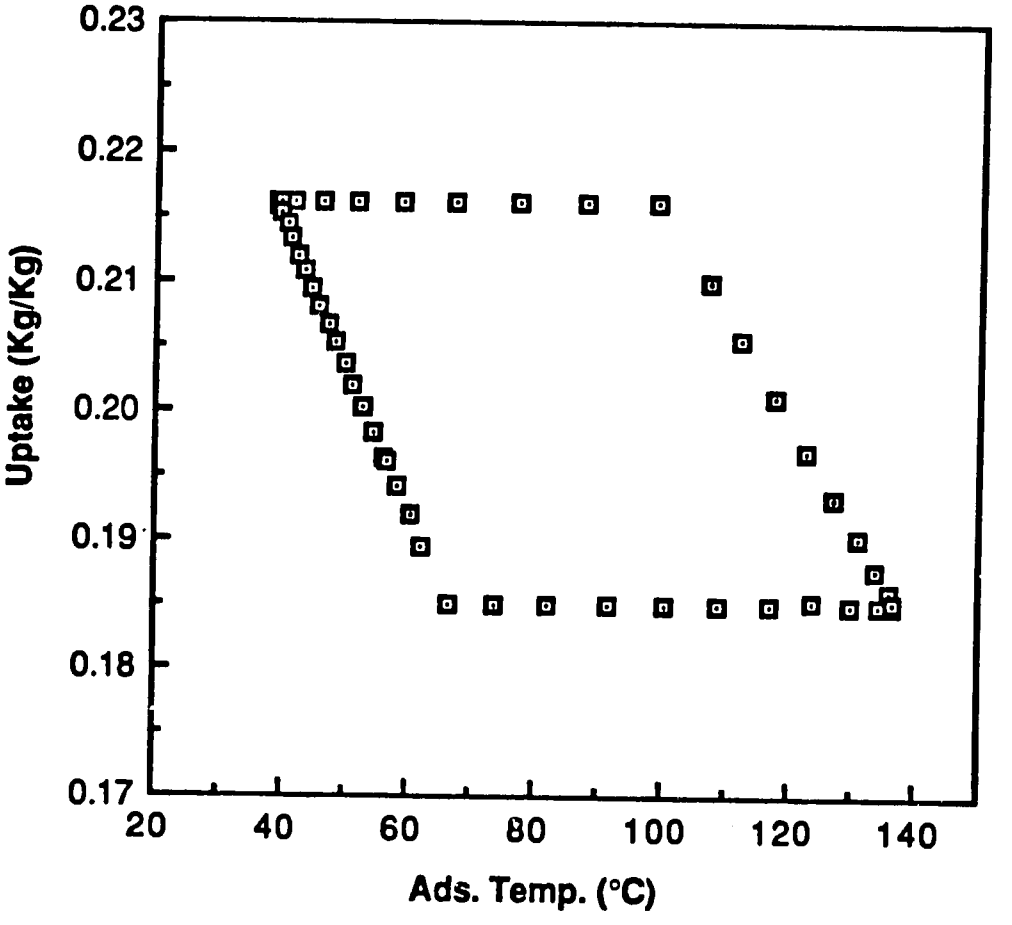

Figure 3-5a: Variation of w with adsorbent temperature.

temperature and the saturation temperature with time. The temperature at the end of adsorption T_{ad} is reached around 7:30 and is equal to about 38°C. The relatively large increase in temperature during the early hours of desorption is due not only to the fact that the energy is mainly transformed to sensible heat but also to the fact that the heat losses are smaller at low temperature. The maximum value T_{re} of adsorbent temperature is about 138°C and is reached around 17:00.

Figures 3-6a,b,c present the variations of the adsorptivity function **G** with time (or indirectly with adsorbent temperature) , uptake w and the saturation temperature respectively. These curves show the relatively constance of **G** during the constant-pressure phases at a value of approximately 1.1×10^{-3} (kg/kg.K). It is also seen that $Ln(G_V)$ varies almost linearly with T_s during the constant-volume phases with values ranging from about 2.0×10^{-7} to 2.0×10^{-6} (Kg/Kg.K) and slightly larger during desorption.

3-6-2 Effects of E_o , ε , T_{co} and T_{ev}:

To perform a parametric study of the closed-cycle adsorption cooling system, the pair Synthetic zeolite-H_2O was chosen and the parameters Eo, ε, T_{co} and T_{ev} were varied. The results are summarized in table 3-1.

E_o is the ratio of the thermal capacity of the inert metal contained in the collector to that of the adsorbent material. The role of the metal is not only to hold the collector structure but also to permit a very good heat transfer through the adsorbent. However the

T_{co}	T_{ev}	E_o	ε	COP_{cycle2}	COP_{solar2}	T_{ad}	T_{re}	w_{min}	w_{max}
20	0	.237	1.0	0.4608	0.18873	45.0	121.7	.1519	.2090
30				0.3983	0.15172	43.2	128.6	.1643	.2111
40				0.3283	0.12042	40.7	133.2	.1761	.2139
50				0.2727	0.09676	38.8	136.9	.1851	.2161
35	0	.237	1.0	0.3643	0.13678	41.3	130.9	.1707	.2133
	5			0.3723	0.14520	42.7	128.4	.1735	.2185
	10			0.4040	0.16099	43.2	127.1	.1749	.2247
35	0	.000	1.0	0.3874	0.14173	41.4	132.3	.1689	.2131
		.474		0.3188	0.12384	42.4	128.4	.1734	.2120
		.949		0.2748	0.10901	44.5	126.4	.1757	.2096
		1.897		0.2063	0.0866	47.3	121.3	.1801	.2065
35	0		0.5	0.3646	0.13687	41.3	130.9	.1707	.2133
			1.5	0.3641	0.13673	41.3	130.9	.1707	2133

Table 3-1: Effect of the parameters T_{co} ,T_{ev},E_o and ε on the machine performance

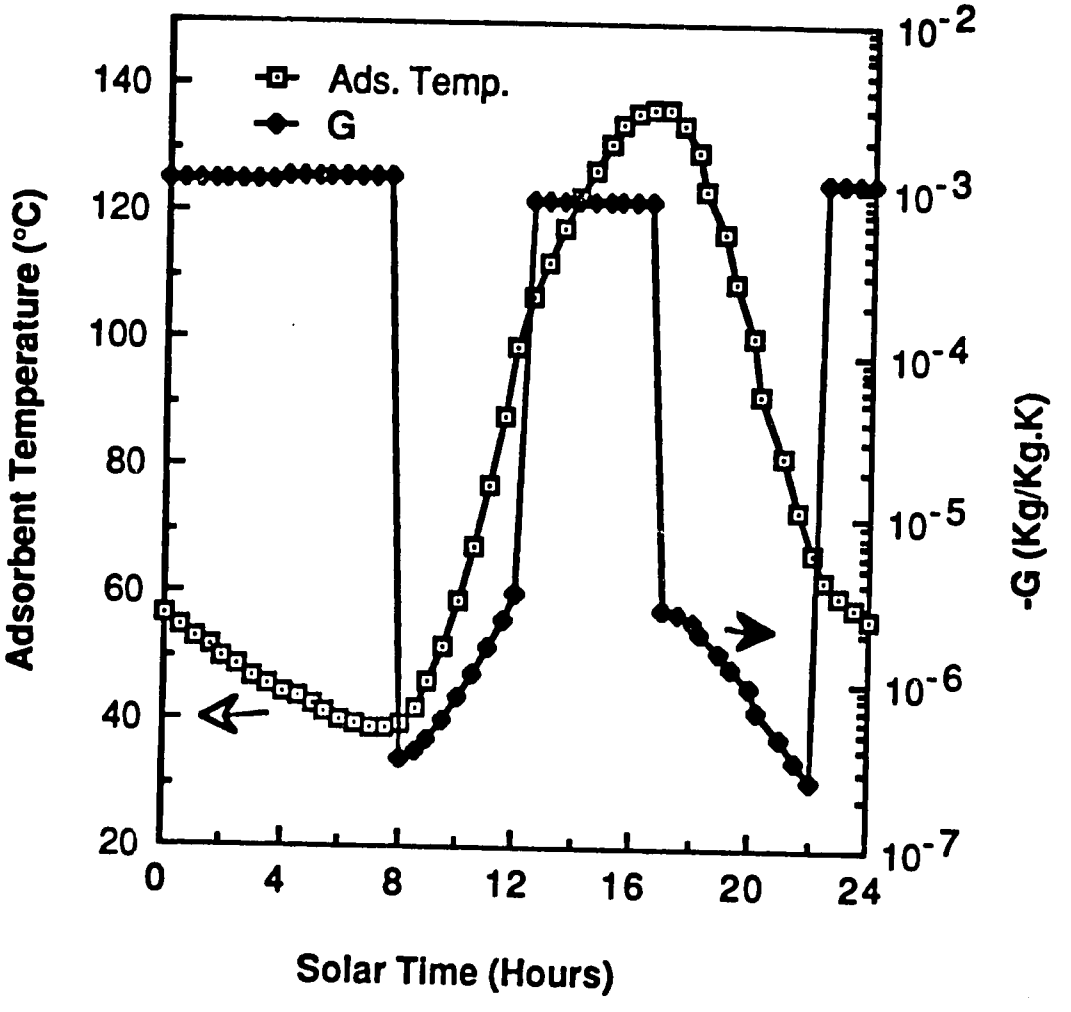

Figure 3-6a: Variations of the function G with adsorbent Temperature

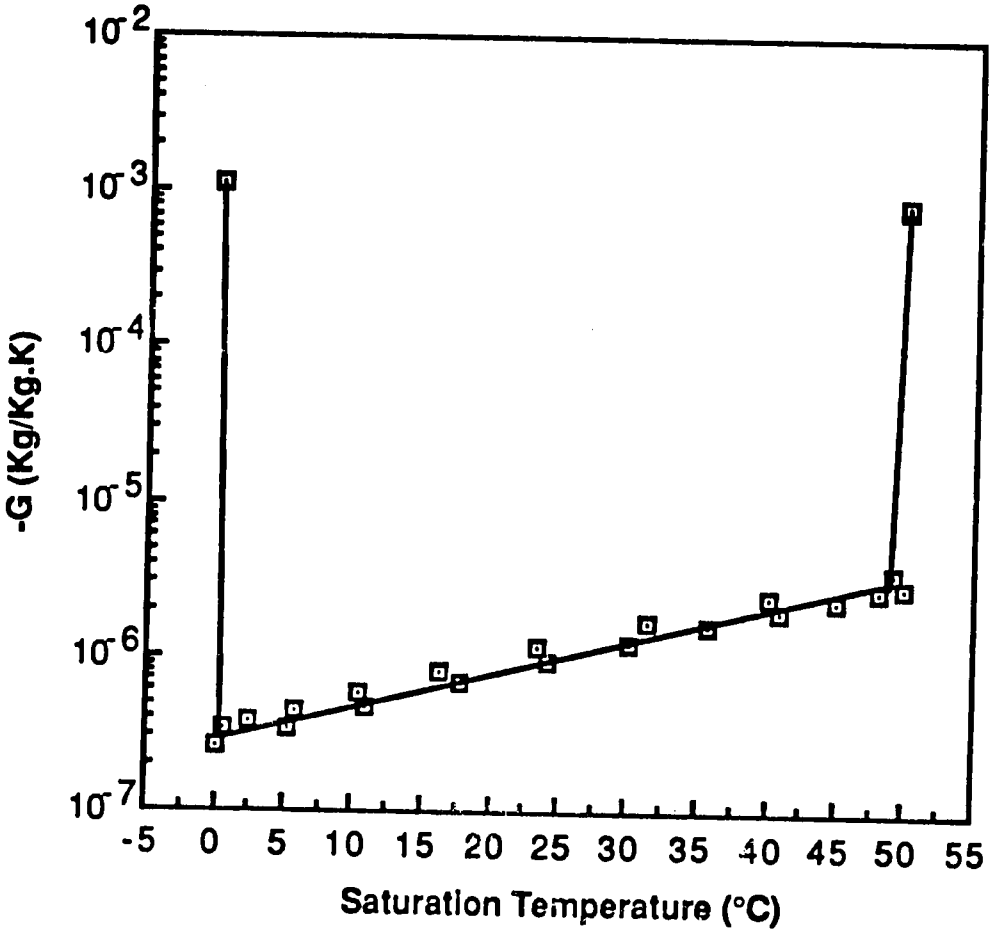

Figure 3-6b: Variations of G as function of the saturation temperature.

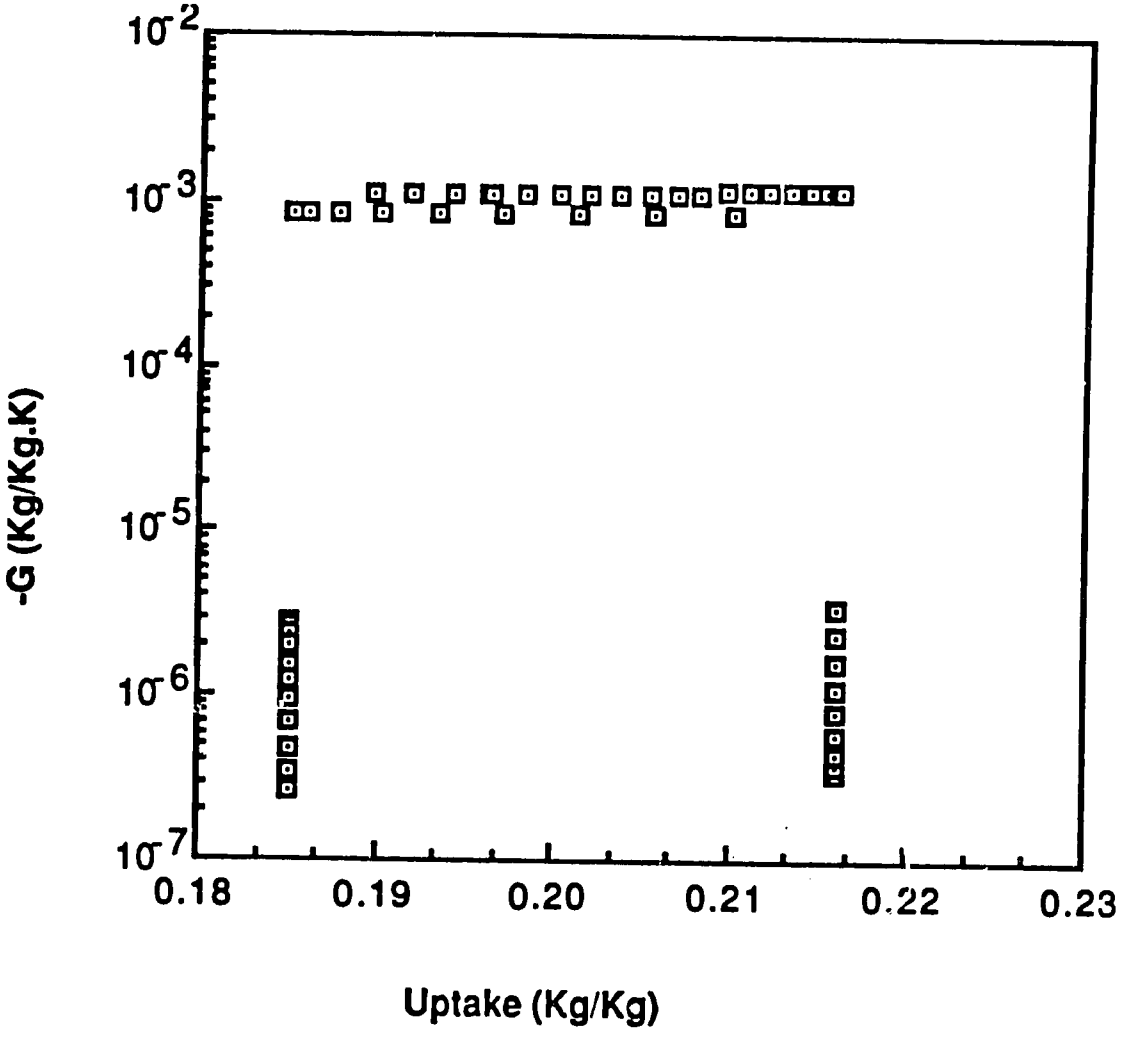

Figure 3-6c: Variations of G as a function of the uptake w.

presence of the metal reduces the fraction of heat used for desorption thus penalizing the COP. Table 3-1 shows that an increase of 0.24 in E_o causes COP_{solar2} to decrease by only 3.7%.

ε is the ratio of the volume of the gas phase to the volume of the adsorbent and depends on the "dead volume" allowed by the design of the collector and also on how the adsorbent is packed (the size of the particles, the interparticle voids...). The effect of ε is negligibly small. The reason is that at low pressures the amount of gas needed to increase the pressure from p_{ev} to p_{co} remains very small even for substantially larger volume the gas phase.

The effects of the T_{co} and T_{ev} - respectively imposed by the condenser and the evaporator are more important. At constant T_{ev}, COP_{solar2} is improved by about 22% for a 10°C decrease of T_{co} and at constant T_{co}, a 5°C increase of T_{ev} causes an improvment of 8%. The difference (T_{co}-T_{ev}) seems to be more decisive in determining the machine performance as seen in figure 3-7.

3-6-3 Below-freezing evaporator temperatures:

The use of refrigerants other than water can allow evaporator temperatures below 0°C. The most used component in solid adsorption cooling is methanol (CH_3OH). The equilibrium data provided by [15] was used to analyse the performance of the pair Chabazite-Methanol and to compare it to the pair Synthetic zeolite 13X-Water. The results are given in this table.

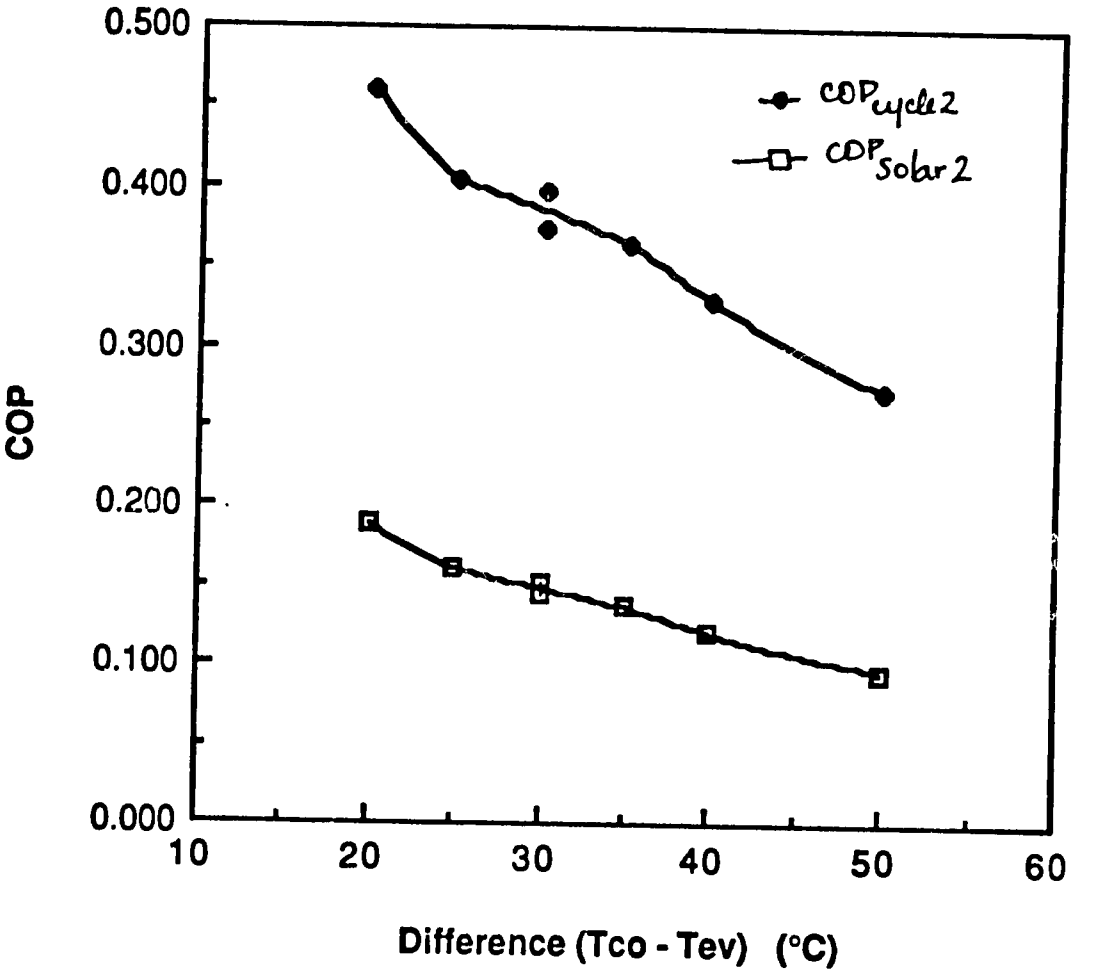

Figure 3-7: Variations of the COP with the difference (Tco - Tev).

T_{ev}	COP_{cycle2}	COP_{solar2}	
0°C	0.24741	0.08388	T_{co}=35°C
-5°C	0.241152	0.08132	ε = 1.0
-10°C	0.21305	0.07042	E_o = 0.237

For comparison between the two adsorption pairs Zeolite 13X-Water and Chabazite-Methanol, figures 3-8a,b give the variations with time of COP_{cycle} and COP_{solar} corresponding for the two pairs at the conditions: T_{co}=30°C , T_{ev}=0°C , ε=1 and E_o=0.237. At low adsorbent temperature (early hours), the COP's of the 2nd pair are larger. But globally Zeolite-Water pair has a much better performance.

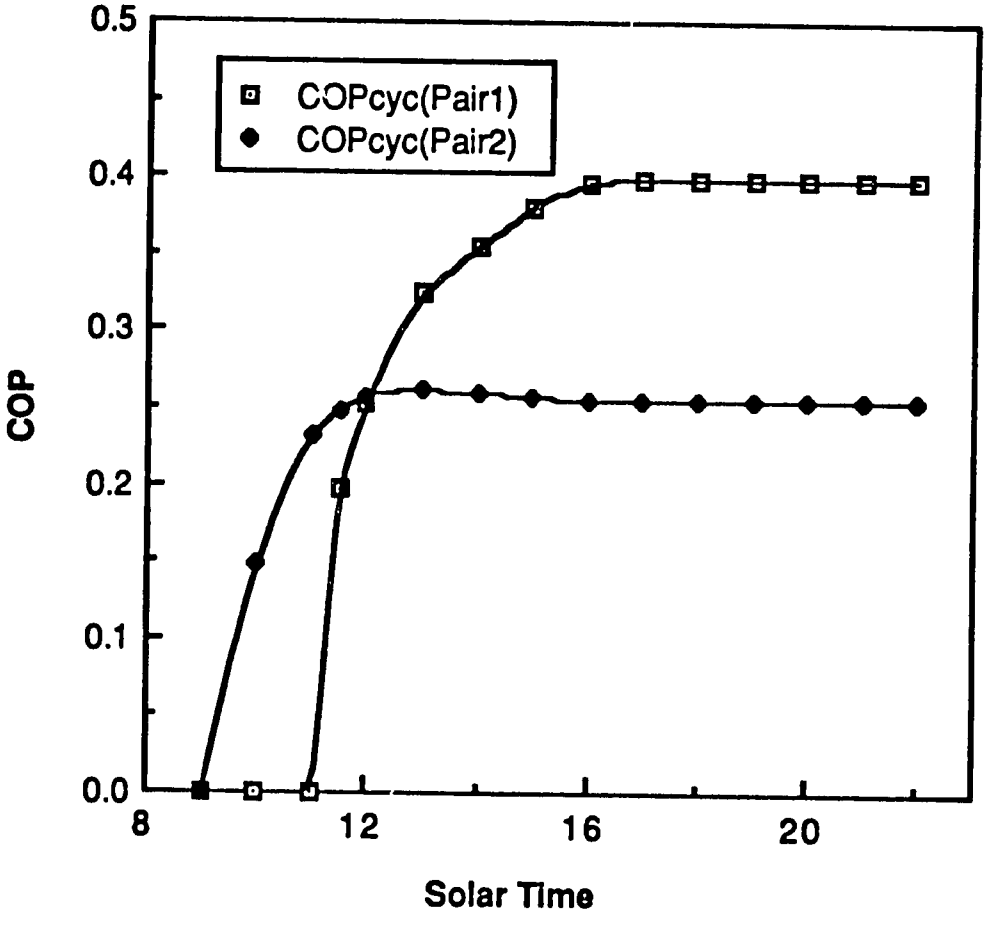

Figure 3-8a: COPcycle2 for the two adsorption pairs:

Zeolite 13X-Water (pair 1) and Chabazite-Methanol (pair2).

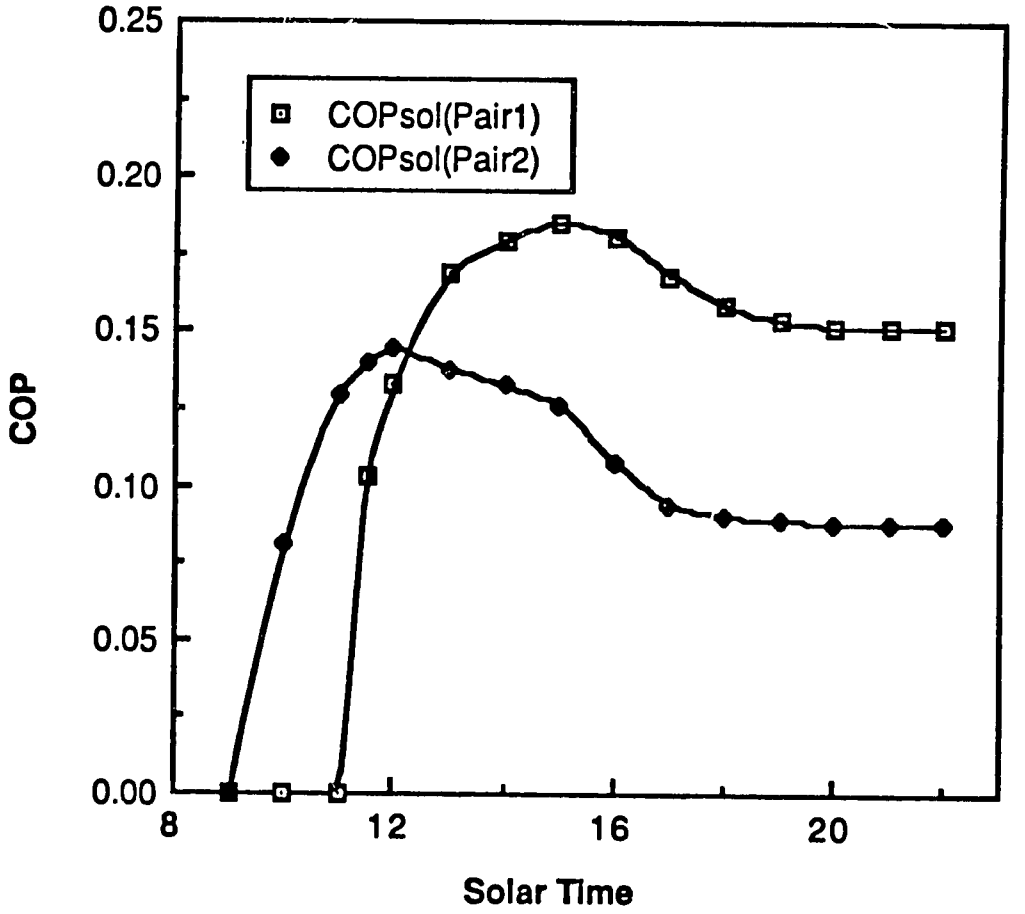

Figure 3-8b: COPsolar2 for the two adsorption pairs:

Zeolite 13X-Water (pair 1) and Chabazite-Methanol (pair2).

Nomenclature

a_L	Constant defined in equation (1-72)
A	Area of collector
A(w)	Function defined in equation (1-32)
B(w)	Function defined in equation (1-32)
C	Specific heat
COP	Coefficient of performance
E_i	Dimensioless parameter defined in section 3-2
F	Equilibrium defined in equation (3-1)
G	Absorptivity function defined in (3-4)
h	coefficient of heat transfer
$\mathcal{I}(t)$	Incident solar flux at time t
L	Characteristic length in section 3-4
L(T)	Latent heat of vaporization at temperature T written in the form $L(T)=L_o + a_L T$
M	Mass
Nu_L	Nusselt Number based on L
Pr	Prandtl Number
q_{st}	Isosteric heat of adsorption
Q	Heat quantity
R	Ideal gas constant
t	Time
T	Temperature
w	uptake (mass of adsorbate/Mass of dry adsorbent)

Greek Symbols:

α	Absorptance

β	Collecor inclination w.r.t. the horizontal plane
ε	Emissivity or void fraction
Φ	Dimensionless F
Γ	Dimensionless G
η	Dimensionless t
$I(\eta)$	Dimensionless $\mathcal{I}(t)$
φ	Dimensionless q_{st}
λ	Dimensionless L
θ	Dimensionless T
ρ	Mass density
τ	Transmittance
$(\tau\alpha)_e$	Effective transmittance-absorptance of the collector

<u>Subscripts:</u>

a	"Dry" adsorbent
ad	Adsorption
co	Condenser
c	Inert parts of the collector
ev	evaporator
g	Glass or gas phase
L	Liquid phase
o	Characteristic value
re	Regeneration
s	Sorbed species or saturation
∞	ambient

References

[1] Meunier F. , B. Mischler, J-J. Guilleminot and P. Simonot, "On the use of Zeolite 13X-H_2O Intermittent Cycle for Application to Solar Climatization of Building", SUN II, vol. **1**, 1979.

[2] Guilleminot J.J., F. Meunier and B. Mischler, "Etude des Cycles Intermittants a adsorption solide pour la refrigeration solaire", Rev. Phys. Ap., **15**, 441, 1980.

[3] Chang, S.C. and J.A. Roux, "Thermodynamic Analysis of a Solar Zeolite Refrigeration System", J. Solar Energy Eng., vol. **107**, 189, 1985.

[4] Duffie, J.A. and W.A. Beckman, "Solar Engineering of Thermal Processes", John Wiley & Sons, 1980.

[5] Monnier, J-B. and M. Dupont, "Zeolite-Water Closed-Cycle Solar Refrigeration: Numerical Optimization and Field Testing", Proceedings of the ASES Annual meeting, 1983.

[6] Adell, A. "Disrtibution des temperatures deans un capteur solaire a adsorpion solide destine a la refrigeration: Resultas experimentaux en climat equatorial", Rev. Gen. Therm., No. **266**, 79-91.

[7] Lloyd, J.R. and W.P. Moran, "Natural Convection Adjacent to Horizontal Surface of Various Planforms", Trans. ASME, J. Heat Transfer, **96**, 443, 1974.

[8] Hollands, K.G, S.E. Unny, G.D. Raithy and L. Konicek, "Free Convective Heat Transfer Across Inclined Air Layers", J. Heat Transfer, **98**, 98, 1976.

[9] Incropera, F.P. and P.P. DeWitt, "Fundamentals of Heat and Mass Transfer", 2nd Ed., John Wiley & Sons, 1980.

[10] Churchil, S.W. and H.H.S Chu, "Correlating Equations for Laminar and Turbulent Free Convection from a Vertical Plate", Int. J. Heat Mass Transfer, **18**, 1323, 1975.

[11] Assouad, Y., "Combinrd Heat and Mass Transfer as Applied to Desalination and Liquid Desiccant Cooling Systems", PhD Thesis, IIT Chicago, 1985.

[12] McAdams, W.H., "Heat Transmission", 3rd Ed., McGraw Hill, N.Y., 1954.

[13] Sparrow, E.M., J.W. Ramsey and E.A. Mass, "Effect of Finite Width on Heat Transfer and Fluid Flow about an Inclined rectangular Plate", Transactions of the ASME, J. Heat Transfer, **102**, 2, 1979.

[14] Tchernev D.I., "Closed-Cycle Regenerative Heat-Pump", Paper presented at at Desiccant Review Conference, Chattanoga, Tennessee, June 1986.

[15] Collier Engineering Services, "determination of Properties of Zeolite-Refrigerant Combinations for Solar Refrigeration Systems", Report to the US Department of Energy, 1986.

RESEARCH AND DEVELOPMENT OF SOLAR-POWERED DESICCANT REFRIGERATION FOR COLD-STORAGE APPLICATIONS

(Grant No. DPE-5542-G-SS-4057-00)

by

Prof. R. H. B. Exell
Dr. S. C. Bhattacharya
Y. R. Upadhyaya.

Asian Institute of Technology
P.O. Box 2754, Bangkok 10501
Thailand

1987

102

CONTENT

I. Zeolite-Water Refrigerator

1.1 Introduction 1
1.2 Specifications 1
1.3 Objectives 3
1.4 Instrumentation and Methodology 3
1.5 Initial Results 3
1.6 Conclusion 10

II. Work Carried Out at AIT on the Charcoal-Methanol Pair 13

III. Future Plan 17

APPENDIX 18

REFERENCES 21

I. ZEOLITE-WATER REFRIGERATOR

1.1 Introduction

A solar zeolite-water refrigerator (model SR-4) manufactured by Zeopower Company, USA has been tested at Asian Institute of Technology. This is a closed cycle intermittent adsorption type refrigerator which has natural zeolite as adsorbent and water as the refrigerant. A view of this refrigerator is shown in Fig. 1. It consists of a solar collector containing zeolite on the top, an air cooled condenser under the solar collector and a receiver/evaporator at the bottom inside a commercial ice box. The solar flat plate collector has a selectively coated absorber. The tilt angle of the absorber is 14° which is equal to the latitude of AIT. The collector contains between 24.95 and 26.3 kg of dry zeolite about 50mm deep. Pipes are provided at the top and the bottom to permit water vapour to enter and leave during adsorption and the desorption. The system operates below atmospheric pressure so it is evacuated, leak tested, filled with required amount of water and sealed. This system has in total about 30.76 wt % water (dry basis). The specifications supplied by the manufacturer (Zeopower Company, USA) are as follows:

1.2 Specifications

Type: Liquid with Solid/Gas Adsorption System.
Model : SR-4
Gross Collector Dimensions : 29" x 47" = 0.8786 m^2
Net Collector Absorbing Surface Area : 25" x 43" = 0.6935 m^2
Overall Dimensions:

Height	46 1/4"	(1.175 m)
Width	30 1/2"	(0.7742 m)
Depth	48 1/2"	(1.232 m)

Refrigeration Capacity : 4 Cubic feet = 0.112 m^3
Ice Making Capacity : 15 lbs or 6.803 kg per day.
Storage Capacity : Three days of bad weather after collector surface has been exposed to a series of three or more sunny days.
Maintenance Requirements : None.
Moving Part : None except the door of the refrigerator box.
Total Weight : 215 lbs (97.505 kg).

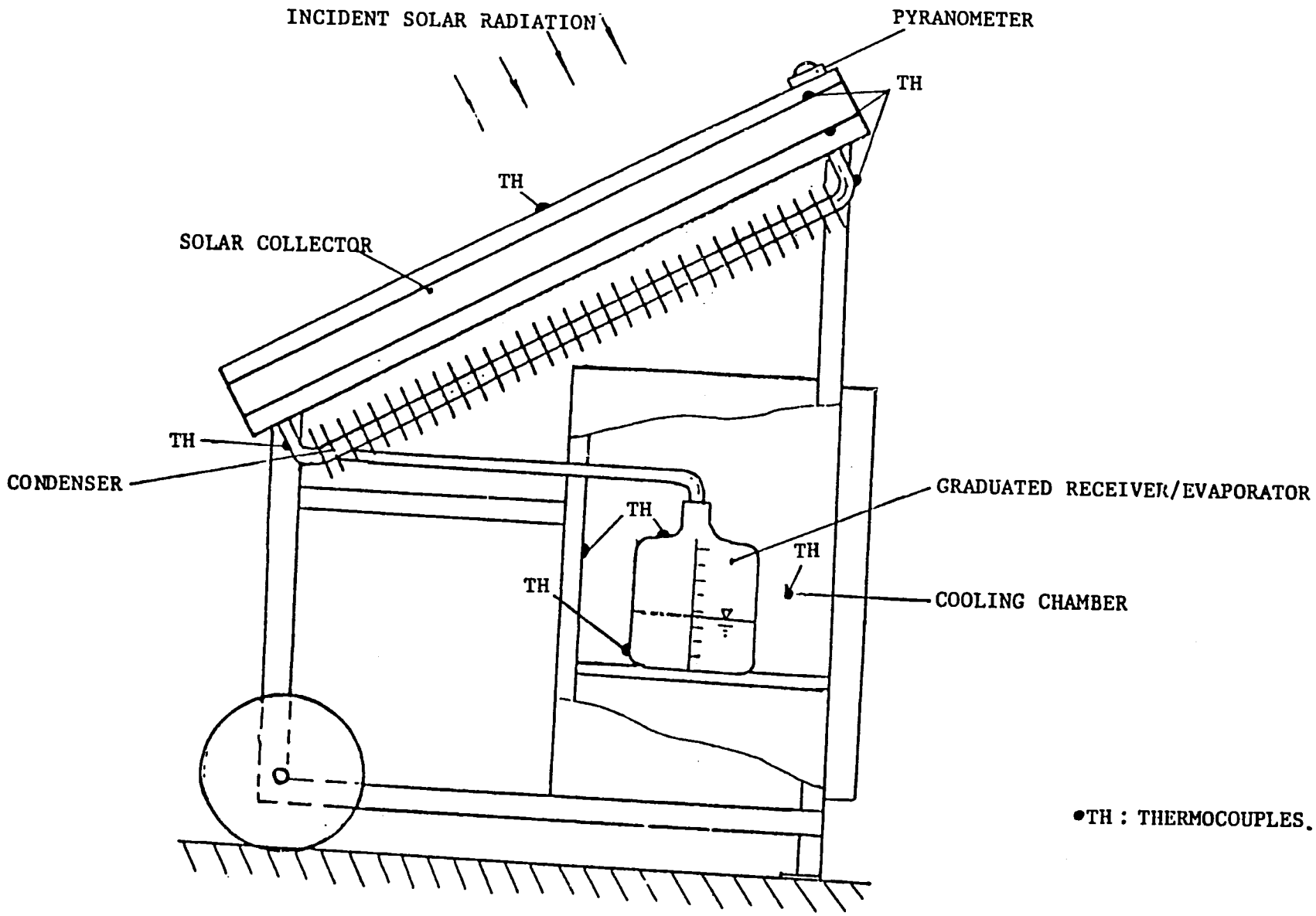

FIG. 1: THE ZEOLITE-WATER REFRIGERATOR MODEL SR-4 (ZEOPOWER COMPANY,USA).

1.3 Objectives

1. The initial objective of the experiment was to study the working and monitor performance, such as approximate temperature ranges, cooling capacity and the solar COP (Overall efficiency of the refrigerator).

2. Analyse the performance of the system in detail to investigate the possibilities for modification.

1.4 Instrumentation and Methodology

To accomplish the above objectives k-type temperature sensors were calibrated against a standard mercury-in-glass thermometer having the precision of 0.1°C and these sensors were installed at different positions: the top and the bottom of the condenser, top and the bottom of the glass bottle (receiver/evaporator), the wall of the refrigerator box; one senser was left hanging in the chamber to monitor the chamber temperature and another was used to read the ambient temperature (see Fig. 1). These temperatures were recorded continuously by a Fuji Chart Recorder.

A calibrated diffused type pyranometer attached to an integrator with digital display (Solar 118) was used to monitor the instanteneous and the integrated values of solar radiation on the surface of the solar collector. The hourly values of integrated and the instanteneous solar radiation were recorded manually.

The zeolite-water refrigerator has a glass receiver/evaporator which was calibrated by the manufacturer in thousands of BTU's. The difference of water level in the morning and the late afternoon gives the heat of condensation of water rejected by the system to the ambient during desorption. Similarily, the difference of readings between late afternoon and the early morning gives the net cooling produced by evaporation of water from the glass bottle during adsorption. The water level in the receiver/evaporator was manually recorded every hour until 24:00 hours.

1.5 Initial Results

According to the manufacturer, the solar refrigerator was

charged with approximately 8.37 kg of water. The refrigerator had been in transit for a couple of weeks and the zeolite had adsorbed approximately 7.9 kg of water (30.7 wt. %, dry basis) as the water left in the receiver/evaporator bottle was approximately 0.5 kg. The unit was placed facing south and its performance was monitored for two weeks (22 Oct to 7 Nov, 1986).

During the first few days the zeolite desorbed comparatively large quantities of water during day time and readsorbed only a fraction of it at night. After several days the amount of water desorbed and adsorbed became approximately equal. During days of average insolation, water started to desorb between 10:00 to 11:00 hours and continued until the peak temperature of the day was reached generally by 15:00 hours. The zeolite should start to adsorb water immediately after it cools from the peak collector temperature but noticeable change in the water level was observed only after 18:00 hours.

A summary of the first series of tests is given in Table 1. The amount of water desorbed during the day and the cooling produced during night are expressed in equivalent heat units as the receiver/evaporator bottle is calibrated in thousands of BTU's. Under ideal conditions, the heat rejected by the system to the ambient during desorption should be practically equal to the net cooling produced during adsorption. As seen from the Table 1, the system took several days to achieve near equilibrium condition as could be seen comparing the amount of heat rejected and the cooling produced. The net cooling produced varied from 316 kJ to 844 kJ. The cooling produced during 5, 6 and 7 Nov is greater for two reasons: (i) the condenser of the system was cooled by two blowers, and (ii) insolation was high during those days. The solar COP of the refrigerator varied between 3 to 8%. A sample calculation for overall coefficient of performance (Solar COP) is shown in the appendix.

As stated by the manufacturer, the system should be able to produce about 6.8 kg of ice during a clear day. To produce that much ice the system should cycle almost 1 kg of water. But even after several days of operation, the receiver/evaporator bottle contained only about 2.45 kg of water (estimated by the measurement of the external dimensions of the glass receiver/evaporator); and only a fraction of this(approximately 130 to a maximum of 360 gm of water) was readsorbed during

Table 1: Experimental Result of the Zeolite-Water Refrigerator for the period of 22 Oct to 7 Nov, 1986.

Date	Ambient Temps Maxm (°C)	Ambient Temps Minm (°C)	Evaporator Temp.(Minm) (°C)	Solar Radiation (MJ/Day)	Heat Rejected (kJ/Day)	Cooling Produced (kJ/Day)	Overall COP (%)
22	31.0	27.5	7.2	12.03	3166.2	527.0	4.4
23	30.6	27.7	7.2	7.52	369.4	485.5	6.5
24	33.4	27.7	7.2	11.12	1224.3	580.5	5.2
25	33.0	28.3	7.1	6.00	52.8	527.7	8.8
26	33.0	28.3	5.8	11.56	949.9	580.5	5.0
27	31.3	28.5	6.6	8.57	369.4	527.7	6.2
28	34.1	27.3	5.8	9.17	527.7	527.7	5.8
30	28.4	25.8	5.1	9.61	527.7	316.6	3.3
31	29.9	26.4	6.4	9.03	316.6	369.4	4.1
1	32.0	27.3	7.2	11.92	949.8	474.9	4.0
2	31.7	27.0	4.1	12.25	633.2	633.2	5.2
3	33.7	27.7	4.1	11.73	738.8	633.2	5.4
4	33.7	25.9	5.1	13.10	686.0	686.0	5.2
5	33.4	23.5	6.0	11.75	633.2	791.5	6.7*
6	36.2	23.8	6.0	12.03	791.6	738.8	6.1*
7	32.7	24.1	5.1	12.17	897.1	844.3	6.5*

* The condenser of the system was cooled by two blowers.

108

cooling. The system was not able to produce ice and the sensor attached to the bottom of the bottle recorded temperatures always above 4°C.

After this initial testing, some changes in the instrumentation were made. Temperature sensors were stuck to the glass, top plate and the back of the zeolite panel. Because it was not possible to break the seal of the system without spoiling the system operation, temperature sensors were not inserted into the zeolite bed. The average of the top and the back temperatures of the zeolite panel was assumed to be the mean zeolite temperature. This system had a valve (valve 1) as shown in Fig. 2. It also had a small piece of copper tube soldered to the valve and a rubber hose with two metal clips. During this set of experiments, it was decided to install a Bourdon vaccum gauge. So an assembly containing a Bourdon vaccum gauge with three isolating refrigerating valves (Castel from Italy) was fabricated (Fig. 2). The joints of this assembly were all soldered to copper tube and it was leak tested. The valve 1 was carefully shut and the rubber hose was removed. At this point air was heard rushing into the system indicating that valve 1 was defective. After soldering this assembly on, the system was evacuated for a few minutes to remove the air and leave it filled only with water vapour.

During the initial tests, condensation was observed on the inside walls of the glass bottle during desorption. During this test, the glass bottle was insulated by packing the refrigerator box with fibre glass to confirm this observation. This was found true as the temperature of the top of the glass bottle turned out to be very high during the condensation period (Fig. 3). With these modifications, the system performance was monitored for three consequitive days. Incidently, those three days were very clear with solar radiation on the surface of the panel between 18 to 19 MJ/m^2 and nights were exceptionally cool (minimum ambient temperature being 19 to 23°C) for this location. The hourly values of the instanteneous and the integrated values of solar radiation, water level in the receiver/evaporator, and the pressure were recorded manually. The instanteneous values of the solar radiation and the temperature profiles for a day are shown in Figs. 4 and 5 respectively. The maximum temperature reached in the zeolite panel was 104°C(219°F). The observed pressure during the condensa on varied between 33 and 78.4 mm Hg which

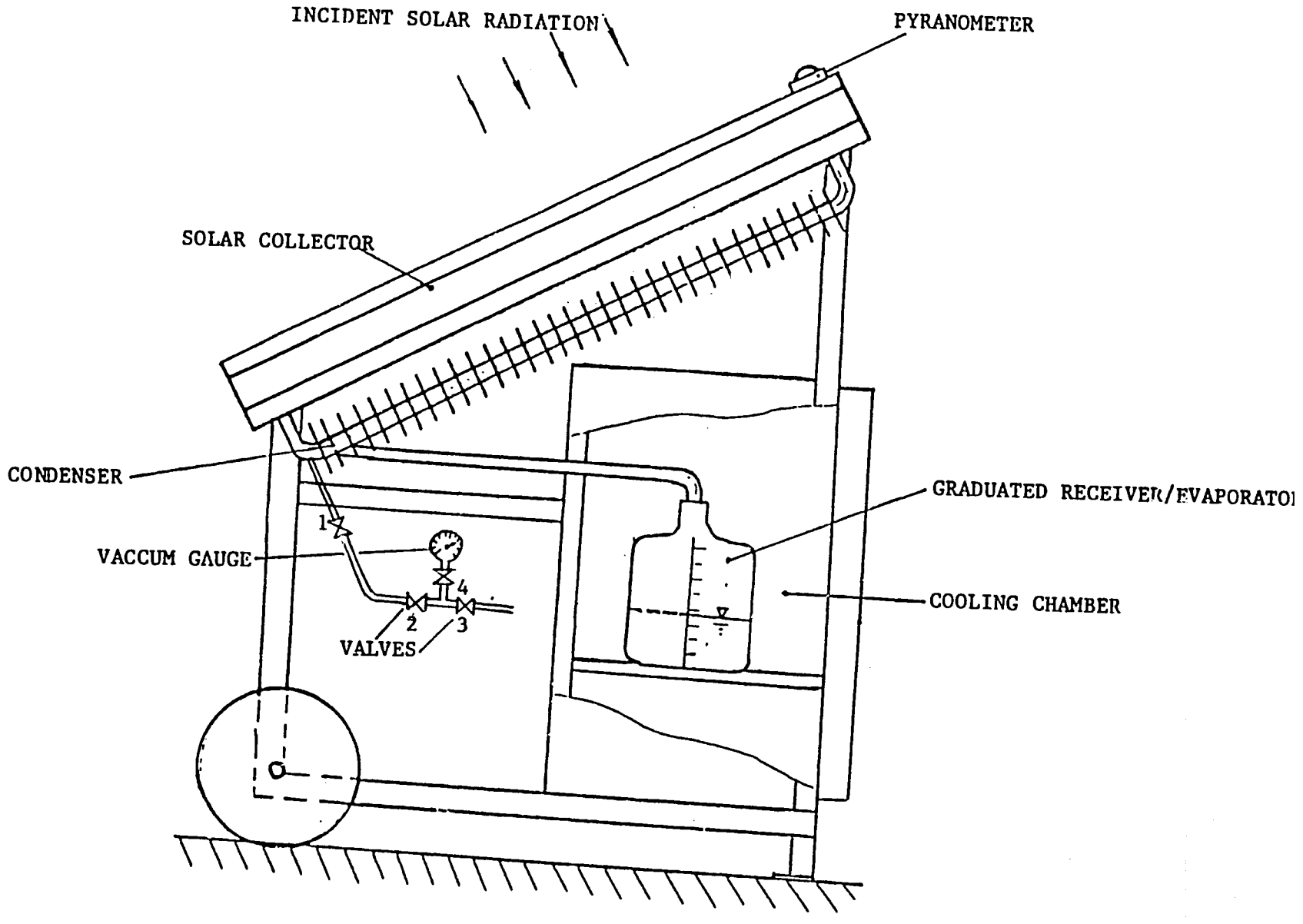

FIG. 2: POSITION OF VACCUM GAUGE IN THE REFRIGERATOR.

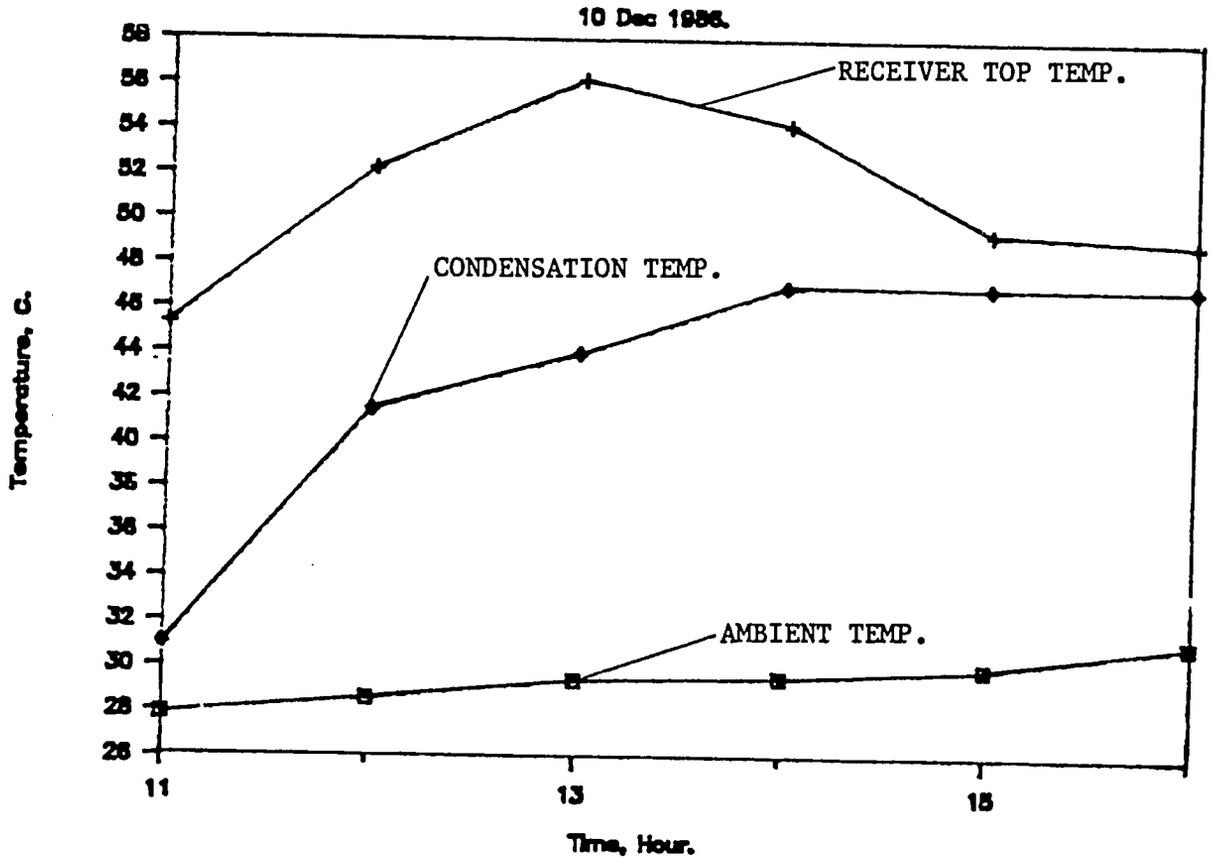

FIG. 3: TEMPERATURE PROFILE DURING CONDENSATION (10 DEC 1986).

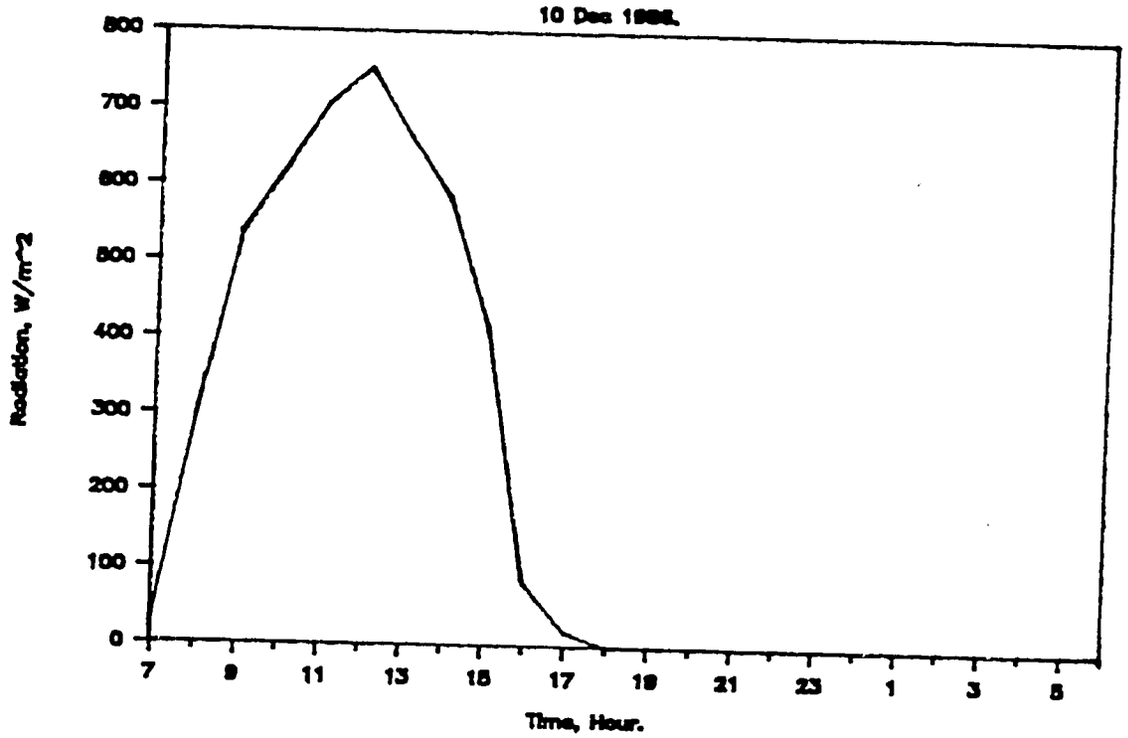

FIG. 4: INSTANTANEOUS SOLAR RADIATION VALUES FOR 10 DEC 1986.

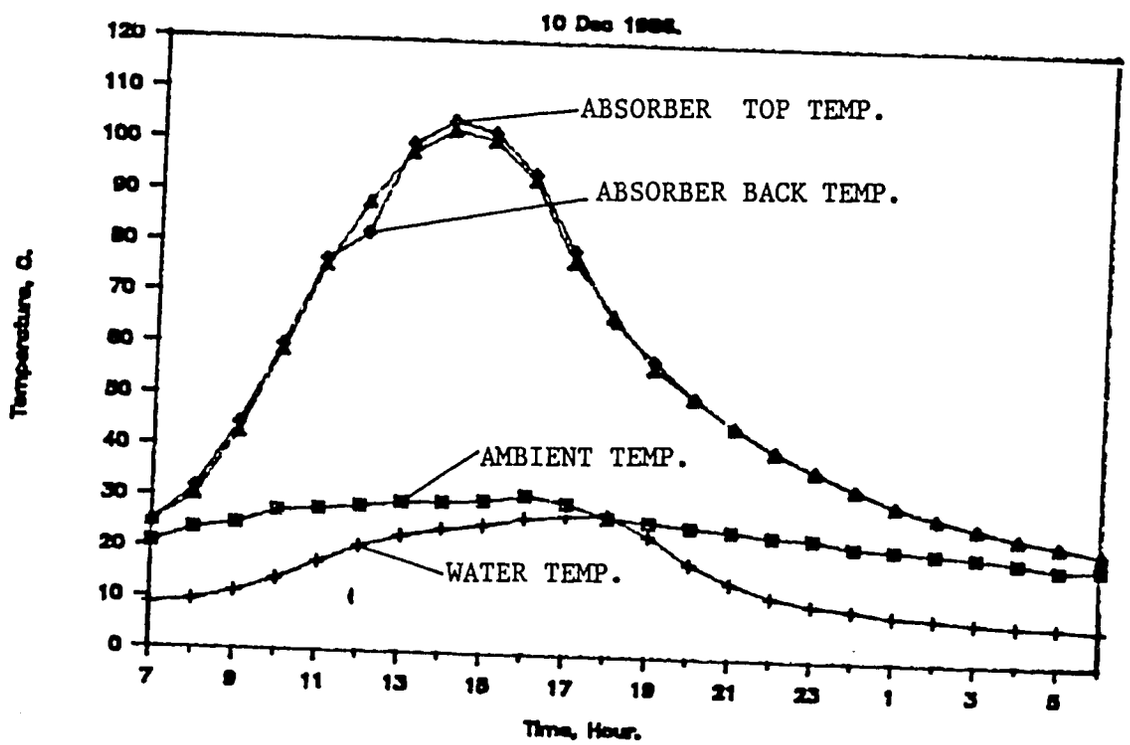

FIG. 5: TEMPERATURE PROFILE FOR 10 DEC 1986.

112

correspond to condenser temperatures of 34 to 47°C(93 to 117°F), the difference between the condenser temperature and the ambient being as high as 17°C. The solar COP of the sytem was between 2.5 to 4%. The measured points were plotted in the pressure-temperature-concentration (p-T-x) chart for zeolite 13X-water (Fig. 6), and based on the available information (Worek, 1986) a mass balance for a day was carried out (see appendix). From the p-T-x chart, the concentration in the early morning was 23 wt. % (dry basis) and the minimum concentration reached during the day was 21%. During adsorption cycle, the concentration changed back to 23%. So, the system cycled 2% water but the recorded value corresponds to concentration change of less than 1%. This difference might be due to three reasons: (i) Actual zeolite temperature might be different than the average of the temperature read at the top and the bottom surface of the zeolite panel; (ii) the p-T-x chart supplied is for zeolite 13X but not for the natural zeolite used in the system, and (iii) the pressure gauge used is not very accurate. Although the minimum temperature corresponding to the pressure read was about 1°C, the sensor attached to the bottom of the bottle recorded 6.6°C. This diffrence might again be due to the low sensitivity of the pressure gauge at very low pressure range. The lowest temperature recorded during the test was 4°C and the system could not produce ice. The net cooling produced for this day was only 316.6 kJ.

1.6 Conclusions

The most important conclusions drawn from these tests are as follows:

1. Although the absorber temperature up to maximum of 104°C was achieved in this system, the temperature was not high enough to result significant desorption as the system cycled less than 1% water. This has resulted into very poor cooling efficiency as low as 2.5%.

2. The condenser temperature is very high and it goes up to 17°C above the ambient which reduces the amount of water desorbed during the desorption cycle which consequently results into low net cooling during adsorption .

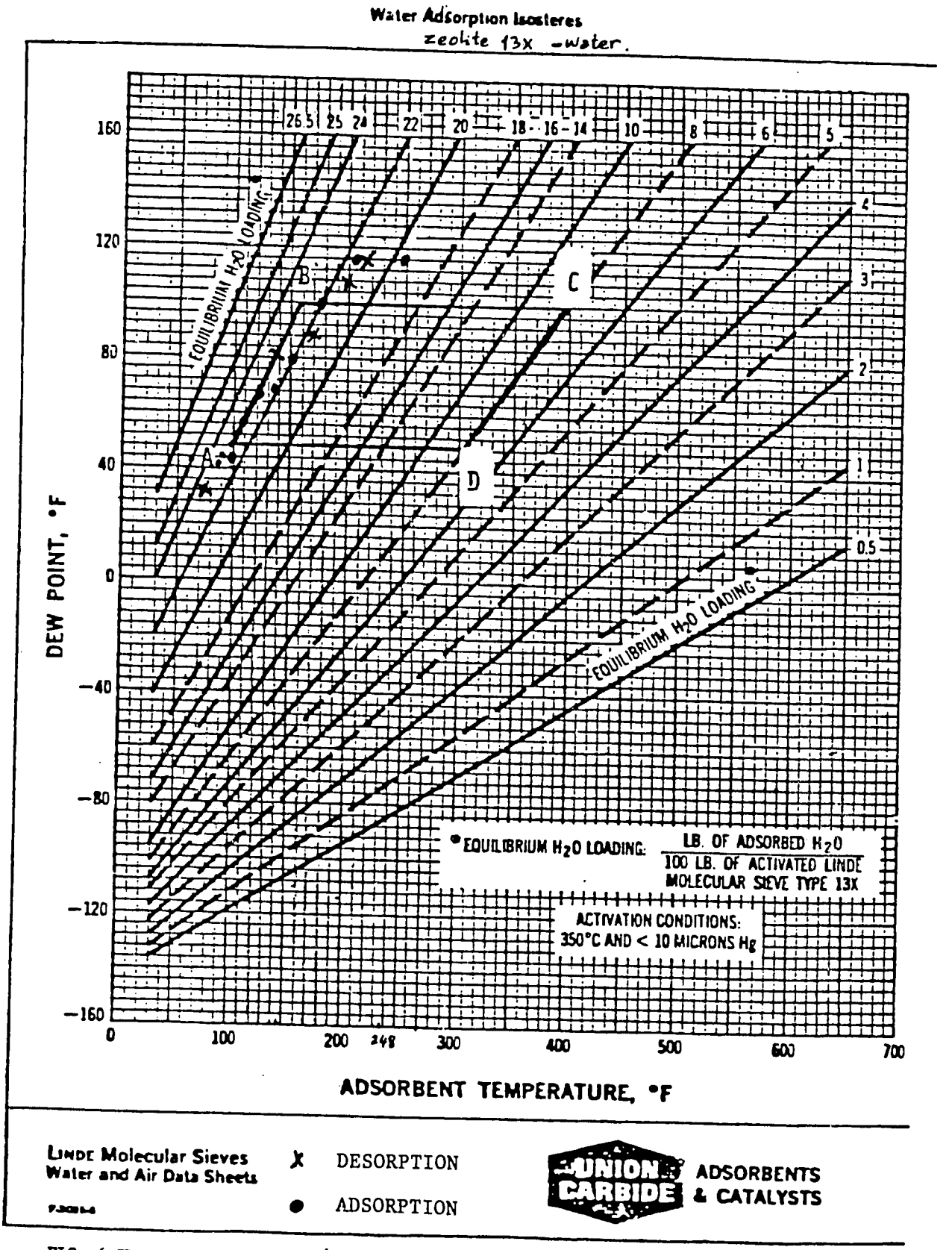

FIG. 6: THE EXPERIMENTAL POINTS IN p-T-x CHART (10 DEC 1986).

114

3. The condensation starts at the evaporator as it is the coldest and continues until the evaporator temperature reaches ambient temperature after which the condensation normally occurs at the condenser. This heats up the water in the bottle and also the cooling chamber during desorption cycle which is undesirable.

II. Work Carried out at AIT on Charcoal-Methanol Pair*

The comparision of synthetic zeolites 5A, 13X and activated charcoal(AC) with different refrigerants R11, R12, R22, and R114 done by Critoph and Vogel (1986) proved charcoal as the preferable adsorbent for solar cooling. We also became aware of the study done by Grenier and Pons(1983), Meunier and others (1986) on synthetic zeolite-methanol and charcoal-methanol pairs. Their study revealed that charcoal-methanol gives a better COP generally, but that when the night-time ambient temperature-evaporating temperature is particularly high then a zeolite-water combination is better. However this will require a higher generating temperature from the solar collector during the day. The comparision of zeolite 13X-water and AC 35-methanol done by Meunier and others(1986) suggest that zeolite combinations will only be superior when the temperature lift (adsorption-evaporating temperature) exceeds 45°C. The COP is based on heat input to the adsorbent rather than the solar collector and so the reduced solar collector efficiency at higher temperatures may actually make charcoal-methanol combinations superior even at higher temperature lifts.

The others reasons for preferring activated charcoal are as follows:

1. Activated charcoals are cheaper than zeolites.

2. Activated charcoals can be made with properties to suit particular applications by varying the activation time and temperature, etc.

3. Activated charcoals (particularly coconut shell charcoal) can be manufactured in the country of origin and use.

Because of above advantages and the encouraging French results it was decided to investigate the methanol-charcoal system under the terms of the USAID contract.

---

*We are indebted to Dr R.E. Critoph of University of Warwick, on leave in AIT during the period Sept - Dec 1986, for this section.

Initially, the data for the AC-35 methanol pair were used for design purposes. Attempts were made to find local suppliers of a suitable granular charcoal suitable for gas adsorption, but without success. Sutcliffe-Speakman in the U.K. were able to supply samples. The cost of charcoal within the U.K. was 4 pounds/kg.

Design calculations were carried out on two versions of a charcoal-methanol referigerator. In both versions, heat was to be supplied at 100°C via condensing steam at atmospheric pressure. This allows the use of variety of heat sources, such as biomass or waste heat, as well as solar. Also, it would allow initial testing to be carried out using electric heating, which is much easier to use experimentally. The ideal cycle, evaporating at -10°C rejecting condenser and adsorber heat at 30°C, and raising the charcoal to 100°C has a COP of 0.51. This neglects the thermal mass of the containing vessels, etc.

The two versions considered were a diurnal cycle and a continuous cycle. In the diurnal cycle the charcoal is heated during the day, and cooled at night. To produce the desired quantity of 25 kg of ice per day, at least 100 kg of charcoal would be needed.

In the continuous cycle, two small adsorption refrigerators are used. Whilst one is heated (via steam from the heat source) the other is cooled by ambient air or water. Based on experience at Warwick with activated charcoals and organic refrigerants we decided to aim at a 30 minute cycle time with 4 kg of charcoal in each adsoprtion vessel. The detailed heat/mass transfer of methanol/charcoal were not known and so part of the experimental work involved, if such a system were to be built, would be measurement of these properties.

Several factors contributed to the decision to build only half of the continuous unit.

(i) The prohibitive cost of obtaining suitable activated charcoal within the time scale.

(ii) The reduced charcoal/methanol inventory of the continuous unit should give lower capital cost,

justifying it even when the materials are locally obtainable.

(iii) The timescale favoured the production of a smaller unit given the limited technical support time available.

At the same time that this experiment was being designed and built using the French p-T-x data, we needed to generate our own p-T-x information on different charcoals in a laboratory test rig. We eventually obtained samples of seven charcoals from Sutcliffe Speakman, UK, and three from India. Two of the charcoals were obtained in 5 kilo quantities for possible use in the larger experiment. These were the Sutcliffe Speakman equivalent of AC 35, and their own recommended grade of coconut shell charcoal.

Considerable difficulties were encountered in building the laboratory rig, most of which related to maintaining the necessary vacumm-tightness. Essentially the rig is quite simple, consisting of a vessel containing charcoal in a temperature controlled oil bath, a glass methanol vessel in a water tank (enabling the liquid level to be read from a graduated scale), a pressure gauge and a vacuum pump, together with connecting pipework and isolating valves. The pressure and temperature of the charcoal can be calculated from a knowledge of the total quantity of methanol present and the liquid level.

Refrigeration valves and pipework were obtained and found adequate. The original pressure gauge used was a mercury manometer. The glass to metal seal proved unreliable, and methanol condensing and then boiling on the glass walls caused problems. Despite the reduced accuracy, a bound-type vaccum gauge was used instead and proved more reliable. The methanol vessel caused problems, being difficult to seal, but these difficulties were solved eventually. An initial set of test results, whilst showing repeated adsorption and desorption did not give identical adsorption and desorption curves because of the thermal lag of the charcoal and water bath. Also the exact temperature of the methanol was difficult to know and could only be inferred from the temperature of the surrounding water bath or from the system pressure.

Both methanol and charcoal containers were redesigned so that their internal temperatures could be determined by a mercury thermometer and thermocouple respectively. This revealed new problems when it was discovered that during desorption the pressure exceeded the saturation pressure by 20 mm Hg or even more, sometimes stopping the desorption process. This was put down to inadequate initial degassing, and a fresh sample is being put through several cycles of adsorption followed by evacuation to try to remove all contaminants. There is still some excess desorption pressure, but the overall performance is adequate. Future samples will be degassed at higher temperatures and for longer.

The samples under test at present are exhibiting reasonable concentration changes, but the thermal lag effect is still very great. Probably only by allowing several hours for each point can true equilibrium conditions be obtained. The apparent difference in concentration between heating and cooling is typically about 4%. This is thought to be hysteresis is due to capillary condensation. Tests are continuing.

Whilst the laboratory work was in progress the larger test rig had to be designed and built. The charcoal was contained in the annular space between a 2" and 4" copper pipe. The outside was well insulated and the inside could either be heated by steam or cooled by water. A water cooled shell and tube condenser was fabricated, as was a receiver and flooded evaporator (capacity 13 kg). Copper was used for all pipework to make leakproof fabrication easier. 1 3/8" OD pipe was used for methanol vapour transport to keep pressure drops insignificant.

One special detail of the generator/adsorber was a stainless steel mesh tube (1" x 1") running axially along the annulus and empty of charcoal. Its function is to transfer the methanol vapour to within a short distance of the adsorbing charcoal with minimum pressure drop.

Initial runs with charcoal 207C produced anomalously high pressures and poor mass and heat transfer. However, this is now thought to be due to the inadequate de-gassing referred to above, and a new de-gassing procedure has been started. The details of the above system and the experimental results will be included in the next report.

An R114-Charcoal refrigerator constructed at Warwick University by Critoph and Vogel (1986) is under test at AIT. The R114-charcoal pair has an ideal COP of 0.15 based on heat input. This system has solar collection area of $1m^2$ and is designed to produce 1 kg ice/day. The refrigerator was shipped to AIT at the expense of Warwick University.

Future Plan

1. In the present arrangement, it seems almost impossible to completely evacuate the water from the zeolite-water refrigerator except by dismantling the arrangement and heating the zeolite to a high temperature. So, before charging methanol in this system, the zeolite-methanol pair will be tested in the test rig. This will also be done to observe whether any catalytic reaction decomposes the methanol as reported by Meunier and others (1986). If the zeolite-methanol pair function satisfactorily in the test rig, the prototype will be charged and tested with methanol.

2. The zeolite-methanol and the charcoal-methanol pairs will be studied.

3. Seven different activated charcoals from Sutcliffe Speakman, U.K., three samples from India and one locally produced sample are being tested in our test rig to find out the most efficient adsorbent for charcoal-methanol pair.

Note: A new factory producing activated carbon from coconut shell has recently been opened in Chonburi(100 km from Bangkok). This factory will be visited, specification of the product will be obtained, and samples will be tested.

APPENDIX

MASS BALANCE

From the basic data supplied by Worek (1986):

Total weight of zeolite and water in the system = 34.0 kg
Dry weight of zeolite is approximately between 24.948 to 26.3 kg (assumed 25.63 kg).
On delivery the amount of water in the receiver/evaporator bottle = 0.5 kg (approximated from the measurement of the external dimensions of the bottle).
Total weight of water in the system = 34.0-25.63 = 8.37 kg
Amount of water initially adsorbed by zeolite = 30.71% (dry basis).

To plot the values on the p-T-x chart, we need the temperature of zeolite in the collector and the dew point temperature of water vapour in the system. The measurements done were based on the following assumptions:

(i) The zeolite temperature is assumed equal to the average between top and the back panel temperatures.

(ii) The dew point temperature is the saturation temperature of water vapour corresponding to the measured value of pressure assuming no other gas is present in the system.

From the p-T-x chart (Fig. 6) for Dec 1986

The concentration of water in zeolite in the early morning = 23% (dry basis).
The concentration at the end of desorption = 21% (dry basis).
The concentration at the end of readsorption = 23% (dry basis).
So, the amount of water cycled during this day = 2% (dry basis)= 0.5125 kg.

The corresponding values were also calculated from observations of the level of water in the bottle. For this case the amount of water in the bottle was estimated measuring the outside diameter of the receiver/evaporator bottle and allowing

121

4mm thickness for the sides and the bottom. The observed values are as follows:

Amount of water initially present in the bottle = 2.149 kg and thus amount of water in the zeolite = (8.37-2.149)/25.63
= 24.27 % (dry basis).

The amount of water in the bottle at the end of desorption
= 2.381 kg and water in the zeolite = (8.37-2.381)/25.63
= 23.367%.

So, amount of water desorbed during the day = 24.27-23.367
= 0.903%.

Water in the bottle at the end of readsorption = 2.242 kg and water in the zeolite = (8.37-2.242)/25.63
= 23.90%.

This is equal to a change of concentration of 0.533% during readsorption.

Thus the amount of water cycled was less than 1% and the minimum temperature reached for the day was 6.6°C.

If the final temperature of zeolite is equal to 120°C(248°F) the condenser temperature being 47°C(97°F), the final concentration of water in the zeolite is 19.5% wt % (dry basis). If the zeolite is able to adsorb the same amount of water during cooling the concentration change will be 3.5% and the amount of water cycled will be 0.8971 kg. If we consider the latent heat of evaporation of 2326 kJ/kg (Tchernev, 1979); the cooling produced can freeze at the maximum 4.5 kg of water initially at 30°C. This is somewhat less than the amount which this system is supposed to produce during a clear day.

Sample Calculation of Overall COP (10 Dec 1986)

The amount of solar radiation incident on the surface of the solar collector inclined at 14° S between 7:00 to 18:00 hours
= 17.97 MJ/m^2.

The effective surface area of the collector/absorber = 0.6935 m^2.

Thus solar radiation incident on the collector = 12.462 MJ/day.

The water level read late afternoon at the end of condensation
= 4.7 thousands of BTU's.

The final water level read next morning(7:00 hours) at the end of cooling part of cycle = 4.4 thousands of BTU's.

So, cooling produced by the system = 1000.0(4.7-4.4)
= 300 BTU = 316.0 kJ
= 0.316 MJ.

Solar COP = Cooling produced by evaporation/Incident Solar Radiation = 0.316/12.462 = 2.5%.

References

Critoph, R.E., and R. Vogel (1986). Possible Adsorption Pairs for Use in Solar Cooling. Submitted for publication to the J. Ambient Energy.

Grenier, Ph., and M. Pons(1983). Experimental and Theoretical Results on the Use of an Activated Carbon CH_3OH Intermittent Cycle for the Application to a Solar Powered Ice Maker. S.V. Szokolay (Ed.). Solar World Congress, Vol. 1. Pergoman Press. pp. 500-506.

Meunier, F., Ph. Grenier, J.J. Guilleminot, and M. Pons (1986). Solar Powered Refrigeration Using Intermittent Solid Adsorption Cycles. To be published in the J. of Solar Energy Engineering.

Tchernev, D.I. (1979). Solar Refrigeration Utilizing Zeolites. Proc. of the 14th Intersociety Energy Conversion Engineering Conference. pp. 2070-2073.

Worek, W. M. (1986). Personal Communications.